UNIVERSITE D'ABOMEY - CALAVI (UAC)

INSTITUT NATIONAL DE L'EAU

Federal Ministry of Education and Research

WASCAL
West African Science Service Center on Climate Change and Adapted Land Use

*Registered under N°:4501-16./UAC/VR-AARU/SA*

**A DISSERTATION**

Submitted in partial fulfilment of the requirement for the degree of
**DOCTOR of Philosophy** (PhD) of University of Abomey-Calavi (Benin Republic)
In the framework of the
**Graduate Research Program on Climate Change and Water Resources (GRP-CCWR)**

by

**Kossi KOMI**

Public defense on: 10/25/2016

======

# FLOOD RISK ASSESSMENT IN POORLY GAUGED RIVER BASINS -A CASE STUDY OF THE OTI RIVER BASIN, TOGO, WEST AFRICA.

======

**Supervisors**

**Mr. Barnabas A. AMISIGO,** Associate Professor**,** CSIR-Water Research Institute, (Ghana)
**Mr. Bernd DIEKKRÜGER,** Professor, University of Bonn (Germany)
**Mr. Moussa BOUKARI,** Professor, University of Abomey-Calavi (Benin Republic)

======

**Reviewers**

Mr. Luc SINTONDJI, Associate Professor, University of Abomey-Calavi (Benin Republic)

Mr. Leonard AMEKUDZI, Associate Professor, KNUST Kumasi (Ghana)

Mr. Kwasi PREKO, Professor, KNUST Kumasi (Ghana)

======

**JURY**

Mr. Norbert Mahouton HOUNKONNOU, Professor, University of Abomey-Calavi, **Chairman**

Mr. Abel AFOUDA, Associate Professor, University of Abomey-Calavi, **Examiner**

Mr. Julien ADOUNKPE, Associate Professor, University of Abomey-Calavi**, Examiner**

Mr. Rabani ADAMOU, Associate Professor, University Abdou Moumouni (Niger), **Examiner**

Mr. Moussa BOUKARI, Professor, University of Abomey-Calavi, **Supervisor**

# DEDICATION

*To the soul of my mother*

## ACKNOWLEDGEMENTS

Doing a PhD is like building a house - many years of work which is not possible without the assistance of some important persons. I would therefore like to thank a great number of people. First, I should thank the German Ministry of Education and Research (BMBF) who funded this project through a three year scholarship, a research budget and a personal computer under the West African Science Service Center on Climate Change and Adapted Land Use (WASCAL) program.

Next, I would like to express my sincerest gratitude to Dr. Barnabas A. Amisigo, Senior researcher at the CSIR-Water Research Institute, Accra and first supervisor of this PhD, who has spent time with me, seeing the details of the PhD work done and offering me the encouragement, advice and help that I needed to improve this study. I am very grateful to Prof. Bernd Diekkrüger at the Department of Geography of the University of Bonn, who was willing to provide some initial ideas of this work and gave me continuous support and constructive criticisms on my changing manuscripts. Also, thanks to both Prof. Moussa Boukari at the University of Abomey-Calavi and Dr. Fabien Hountondji at the University of Parakou for their contribution to this work. I am also grateful to Dr. Jeff Neal at the University of Bristol (England) for giving me the opportunity to undertake part of this work at the School of Geographical Sciences, providing me with data and scientific assistance which were necessary to improve this work. I would like to thank Mark and Stephanie Trigg for their technical and scientific contributions to this work and the language help.

I express my gratitude to Prof. Abel Afouda and Dr. Julien Adounkpe, respectively Director and Coordinator of the WASCAL Graduate Research Program (GRP) on Climate

Change and Water Resources at the University of Abomey-Calavi, as well as to Prof. Emmanuel Lawin and all the staff of the WASCAL-GRP in Benin Republic. I would like to thank Mrs. Minnattallah Boutros for all the assistance during my scientific visit. Thanks to Erin Couglan, Janot Mendler de Suarez, Dr. Peter Burek, Dr. Bernard Bisselink, Dr. Brenden Jongman and Prof. Ad De Roo, for their contribution in the calibration of LISFLOOD hydrological model.

I would like to thank Professor Kouame Kokou and Professor Kissoa Gnandi at the University of Lomé for the support during my application to this PhD program. Fellow students Jean Hounkpe and Felicien Badou are thanked for their help and useful opinions. I should also thank Thierry for writing the Scilab code. Finally, I would like to thank Dr. Jean Gabriel Baba and his family, Tchankoni Koffi, Naimath, Dr. Kodjo Glato and Saibou Anzoumana for their support.

# ABSTRACT

In many parts of the world, hydrological extremes have been observed and grave consequences on human life, socio-economic activities and ecosystems have been reported. Over the last few years, West Africa has increasingly experienced severe floods that have affected millions of people and hampered economic development in the region. Floods in Oti River Basin result in loss of life and property, damages of growing crops and infrastructure, and disruption of social and economic activities. These consequences could be exacerbated by the effects of human-induced climate change. Therefore, managing the risk of extreme events and disasters is important for an efficient climate change adaptation. In West Africa, the management of floods becomes a strategic priority at local, national and regional levels, particularly in the aftermath of the severe floods in 2007, 2008 and 2010. Flood risk assessment is the first step of any flood risk management project. Such assessment gives insight on what can be expected and opens up the discussion on how to tackle the situation. However, flood risk information is missing in many West African catchments basically in the Oti River Basin due to the lack of the hydrological data required to estimate it. The urgency of this subject and the existing research gaps in the study area are the main motivation for the present work. This thesis is an initial detailed flood risk assessment in the Oti River Basin (Togo). The research methodology was articulated in four main steps namely (*i*) regional flood frequency analysis based on L-moments (*ii*) hydrological modelling for flood prediction, (*iii*) flood hazard mapping using flood inundation model and (*iv*) community-based flood risk assessment via a combination of flood hazard map, survey data on vulnerability, exposure and coping capacity. The results of this study showed that Generalized

Extreme Values (GEV) and Generalized Pareto (GPA) are the best probability distributions to estimate flood frequency in the Oti River Basin. For the hydrological modelling, Nash-Sutcliffe coefficients of 0.87 and 0.94 were respectively obtained for the calibration and validation periods. Moreover, the present study showed that flood extends in the Oti River Basin doesn't change drastically for higher return period floods. This thesis showed also that flood risk in the Oti River Basin is moderate and predominantly driven by high vulnerability and hazard. Both exposure and coping capacity are relatively low. Finally, further research is needed to understand the effects of rainfall on the variability of L-moments of annual maximum discharges, to analyze the combined effects of climate and land use changes on flood risk and to implement advanced flood early warning system in the Oti River Basin of Togo.

# RESUME

Dans plusieurs régions du monde, des extrêmes hydrologiques ont été observées avec de lourdes conséquences sur la vie humaine, les activités socio-économiques et les écosystèmes. Par ailleurs, durant ces dernières années, L'Afrique de l'Ouest a été touchée par des inondations sans cesse croissantes qui ont affecté plusieurs millions de personnes et ralenti le développement socio-économique de cette région. Les inondations dans le bassin versant de l'Oti causent d'importantes pertes en vie humaines, destruction d'infrastructures et de champs et interruption des activités socio-économiques. Ces conséquences pourraient être aggravées par les effets des changements climatiques. Par conséquent, il est important de bien gérer les aléas et catastrophes naturelles pour une meilleure adaptation aux changements climatiques. En Afrique de l'Ouest, la gestion des inondations est une priorité à l'échelle locale, nationale et régionale, particulièrement après les inondations dévastatrices des années 2007, 2008 et 2010. L'évaluation des risques d'inondations est la première étape de tout projet de gestion durable de risques d'inondations. Cette évaluation permet de savoir à quoi l'on peut s'attendre et ouvre le débat sur les solutions à apporter au problème. Cependant, les informations sur les risques d'inondation sont manquantes dans plusieurs bassins versants Ouest africains tel que le bassin du fleuve Oti à cause du manque ou d'insuffisance de données hydrologiques nécessaires à leur estimation. Cette thèse constitue une analyse initiale et détaillée du risque d'inondation dans le bassin du fleuve Oti au Togo. La démarche méthodologique est articulée autour de quatre points principaux à savoir (*i*) l'analyse régionale fréquentielle des crues basée sur les moments linéaires, (*ii*) la modélisation hydrologique pour la prédiction des crues, ( *iii*) la cartographie des zones inondables à l'aide d'un modèle hydraulique et (*iv*) l'évaluation du risque d'inondation à l'échelle communale en

associant des informations sur la vulnérabilité, l'exposition, la capacité de gestion et l'aléa hydrométéorologique. Les résultats de cette étude ont montré que la distribution des valeurs extrêmes généralisées et la distribution généralisée de Pareto sont les meilleures fonctions de distributions pour l'estimation de la fréquence des crues dans le bassin de l'Oti. Ensuite, des coefficients de Nash-Sutcliffe de 0.87 et 0.94 ont été obtenus respectivement pendant la calibration et la validation du modèle hydrologique. Les étendues des inondations pour les crues de périodes de retour élevées ne changent pas considérablement. Cette étude a aussi montré que le risque d'inondation dans le bassin de l'Oti au Togo est relativement modéré et caractérisé par des indices élevés de vulnérabilité et d'alea hydrométéorologique. L'exposition et la capacité de gestion sont relativement faibles. Enfin, des recherches supplémentaires sont nécessaires pour comprendre l'effet des pluies sur la variabilité des moments linéaires de débits maximaux annuels d'une part et d'autre part pour analyser l'effet des changements climatiques et d'utilisation des terres sur les risques d'inondations dans le bassin versant de l' Oti au Togo.

# Table of Contents

# LIST OF FIGURES

# LIST OF TABLES

## LISTE OF ABBREVIATIONS

AMAX: Annual Maximum

BMBF: German Ministry of Education and Research

CBDRI: Community-Based Disaster Risk Index

CRU: Climate Research Unit

CRED: Centre for Research on Epidemiology of Disasters (Belgium)

DEM: Digital Elevation Model.

DGSCN : Direction Générale de la Statistique et de la Comptabilité Nationale (Togo)

ETo: Reference evapotranspiration

ES0: Potential evaporation from a bare soil surface.

EW0: Potential evaporation of open water surface.

FAO: Food and Agriculture Organization.

GEV: Generalized Extreme Value distribution.

GIS: Geographic Information System.

GLO: Generalized Logistic distribution.

GNO: Generalized Normal distribution.

GRP: Graduate Research Program.

GPA: Generalized Pareto distribution.

GTZ: German Technical Cooperation Agency.

HWSD: Harmonized World Soil Database.

ICSU : International Council for Science Unions

IFRCRCS: International Federation of Red Cross and Red Crescent Societies.

ISDR: International Strategy for Disaster Reduction

IPCC: The Intergovernmental Panel on Climate Change.

ISRIC: International Soil Reference and Information Centre.

ITCZ: Intertropical Convergence Zone.

LAI: Leaf Area Index.

NASA: National Aeronautics and Space Administration (United State of America).

NERC: Natural Environment Research Council (United Kingdom)

NSE: Nash-Sutcliffe coefficient.

PD: Percentage deviation.

PDNA: Post Disaster Need Assessment

PE3: Pearson type III distribution

PWM: Probability Weighted Moment.

RFFA: Regional Flood Frequency Analysis.

RMSE: Root Mean Square Error.

SRTM: Shuttle Radar Topography Mission.

TRMM: Tropical Rainfall Measuring Mission.

VBRP: Volta Basin Research Project

WASCAL: West African Science Service Center on Climate Change and Adapted Land Use.

# 1. GENERAL INTRODUCTION

## 1.1. Background and problem statement

Climate change and its negative impacts have become a major concern for scientific community, governments and civil society. The Intergovernmental Panel on Climate Change (IPCC) defines climate change as a change in the state of the climate that can be identified by changes in the mean and/or the variability of its properties and that persists for an extended period, typically decades or longer (IPCC, 2012). The IPCC fifth report showed that climate change threats will have major impacts on both the environment and economy worldwide (IPCC, 2014). Observational records and climate projections provide abundant evidence that water resources are vulnerable and are strongly impacted by the effects of climate change, with wide-ranging consequences for human societies and ecosystems (Bates et al., 2008). Changes in the hydrological cycle due to climate change and variability have led to negative consequences on water resources in many African countries (Ardoin-Bardin, 2004; Goula et al., 2006; Goula et al., 2009) and the severe floods in 2007, as well as the droughts of the years 1983/1984 and 1973/1974 are some examples of the impacts of climate change and variability in Africa. Furthermore, studies have shown that discharge evolutions in West Africa would be affected by rainfall variations linked to climate change and climate variability. For instance, a 10% drop in rainfall would result in reduction in river flow of approximatively 25% (Roudier et al., 2014). Moreover, McCartney et al. (2012) have shown that by the end of this century, the magnitude of floods with return periods less than 10 years would decrease in the Volta Basin, while the trend for higher return period floods is not consistent from station to station.

It is important to note that change in the frequency of flood and drought are the most important observed and potential impacts of climate change in Africa. For instance, according to

the International Council for Science Unions (ICSU), from 1900 to 2006, floods in Africa killed 20,000 people (ICSU, 2007). Heavy rainfall in September 2007 caused the worst floods that West Africa had ever faced since many decades. The hardest hit countries were Togo, Burkina Faso and Ghana with 23, 46 and 56 persons killed respectively (Tschakert et al., 2010). More recently, 38 people were reported killed and 9,000 homes were destroyed in the August-September 2016 floods of the Niger River (OCHA, 2016).

Moreover, in the Oti River Basin (ORB) heavy rainfalls in 1998, 2007, 2008 and 2010 caused damaging floods and people were made homeless with severe damages and loss of live. According to the International Federation of Red Cross and Red Crescent Societies (IFRCRCS), 14,620 persons were affected in Togo by the October 1998 floods of the Oti River (IFRCRCS, 1998). The severe flood of September 2007 killed 25 people and injured critically 97 critically in Togo part of the Oti River Basin (IFRCRCS, 2007). About 11,628 hectares of cultivated land and 11 main bridges were destroyed by the 2008 floods of the Oti River in Togo (MERF, 2009). Also, extreme floods in 2010 made 836 persons homeless at Cobli in Benin Republic part of ORB (PDNA-Benin, 2011). Further back in time, Oti River experienced historical extreme floods on October 6, 1957 (10.0 m of water level) and September 21, 1962 (10.64 m of water level) at Mango in Togo; on September 2, 1951(1.0 m of water above a bridge on the Kara River at Lama-Kara in Togo); the extreme flood of 1963 affected the whole Volta Basin with grave consequences in Ghana (Moniod et al., 1977).

Since a flood is a product of the hydrologic cycle that is influenced significantly by two major group of factors namely climatic and physiographic factors (Chow, 1956), flood frequency in the Volta Basin may increase in future due to climate change and human activities. In 2012, a special report on extreme events of the IPCC emphasized the necessity of managing the risks of

extreme events at the local level (IPCC, 2012). Some approaches for accurately managing flood risk and adapting to climate change involve the identification of the risk issue and the definition of methodologies for assessing this risk (Simonovic, 2012). Moreover, in 2005, the World Conference on Disaster Reduction emphasized the necessity to incorporate disaster risk assessment into rural planning and management in order to mitigate disaster risk (ISDR, 2005).

To the best of our knowledge, the first research on floods in the Oti River were performed by the French Research Institute for Development (former ORSTOM) and published in a Monograph of the Volta Basin (Moniod et al., 1977). In addition, McCartney et al. (2012) studied the impacts of climate change on the magnitude of floods for different return periods in the Volta Basin including the Oti River Basin. However, there is a lack of information on flood risk in the Oti River Basin.

## 1.2. The Oti River Basin

The ORB is a sub catchment of the Volta Basin which is one of the largest catchments in West Africa (Figure 1.1). The topography of the ORB is the steepest in the Volta Basin with an elevation between 42 and 874 m. The Oti River begins in the Atakora hills of Benin where it is called Pendjari River. Then, it flows along the border between Benin and Burkina Faso before entering Togo with an annual stream flow of about 3.0 $km^3$. The Oti River passes along the border between Togo and Ghana and it reaches the main Volta River in Ghana with an annual discharge of about 12.0 $km^3$(Amisigo, 2005). With only 18% of the total surface area of the Volta Basin, the contribution of the Oti River ranges between 30% and 40% of the total annual discharge of the Volta River System (UNEP-GEF, 2012).

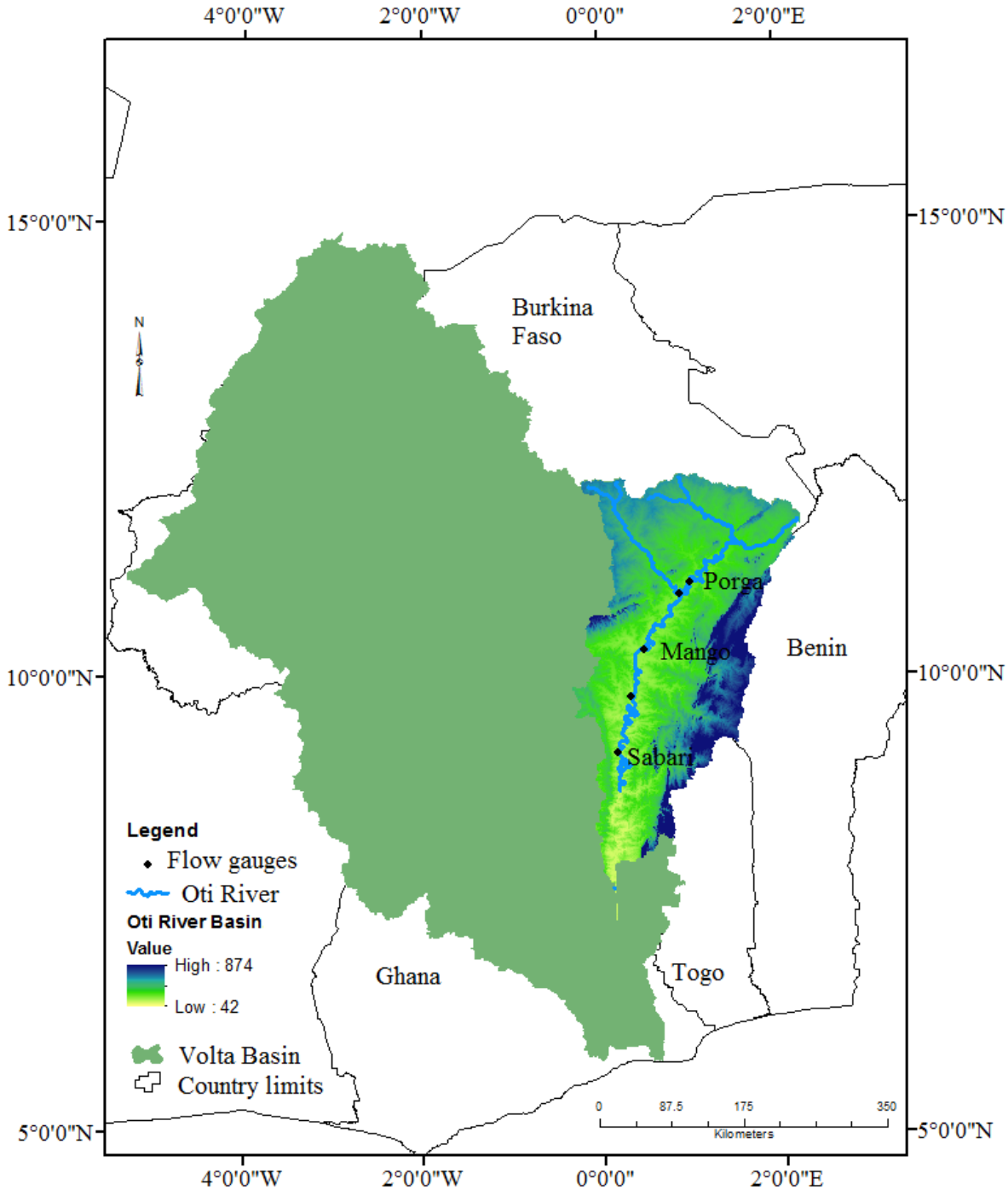


*Figure 1. 1.Location of the Oti River Basin*

### 1.2.1. Climate

The climate of the ORB is tropical semi-arid to sub-humid and it is determined by its location within the West African Monsoon (WAM) which is documented in both Sultan et al. (2003) and Sultan and Janicot (2003). The key components of the WAM system are the Inter Tropical Convergence Zone (ITCZ), the African Easterly Jet (AEJ), the Tropical Easterly Jet (TEJ) and African Easterly Waves (AEWs). ITCZ is the interface between two winds namely the harmattan, blowing from the Sahara desert and the monsoon which blows from the Atlantic Ocean. The AEJ is a middle tropospheric jet located over much of tropical northern Africa during the northern hemisphere summer. The TEJ is an upper tropospheric easterly jet that extends across the tropics from the eastern Indian Ocean to western Africa. The AEWs are westward-travelling waves that originate over northern Africa primarily between June and October. The onset and end of the rainy season, the length of rainfall period and the annual rainfall amount are controlled by the northward progression of the West African Monsoon (Omotosho, 1985). The West African Monsoon is a large scale air circulation which forms from the seasonal change in direction of winds because of the land-sea temperature difference between the Sahara desert and the Atlantic Ocean.

Over West Africa, the most important amount of rainfall forms from convective systems such as squall lines and ITCZ (Peters and Tetzlaff, 1988; Mohr and Thorncroft, 2006). Moreover, one of the characteristics of West African rainfall is its high annual and seasonal variability (Nicholson, 2001; Le Barbe et al., 2002; Sultan et al., 2003). Annual rainfall in the ORB varies from 900 mm to 1,400 mm and the maximum rain falls in August (Figure 1.2)

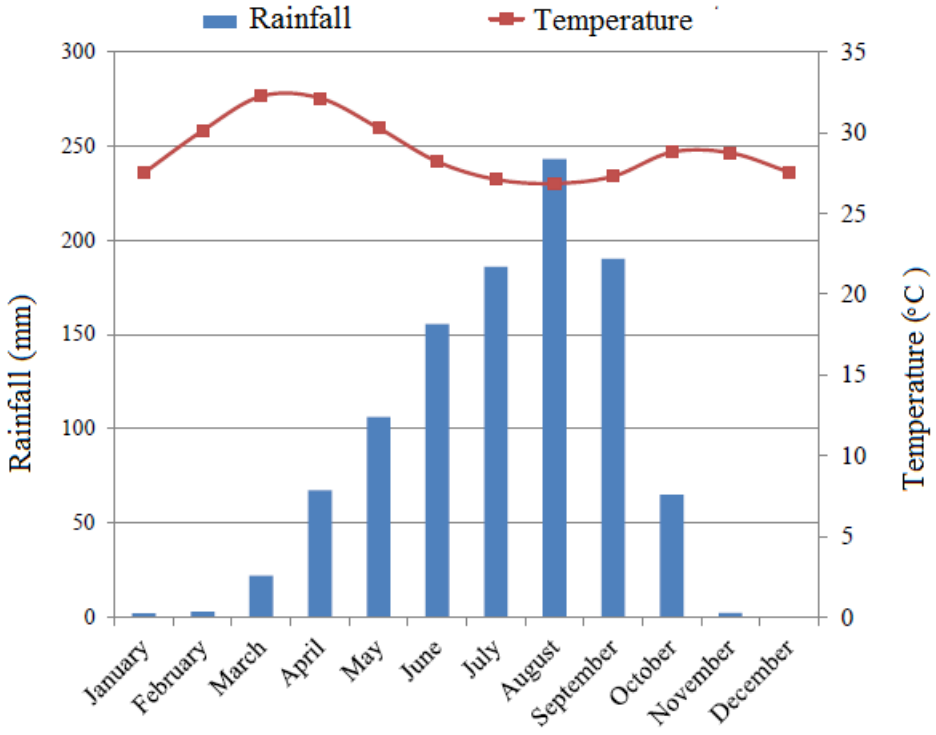


*Figure 1. 2.Average monthly rainfall and temperature at Mango (1980-2010). [ Data source: Togo meteorological service]*

### 1.2.2. Land use and Land cover

Land use and land cover in the ORB are characterized by extensive bush fallow cultivation and grazing with tree regrowth and small patches of reserved forest areas on the hills in the southeast (Barry et al., 2005). The natural vegetation is dominated by savannah (grassland interspersed with shrubs and trees), light forest as well as park forest and small dense forest. Urbanization in the ORB is relatively small.

### 1.2.3. Geology and soils

The Oti River Basin lies on the Voltaian system, the Togo series and the Buem formation (UNEP-GEF, 2012). The Voltaian system includes the Bombouaka Supergroup and the Oti-

Pendjari Supergroup. The Bombouaka Supergroup is dominated by sandstones and other sedimentary rocks. The Oti-Pendjari Supergroup includes mainly sandstones, silexite, tilites and conglomerates. The Togo series is mainly composed of metamorphic rocks such as migmatites, gneisses, micaschists. The Buem system consists of a sequence of shale, sandstone, and volcanic rocks.

The dominant soils of the ORB are gleyic luvisols, fluvisols, ferric luvisols and chromic vertisol (Figure 1.3). Luvisols are soils in which clay is washed down from the soil surface to an accumulation horizon. They are common in flat or not very steep land in regions with distinct wet and dry seasons (http://www.isric.org). Gleyic properties of soil are associated with the movement of the groundwater table and prolonged saturation (http://www.isric.org). Because of their medium stage of weathering and high base saturation, luvisols are suitable for agricultural uses (http:// www.isric.org). Fluvisols are young soils developed from fluvial, lacustrine or marine deposits in all types of climate. The periodic floods in these soils make them wet in all parts of the soil profile. They are suitable to grow crops or grazing grasses. The ferric properties of soils are associated with segregation of iron which leads to the formation of large mottles. According to the International Soil Reference and Information Centre (ISRIC), vertisols are churning heavy soils which are formed from either sediments that contain a high proportion of smectite clay, or rocks weathering that have the properties of smectite clay. They are common in tropical, semi-arid to humid and Mediterranean climates with distinct wet and dry seasons. Infiltration rate in cracked vertisols with surface mulch is initially very high. But, once the soil surface becomes wet and the crack are closed, the infiltration of water is almost nil (http://www.isric.org). Consequently, vertisols flood quickly.

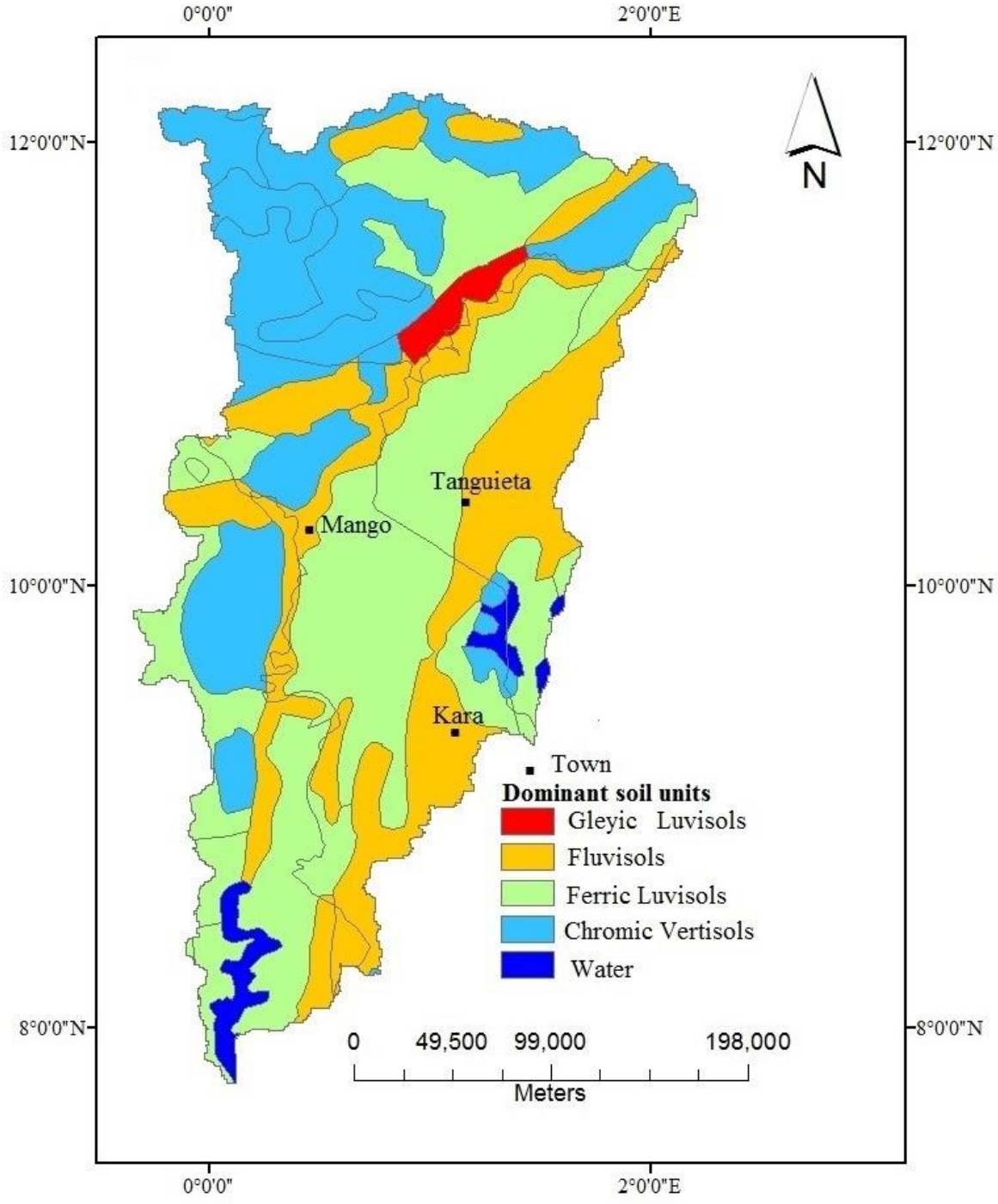


*Figure 1. 3.Soil map of the Oti River Basin (FAO/UNESCO, 1995)*

### 1.2.4. Flood risk reduction measures

In the aftermath of the disastrous floods of 2007 and 2008 in Togo, some strategies to manage and mitigate floods have been established. For instance, the World Bank funded an integrated disaster and land management project to provide support to the Togolese government and strengthens institutional capacities in order to manage the risk of flooding and land degradation in rural and urban areas in the country (World Bank, 2011). The Togolese Red Cross (with the assistance of the German Red Cross) has implemented simple early warning systems in some flood prone areas of ORB. Moreover, on October 2016, HKV CONSULTANTS (http://www.hkv.nl) started the implementation of the Oti River flood risk assessment project funded by the WordBank. The objective of this project is to estimate flood risk, effectiveness of flood mitigation measures as well as to implement a flood early warning systems in the flood prone areas of the ORB in Togo and Ghana (source: http://www.hkv.nl/nl/actueel).

## 1.3. Research objectives and strategy

Given the gaps in the scientific research on flood risk in the ORB, as well as the fact that the study area experiences frequent damaging floods and is poorly gauged, the main objective of this work is to develop methods for flood risk assessment in data scarce areas of West Africa river basins taking the ORB as case study. Specifically, the research objectives of this study are to:

i. Select the appropriate probability distributions to analyze flood frequency (RO1)
ii. Simulate the extend of flood for different return periods (RO2)
iii. Identify the major factors that contribute to flood risk (RO3)
iv. Suggest flood risk mitigation measures (RO4)

In order to achieve these goals, a research strategy has been developed (Figure 1.4)

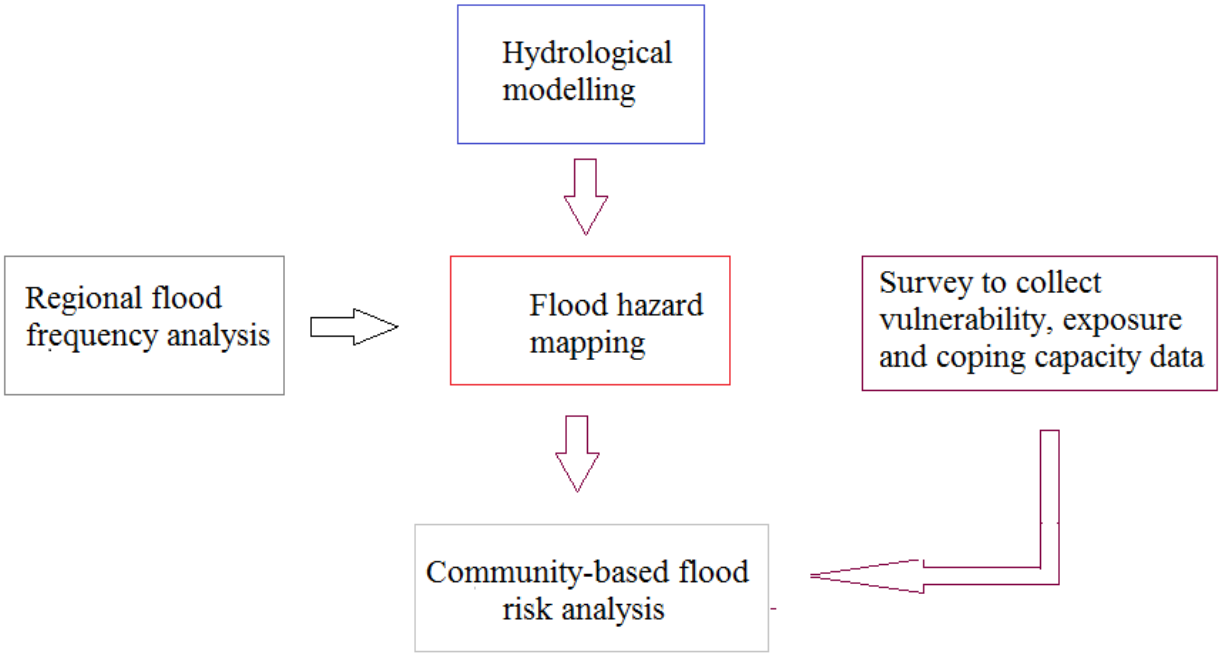


*Figure 1. 4. Research strategy for assessing flood risk in the Oti River Basin*

In a first step, a regional flood analysis is performed for the whole Volta Basin in order to select the suitable flood frequency distributions (OR1). The whole Volta Basin was chosen for the frequency analysis in order to reduce the uncertainty in the estimation of design floods because of the insufficiency of observed discharge data and the short length of the available streamflow time series in the ORB. In addition, a hydrological modelling for flood prediction was applied for the ORB. In a second step, the flood frequency models and the hydrological model were used to estimate the design floods and simulate input hydrographs for the flood hazard mapping (OR2). Finally, vulnerability, exposure as well as coping capacity data were collected from surveys .These data were combined with a simulated flood hazard map to perform a community-based flood risk analysis in order to identify the major factors that contribute to floor risk (OR3) and suggest some recommendations to mitigate flood risk in the ORB (RO4).

## 1.4. Structure of the thesis

This PhD thesis is organized in five (5) chapters. The general introduction to the thesis is given in the first chapter. Chapter 2 provides a review of the literature relevant to this research. This section is dominated by some concepts related to flood risk and an overview of the different methods to both predict floods in ungauged basins and assess flood risk. Chapter 3 presents the 'materials and methods' while Chapter 4 presents the 'results and discussion'. Finally, Chapter 5 provides the conclusions with reference to the research objectives specified above, indicates the limits of this research, and suggests some recommendations for both future research and policy. It is important to mention that two articles have been produced from this PhD thesis. The first one is entitled 'Regional flood frequency analysis in the Volta River Basin, West Africa' (see Appendix 1a) and the second article is entitled 'Integrated flood risk assessment of rural communities in the Oti River Basin, West Africa' (see Appendix 1b).

# 2.LITERATURE REVIEW

## 2.1. Flood risk concepts.

### 2.1.1. Typology of floods

The term flood has many definitions. From a hydrologic standpoint, a flood is a relatively high flow which overtaxes the natural channel provided for the runoff (Chow, 1956). Flood is also defined as the temporary inundation of normally dry land areas resulting from the overflowing of the natural or artificial confines of a river or other body of water (Wisner et al., 2004). According to Natural Environment Research Council (NERC), flood can take many forms such as riverine flood, pluvial flood, tidal flood and groundwater flood ( www.nerc.ac.uk). Riverine flood is typically caused by hydro-meteorological conditions. It occurs in floodplain of rivers when the capacity of the river to contain the water is exceeded as a result of rainfall and the excess water spills out from the river onto the floodplain. Where the riverine flood is very rapid, it is called flash flood. Pluvial flood occurs in rural and urban lands where the intensity of the rainfall exceeds the infiltration rate of the soil. This type of flooding is exacerbated by urbanization which decreases the proportion of permeable surfaces and inadequate urban drainage systems. Tidal flood occurs in estuaries where there is interaction between the tides and river flows. In estuaries, a high flow in rivers, combined with a high tide from the sea, increases water level in rivers which can flow over river banks. Groundwater flood occurs when the water table in the subsoil rises to the ground surface as a result of intense or prolonged rainfall (www.nerc.ac.uk).

### 2.1.2. Flood risk as a concept

The term “risk” in relation to flood was introduced by Knight in 1921, and is actually used in different contexts showing how adaptive any definition can be (Sayers et al., 2002). Hence, many definitions of risk can be found in the literature. For instance, risk is defined as the sum of expected losses and damages caused by a given natural phenomenon as function of the hazard and the vulnerability of the elements at risk (UNDRO, 1991). According to Stenchion (1997), risk might be defined simply as the probability of occurrence of an undesired event [but might] be better described as the probability of a hazard contributing to a potential disaster. Importantly, it involves consideration of vulnerability to the hazard. In some cases, risk is defined as the expected number of lives lost, persons injured, damage to property and disruption of economic activity due to a particular natural phenomenon (e.g. Granger, 1999) and in others as a combination of the chance of a particular event, with the impacts that the event would cause if it occurred (e.g. Simonovic, 2012). Wisner et al. (2004) define risk as a compound function of the natural hazard and the number of people, characterized by their varying degrees of vulnerability to that specific hazard, who occupy the space and time of exposure to the hazard event. Risk of disaster is also thought as the probability of harmful consequences, or expected losses resulting from interactions between natural or human-induced hazards and vulnerable conditions (ISDR, 2004) or as the likelihood of severe alterations in the normal functioning of a community due to hazardous physical events interacting with vulnerable social conditions, leading to widespread adverse effects that require immediate emergency response to satisfy critical human needs (IPCC, 2012). Besides, Cardona et al. (2012) defines disaster risk as the possibility of adverse impacts in the future and it derives from the interaction of social and environmental processes, as well as from the combination of physical hazards and the vulnerabilities of exposed elements.

Defining risk as the product of hazard and vulnerability (Sayers et al., 2003; Apel et al., 2009) may suggest that risks with the same numerical value have the same significance; but it is not often the case because the combination of low probability and high consequence events at one hand as well as the combination of high probability and low consequences events at another hand are perceived differently. Furthermore, the definition of risk as the frequency of occurrence and magnitude of consequences does not automatically imply negative or undesirable effects caused by the hazard. It is also important to note that the various definitions of risk are interrelated and each of them has a certain advantage in different applications (e.g. Sayers et al., 2002; Merz et al., 2007) but they are not universally applicable. Each scientist agree on a risk definition according to his discipline and the application that is made (Kelman, 2003).

Although the majority of these approaches to risk consider the vulnerability and exposure to the hazard, they do not take into account the coping capacity of the exposed population. In this study, risk is defined as the hazard-related potential adverse effects and total economic loss expected in a region as a composite function of hazard, exposure, vulnerability and management ability (Davidson and Lambert, 2001).

### 2.1.3. Factors of risk

#### 2.1.3.1. Hazard

A hazard stands for a potentially damaging physical event, phenomenon or human activity that may cause the loss of life or injury, property damage, social and economic disruption or environmental degradation (ISDR, 2004). It can occur with different probabilities and magnitudes. For example, an infrastructure located in a floodplain may be damaged by a 10-year flood and 0.5 m water level as well as by a 50-year flood and 1.5 m water level. At some times,

hazard was ascribed the same meaning as risk, but it is now widely accepted that it is a component of risk and not risk itself (Cardona et al., 2012). Flood, earthquake, volcanic eruption are some examples of natural hazards.

#### 2.1.3.2. Vulnerability

In relation to hazard, vulnerability is broadly defined as the "potential for loss" (Mitchell , 1989) or the "the capacity to suffer harm and react adversely" (Kates, 1985). Depending on the research application, the term vulnerability has many definitions. For example, Cutter (1993) defined vulnerability as the likelihood that an individual or group will be exposed to and adversely affected by a hazard, whereas Alexander (1993) defined vulnerability as a function of the costs and benefits of inhabiting areas at risk from natural disaster. In some cases, vulnerability is defined as the characteristics of a person or group in terms of their capacity to anticipate, cope with, resist and recover from the impacts of natural hazard (Blaikie et al., 1994), and in others in terms of exposure, capacity and potentiality (Watts and Bohle 1993). According to the latter definition, measures to reduce vulnerability should reduce exposure, enhance coping capacity and minimize damaging consequences too.

In this study, vulnerability is defined as the conditions determined by physical, social, economic, and environmental factors or processes, which increase the susceptibility of a community to the impact of hazards (ISDR, 2004). Vulnerability to flood is considered as a combination of different types of vulnerabilities such as social, physical, economic and environmental. Social vulnerability focuses on the population, particularly the reaction, response and resistance of people to a flood event. Among the various characteristics which impact social vulnerability to environmental hazards, there are age, gender, education as well as densities, whether the population is rural or urban; livelihoods, family structure, access to medical services,

access to information, institutional capacity, etc. (Cutter et al., 2003). Physical vulnerability refers mainly to the type of house unit and the density of the population. People who are living in flood-prone areas with unplanned and weak houses are considered at higher flood risk than those who are living in formal settlements. In addition, when people are concentrated in a limited area, a flood hazard will have a greater impact than if people are dispersed (Bollin et al., 2003). Economic vulnerability stands for the susceptibility of an economic system, including public and private sectors, to potential disaster damage and loss (Rose, 2004; Mechler et al., 2010) and refers to the inability of affected individuals, communities, businesses, and governments to absorb the damage (Rose, 2004). Besides, Cardona et al. (2012) note that economic vulnerability to natural hazards has been inexactly defined in the literature and conceptualizations often have overlapped with risk, resilience or exposure. Environmental vulnerability includes environmental conditions and environmental degradation. For instance, the presence of forests increases the infiltration rate of the soil and reduces the overland flow which contributes to a reduced flood. Environmental degradation increases the intensity of natural hazards and is often the factor that transforms the hazard into a disaster (ISDR, 2004)

#### 2.1.3.3. Exposure and coping capacity

Exposure describes the people, the value of infrastructures and economic activities that will experience a natural hazard and may be adversely impacted by it (Bollin et al., 2003). Broadly, exposure refers to an inventory of elements in an area where hazard event may occur (ISDR 2004). It is worth noting that the literature mistakenly combines exposure and vulnerability but they are distinct because it is possible to be exposed to a hazard but not vulnerable (Cardona et al., 2012). For instance one can live in a floodplain and has sufficient means to modify building structure and behavior to reduce potential damages.

Coping capacity is defined as the "ability of people, organizations and systems, using available skills and resources, to face and manage adverse conditions, emergencies, or disasters" (ISDR, 2009). The strengthening of coping capacities usually builds resilience (capacity of an exposed systems or community to adapt by resisting) to withstand the effects of natural and human-induced hazards (ISDR, 2004). It is worth mentioning that the relationship between coping capacity and vulnerability is described in the literature by two schools of thought (IPCC, 2001; Bohle, 2001; Moss et al., 2001; Yodmani, 2001; Brooks et al., 2005; Gaillard, 2010): the first considers vulnerability as the lack of coping capacity while the second considers vulnerability and coping capacity as opposite so that increasing coping capacity leads to a reduced vulnerability and high vulnerability means low capacity.

## 2.2. Flood prediction methods in poorly gauged and ungauged basins

Flood risk is commonly estimated as a convolution of hazard, vulnerability and exposure (e.g. Granger et al., 1999; Davidson and Lambert 2001). The calculation of the different factors of risk can be performed separately in the first step but have to be combined for the final risk analysis (Apel et al., 2009). When calculating the hazard factor, one of the challenge is the estimation of the flood magnitude for different return periods (Apel et al., 2004; Merz and Thieken 2009). Generally, when sufficient observed data are available for the sites of interest, the estimation consists of fitting directly a probability distribution to the observed flow data. However, in many regions (e.g. Oti River Basin) there may be no observed discharge for the site of interest or the length of the time series is too short for accurate estimation of design floods. In this case, statistical and 'process-based methods' have been proposed to solve the problem of data scarcity. Statistical methods involve regression models, index flood method and geostatistical methods whilst process-based methods are composed of rainfall-runoff models and

derived distribution methods (Rosbjerg et al., 2013). According to the same authors, regression models find correlations between flood and catchment characteristics or/and its meteorological variables but this does not ensure a causal relationship. The typical regression model used to estimate flood at ungauged or site with short peak flow data uses the power model structure shown in Equation 2.1:

$$Q = aX_1^{c_1}X_2^{c_2} \ldots\ldots X_p^{c_p} \quad (2.1)$$

Where, $Q$ is the flood discharge (dependent variable), $a, c_1$ , $c_2$ , $c_p$ are the parameters of the regression model, $X_1$, $X_2$, $X_p$ are the catchment characteristics or/and its meteorological variables. Usually, the most important catchment characteristic is the drainage area and the other independent variables include slope, land use type. The meteorological variables considered for the regression model are generally the various forms of precipitations. The index flood method uses statistical analyses of peak flows at similar gauge sites to develop a flood frequency curve at ungauged sites. Geostatistics offer some means of describing the spatial variation of stream flows in a river basin and allow the estimation of flood discharge at ungauged sites. Two geostatistical methods such as ordinary kriging and topological kriging are used for this purpose. In contrast to the ordinary kriging, the topological kriging was developed by Skøien et al. (2006) to take into account both the area and the nested nature of the catchment. The topological kriging integrates a point variogram of runoff generation over nested catchments; whereas in the ordinary kriging flood data on the main stream and the tributaries are considered identically (Rosbjerg et al., 2013). Moreover, because rainfall time series are usually longer than the observed discharge time series, rainfall-runoff models are used to transform rainfall into flood discharge. This is done by first calibrating the hydrological model at a gauged site and then transferring the model parameters to ungauged sites via regression or similar basins (Rosbjerg et al., 2013). In addition,

according to Moores et al. (2006), distributed hydrological models can be calibrated to a gauged catchment and re-applied to a target ungauged site which is located in the catchment used for calibration. Finally, the rational method is the typical example of the derived distribution methods. According to McCuen et al. (2002), the rational method is based on five assumptions: (i) the rainfall intensity is constant over the storm duration; (ii) the rainfall is uniformly distributed over the catchment; (iii) the maximum discharge will occur when runoff is being contributed to the outlet from the entire catchment; (iv) the peak discharge equals some fraction of the rainfall intensity and (v) the catchment system is linear. The formula of the rational method is given by Equation 2.2 (Rosbjerg et al., 2013):

$$Q_T = C_T \, I_{T,tc} \, A \qquad (2.2)$$

where $C_T$ is the runoff coefficient, $I_{T,tc}$ the annual maximum rainfall intensity with a return period T averaged over duration $t_c$ which is the mean response time of the catchment , $A$ the catchment surface area and $Q_T$ the peak discharge of return period T. It is worth noting that the rational method should not be used for the estimation of floods for large river basins because the assumptions do not hold true in many cases. For instance, the catchment system is non-linear and the runoff rate within the catchment varies from place to place because of different soil properties and antecedent conditions. In addition, it is rare that the rainfall intensity remains constant during the duration of the storm and the runoff coefficient is independent of rainfall intensity as it is assumed in the rational method (http://www.engineeringcivil.com).

In flood frequency analysis, the return period is the average time between the occurrences of a flood whose magnitude is greater or equal to $Q_T$ over a long record. This means that a given flood $q$ of return period T may be exceeded once in T years. Hence, a relationship between the

probability of exceedance ($P(Q_T > q)$ of a flood and the corresponding return period is given by Equation 2.3:

$$P(Q_T > q) = 1/T \quad (2.3)$$

## 2.3. Methods of flood risk assessment.

A risk assessment is a methodology to determine the nature and extent of risk by analyzing potential hazards and evaluating existing conditions of vulnerability that could pose a potential threat or harm to people, property, livelihoods and the environment on which they depend (ISDR, 2004). Several methods have been used to assess flood risk.

### 2.3.1. Hydrologic and hydraulic approach

Many studies have used hydrologic and hydraulic models to analyze flood hazard for risk assessment. For instance, Mentzafou and Dimitriou (2015) used a hydrological and hydraulic models to perform flood risk assessment of the Pikrodafni catchment in Greece. The hydraulic model takes discharge data (among other input data) to simulate flood extent and depth. Due to the lack of discharge data during the flood event of interest (February 2013), the MIKE SHE hydrological model was used to retrieve the flood hydrograph of February 2013 which was used as input for a calibrated one dimensional hydraulic model (MIKE 11) to simulate the flood depth of February 2013 flood event. Then, the flood risk was assessed based on the simulated water depth. Ward et al. (2013) developed and validated a model cascade to assess flood risk at the global scale. The cascade include hydrological and hydraulic modelling, extreme value statistics, flood impact modelling and estimation of annual expected impacts. Because of the small time requiredfor the simulations and the good performance of the model cascade, the authors concluded that it could be used to carry out assessment of changes in flood risk.

### 2.3.2. Remote sensing and GIS approach

Remote sensing and Geographic Information System (GIS) are becoming the common methods for the delineation of flood zone for flood risk analysis. The direct use of radar satellite images for flood risk mapping was illustrated by Schumann and Di Baldassarre (2010) who generated an event-specific weighted hazard map based on flood area observation from satellite recorded event. Then, this map was fused with vulnerability-weighted land cover vector data in GIS environment to produce the flood risk map. Elkhrachy (2015) used a satellite image and GIS tools to produce flash flood hazard map for Najran city in Saudi Arabia. To achieve this goal, two different resolution digital elevation models (one from SPOT 5 satellite and the other from Shuttle Radar Topography Mission), a composite flood hazard index obtained from flood causative factors (runoff, soil type, surface slope, surface roughness, drainage density, distance to main channel and land use) were integrated in ArcGIS software to prepare a final flood hazard map for the study area; and the areas in high risk flood zones are obtained by overlaying the flood hazard index map with the zone boundaries layer. Safaripour et al. (2012) used Landsat ETM+ images and Digital Elevation Model (DEM) data to perform flood risk assessment for Gorganroud catchment in Iran. By overlaying and weighting layers of flood-prone areas in ArcGIS software, a map of flood hazard intensity was obtained by the authors. Next, by using obtained numbers and scoring, an overuse land ‘priorities’ map was generated. Then, these two maps were overlaid via a two-dimensional matrix and the final map of flood risk was obtained. Forkuo (2011) has developed a methodology for preparing flood hazard maps in Ghana, taking the Volta River Basin as case study. The ASTER imagery, topographic map covering the study area at a scale of 1:50000, the contours generated DEM, land cover and demographic data have

been used to create a district level map indicating flood hazard index for district scale using an 'additive' model which was adapted for this study.

### 2.3.3. Other methods

Other methods have been used to assess flood risk. Jiang and Tatano (2015) used a rainfall design for spatial flood risk assessment in the southern part of Osaka prefecture (Japan) by considering the relationship between response characteristics of many flood sources. First, rainfall data and basin information were collected and based on basin information, the flood assessment area was defined. Centered on the risk assessment area, the flood risk sources were traced and the concentration time from flood risk sources to flood risk assessment area were calculated. The concentration time of a flood is defined by the authors as the critical rainfall duration, in which rainfall, including peak rainfall, will form the flood peak volume. Moreover, rainfall time series were produced and divided into rainfall events using the interval time method. Then, the correlation of rainfall amounts with different critical rainfall durations such 1 h rainfall, 2 h rainfall and 3 h rainfall was estimated using the copula method. For each rainfall duration, a probability distribution was fitted. Next, the joint probability distribution was used to generate critical rainfall durations according to return periods. Finally, the generated correlated critical rainfall duration was used to produce rainfall events. Musungu et al. (2012) proposed a methodology of integration of community-based information into a GIS for flood risk assessment of an informal settlement in Cape Town (Republic of South Africa). First, a questionnaire was used to collect community-based information. The shack outlines of the informal settlement were digitized using aerial imagery. Next, the questionnaires were linked to the corresponding shacks in the GIS. Risk weights were subsequently calculated using pairwise comparisons for each household, based on their responses to the questionnaires. Then, the risk weights were mapped in

the GIS to show the spatialdisparities in flood risk. Guarín (2008) integrated local knowledge into GIS-based flood risk assessment of Triangulo and Mabolo communities in Naga city (Philippines). The methodology includes analysis of local community risk-related knowledge and perceptions, flood modelling approach, vulnerability analysis and assessment, as well as risk assessment. The community perception of flood in terms of water depth and flood duration was used as input into hydrodynamic modelling, using the SOBEK hydrodynamic software. Three scenarios with return period of 2, 10 and 20 years were modelled for past, present and future development situations. In addition, many aspects which determine the spatial vulnerability patterns found in the two communities were analyzed based on the results of participatory exercises. Factors that were taken into account are related to occupation, livelihood means, type of housing, land ownership, education, health status, quality of the environment, access to drinking water and services, development-related infrastructure and availability of assistance during flood event. Then, the vulnerability information was combined with hazard scenarios to perform both qualitative and quantitative flood risk assessment for the various flood scenarios.

# 3.MATERIALS AND METHODS

## 3.1. Description of study areas and datasets

The study area considered for the regional flood frequency analysis (see Figure 1.4) refers to the Volta Basin located in West Africa with geographic coordinates ranging from $5^0$W to $2^0$E longitude to $5^0$ N to $14^0$N latitude. It covers a total area of about 400,000 $km^2$ and it is drained by four main rivers namely Black Volta, White Volta, Oti and Main Volta Rivers (Figure 3.1). According to Amisigo (2005), the mean annual discharge of the Black Volta River near its source is around 0.4 $km^3$ , the mean annual discharge of the White Volta River is about 0.2 $km^3$ downstream of its source and the Oti River joins the Main Volta with a flow of about 12.7 $km^3$/year. In addition, the actual study sites are located upstream of the large Volta Lake created by the Akosombo Dam in Ghana.

Twenty three flow gauging stations were selected for the regional flood frequency analysis and the main criteria used to choose the sites were based on the length of record periods (minimum of thirteen years) and continuity (no consecutive gaps). In addition, only AMAX discharge data that are prior the operation of the important dams (Bagre and Kompiega) in the Volta Basin were selected. Specifically, they were obtained for the years 1950 -1973 for the White Volta and Black Volta from (Moniod et al., 1977) and for the years 1959 -1990 for the Oti River. The mean annual precipitation values for the sites of White and Black Volta Sub-basins were obtained from Moniod et al. (1977) while some mean annual precipitation values for the Oti River sub-basin were computed based on observed daily rainfall data. Table 3.1 and Table 3.2 show respectively the characteristics of the sub-basins (sites) and the inter-site correlation of the AMAX.

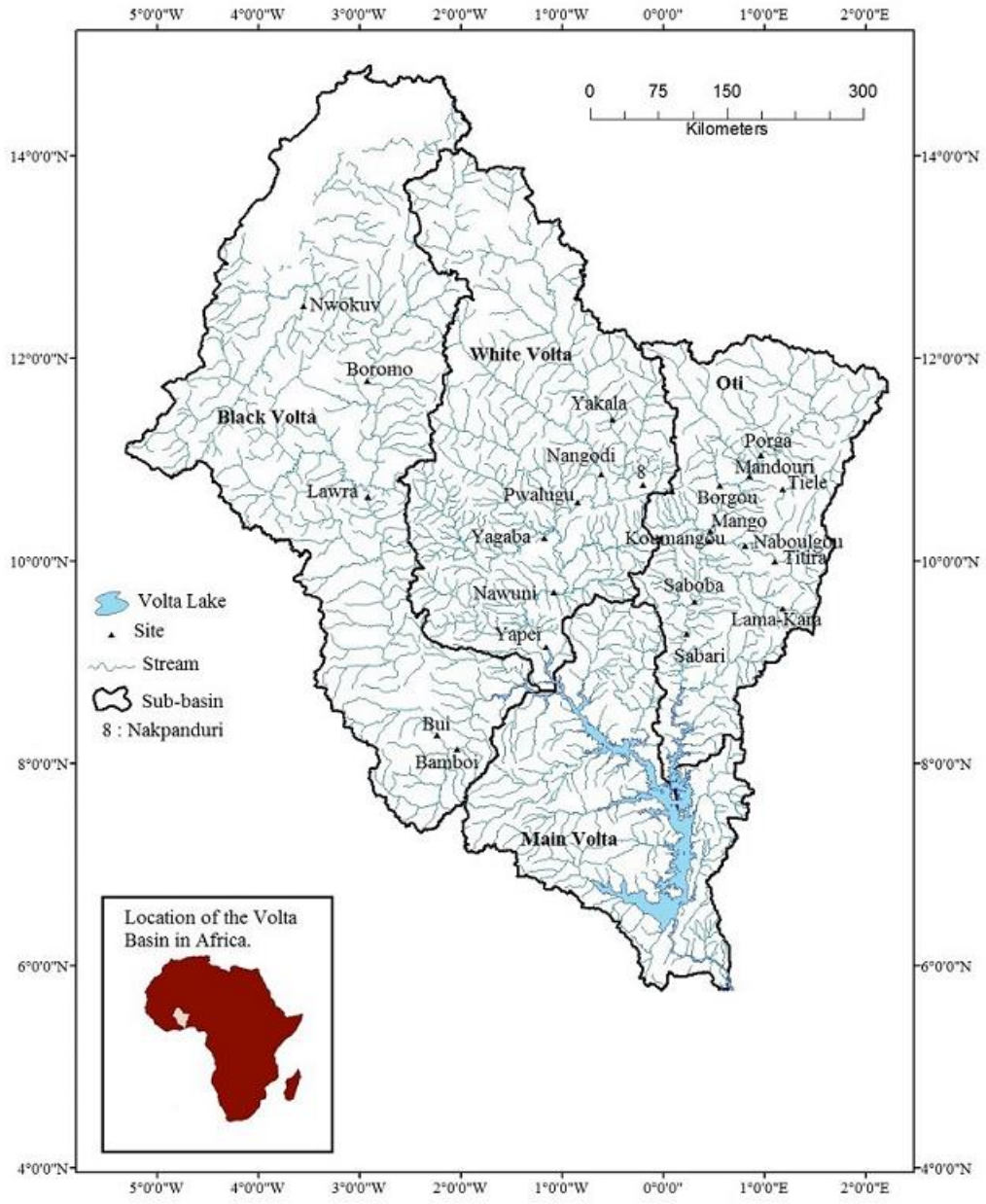


*Figure 3. 1.Location of flow gauge sites used for regional flood frequency analysis*

*Table 3. 1.Site characteristics used in the regional flood frequency analysis*

| Number | Site name | River | Area ($km^2$) | Mean slope (%) | Sample length (year) | L-cv | L-skew | L-kur |
|---|---|---|---|---|---|---|---|---|
| 1 | Nwokuy | Black Volta | 14 800 | 0.70 | 20 | 0.20 | 0.06 | 0.24 |
| 2 | Boromo | Black Volta | 35 000 | 0.40 | 19 | 0.15 | 0.01 | 0.06 |
| 3 | Lawra | Black Volta | 66 820 | 1.10 | 23 | 0.23 | 0.15 | 0.10 |
| 4 | Bui | Black Volta | 96 000 | 1.47 | 20 | 0.26 | 0.25 | 0.30 |
| 5 | Bamboi | Black Volta | 134 200 | 0.11 | 24 | 0.25 | 0.20 | 0.19 |
| 6 | Yakala | White Volta | 31 680 | 1.19 | 18 | 0.22 | -0.03 | -0.04 |
| 7 | Nangodi | Red Volta | 11 570 | 1.41 | 16 | 0.25 | 0.03 | 0.10 |
| 8 | Nakpanduri | White Volta | 1 530 | 1.47 | 15 | 0.23 | -0.05 | 0.04 |
| 9 | Pwalugu | White Volta | 63 350 | 1.09 | 16 | 0.22 | 0.00 | 0.07 |
| 10 | Yagaba | White Volta | 10 600 | 0.45 | 16 | 0.26 | -0.23 | 0.11 |
| 11 | Nawuni | White Volta | 92 950 | 1.05 | 21 | 0.13 | -0.31 | 0.20 |
| 12 | Yapei | White Volta | 102 170 | 1.11 | 17 | 0.19 | 0.04 | 0.09 |
| 13 | Tiele | Magou | 836 | 1.56 | 13 | 0.17 | 0.21 | 0.16 |
| 14 | Porga | Pendjari | 22 280 | 0.33 | 27 | 0.28 | 0.13 | 0.13 |
| 15 | Mandouri | Oti | 29 100 | 0.80 | 21 | 0.21 | 0.01 | -0.03 |
| 16 | Borgou | Sansargou | 2 280 | 0.99 | 28 | 0.31 | -0.03 | 0.06 |
| 17 | Mango | Oti | 35 650 | 0.33 | 37 | 0.32 | 0.23 | 0.07 |
| 18 | Titira | Keran | 3 695 | 0.89 | 26 | 0.31 | 0.06 | -0.04 |
| 19 | Naboulgou | Keran | 5 470 | 1.15 | 26 | 0.19 | 0.01 | 0.06 |
| 20 | Koumangou | Koumangou | 6 730 | 0.70 | 29 | 0.14 | -0.03 | 0.19 |
| 21 | Lama-Kara | Kara | 1 560 | 2.52 | 34 | 0.26 | 0.06 | 0.06 |
| 22 | Saboba | Oti | 53 090 | 1.44 | 32 | 0.24 | 0.11 | 0.01 |
| 23 | Sabari | Oti | 58 670 | 0.49 | 32 | 0.28 | 0.10 | 0.01 |

*Table 3. 2. Inter-site correlation of AMAX in the Volta River Basin*

| Stations | Periods | Inter-site correlation squared ($R^2$) |
|---|---|---|
| Nwokuy, Boromo | 1955 - 1973 | 0.19 |
| Boromo, Lawra | 1955 - 1973 | 0.06 |
| Lawra, Bui | 1954 - 1973 | 0.01 |
| Bui, Bamboi | 1954 -1973 | 0.01 |
| Yakala, Nangodi | 1958 -1973 | 0.10 |
| Nangodi, Nakpanduri | 1958 - 1972 | 0.37 |
| Nakpanduri,Pwalugu | 1958 - 1972 | 0.21 |
| Pwalugu, Yagaba | 1958 - 1973 | 0.00 |
| Yagaba,Nawuni | 1958 -1973 | 0.00 |
| Nawuni, Yapei | 1953 -1967 | 0.00 |
| Tiele, Porga | 1963 -1973 | 0.21 |
| Porga,Mandouri | 1963 -1979 | 0.00 |
| Mandouri,Borgou | 1960 -1979 | 0.00 |
| Borgou,Mango | 1960 -1987 | 0.00 |
| Mandouri,Mango | 1959 -1979 | 0.01 |
| Mango, Titira | 1962 -1987 | 0.11 |
| Titira, Naboulgou | 1962 -1987 | 0.62 |
| Naboulgou,Koumangou | 1962 -1987 | 0.00 |
| Koumangou, Lama-Kara | 1959 -1987 | 0.03 |
| Lama-Kara, Saboba | 1959 -1987 | 0.00 |
| Mango, Saboba | 1959 -1989 | 0.00 |
| Saboba, Sabari | 1959 -1990 | 0.71 |

The study area considered for the hydrological modelling (see Figure 1.4) refers to the Oti River Basin. The Oti River Basin is a sub-catchment of the Volta Basin which is one of the largest catchment in West Africa. The Oti River Basin is situated between latitudes 7° 33"N and 12° 23"N and longitudes 0° 34" W and 2° 20" E. It has an area of 72,778 $km^2$ and is shared by four countries: Togo (36%), Burkina Faso (28%), Ghana (22%), and Benin (14%).The Oti Basin represents 47% of the total area of Togo and covers mainly the northern and central parts of the country. The elevation of the basin ranges from 42 to 874m (Figure 3. 2).

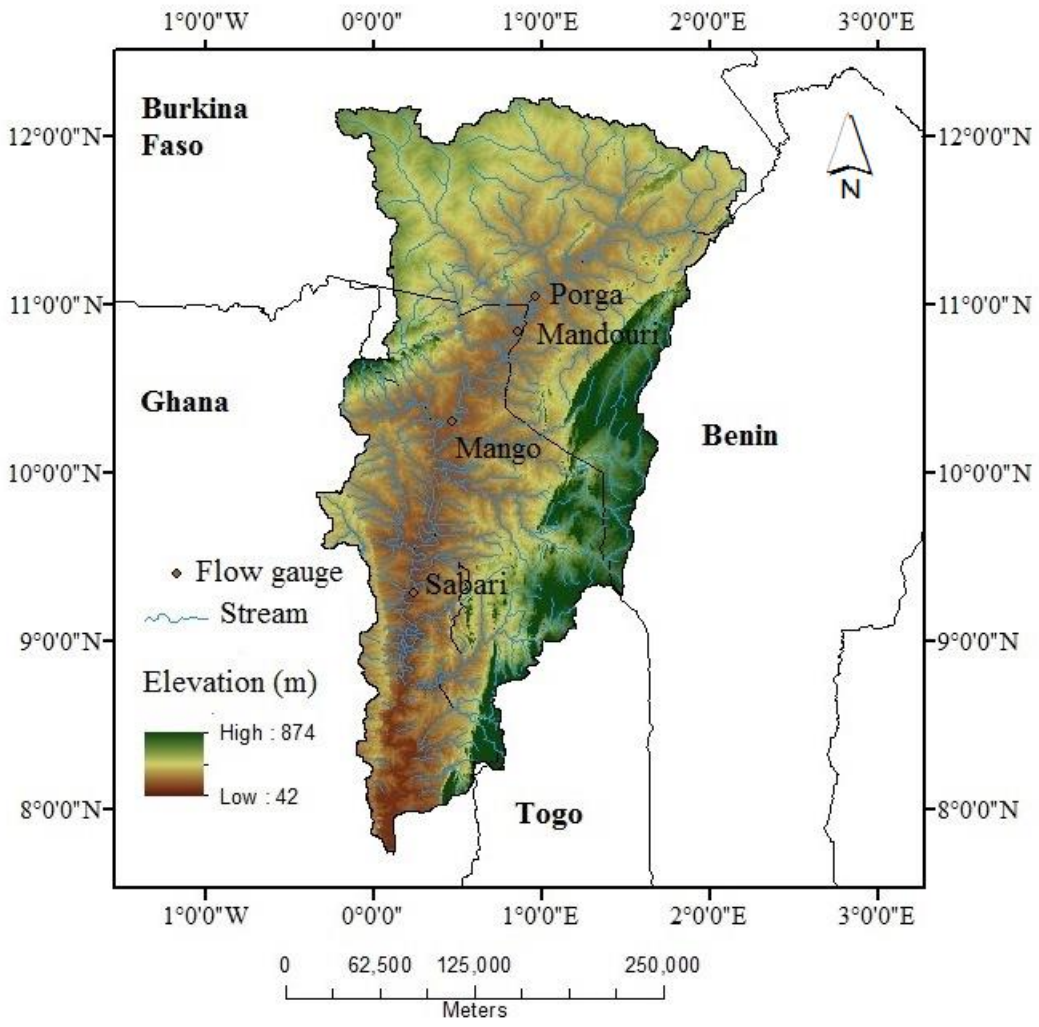


*Figure 3. 2.Location of the Oti River Basin: only the flow gauge stations at Porga (Benin) and Sabari (Ghana) are currently operating*

Moreover, remote sensing data and in-situ measurements were used in the hydrological modelling. The remote sensing products used for this study are daily rainfall at 0.250 grid resolution obtained from Tropical Rainfall Measuring Mission (TRMM), minimum and maximum temperature at 0.50 grid resolution obtained from Climate Research Unit (CRU), Digital Elevation Model (DEM) obtained from the SRTM, land cover/land use in 2000 from Landsat ETM+ (Figure 3.3) and Leaf Area Index from Satellite Application Facility (SAF).

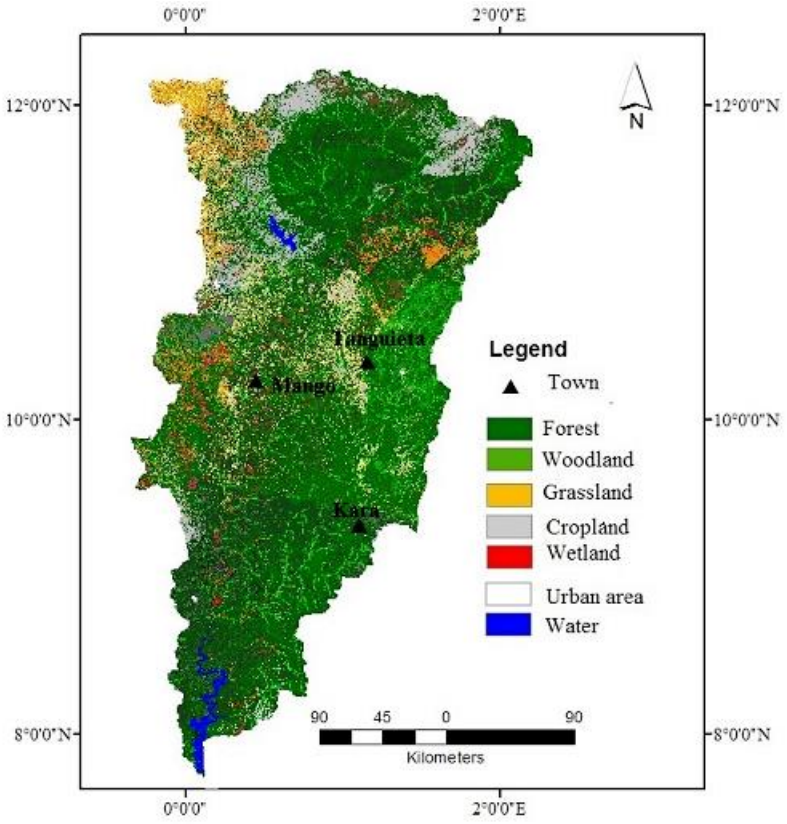


*Figure 3. 3. Land use/ land cover map of the Oti River Basin in 2000*

The in-situ data are observed daily discharge data which were obtained from national hydrological service of Ghana while observed daily rainfall data were obtained from the national meteorological services of Ghana and Togo. Figure 3.4 shows the observed daily discharges at Sabari gauge station and average gauged rainfall for the years 2005, 2006 and 2007.

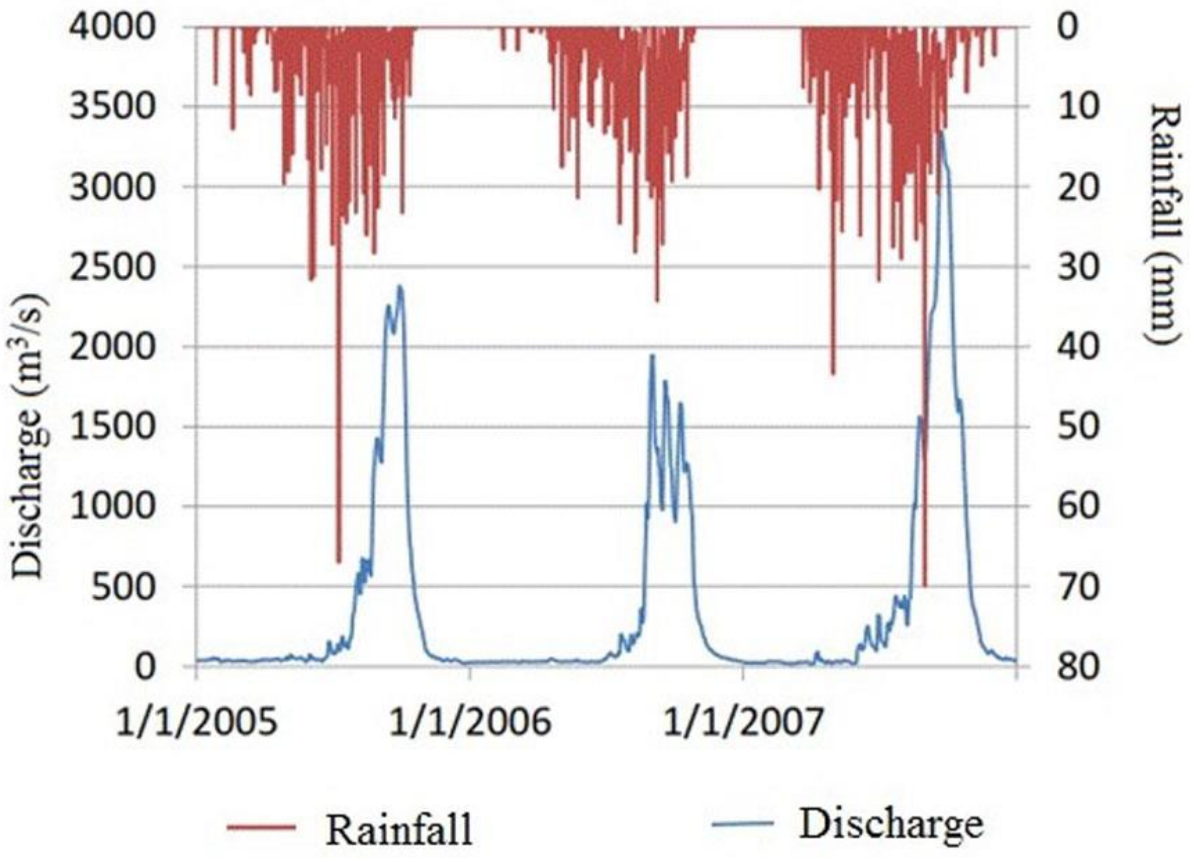


*Figure 3. 4.Observed discharge (blue) at Sabari gauge station and averaged gauged rainfall (red). [Source: national hydrological and meteorological services of Ghana and national meteorological service of Togo]*

In the flood hazard mapping (see Figure 1.4), we consider approximately 140 km of the Oti River starting from the Mandouri gauge station (Figure 3.5) and ending just downstream of Mango gauge station. The average width of the river in the study reach is 60 m and the model domain is between latitudes 10.20 and 10.84°N and longitudes 0.02 and 1.15°E. The study area is a rural catchment which is mainly characterized by agricultural land use with a range of floodplain elevation from 103 m to 559 m over the model domain (Figure 3.6 a). Figure 3.6b shows the observed extent of the severe flood in 2007 which was used for the calibration of the hydraulic model for the flood hazard mapping.

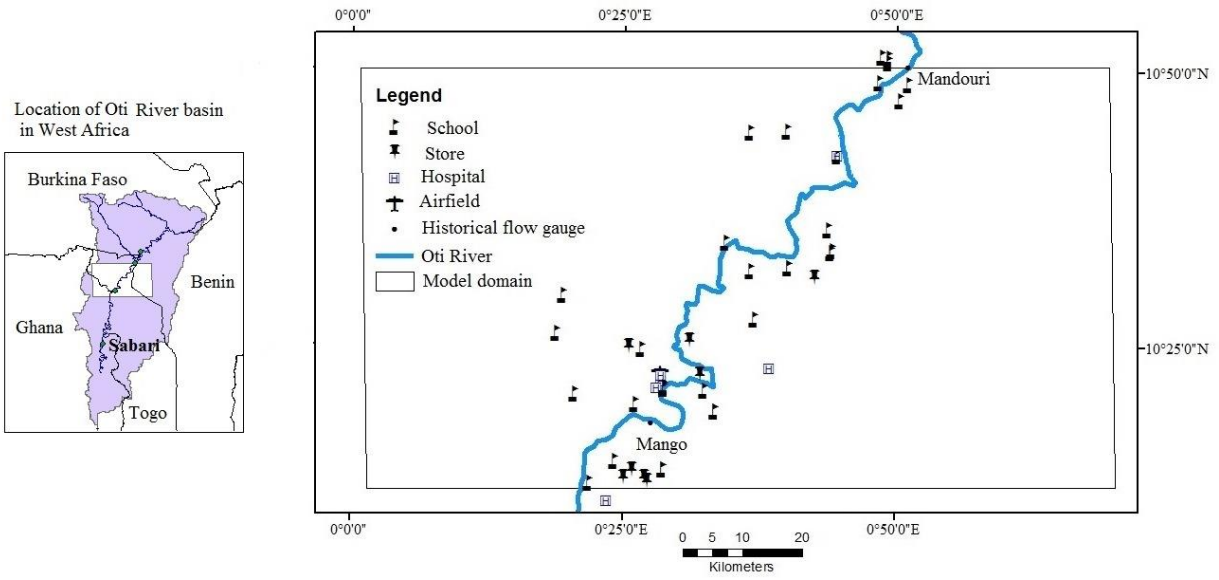


*Figure 3. 5.Location of the study area in the flood hazard mapping showing the model domain, main settlements along the Oti River in Togo and historical flow gauges.*

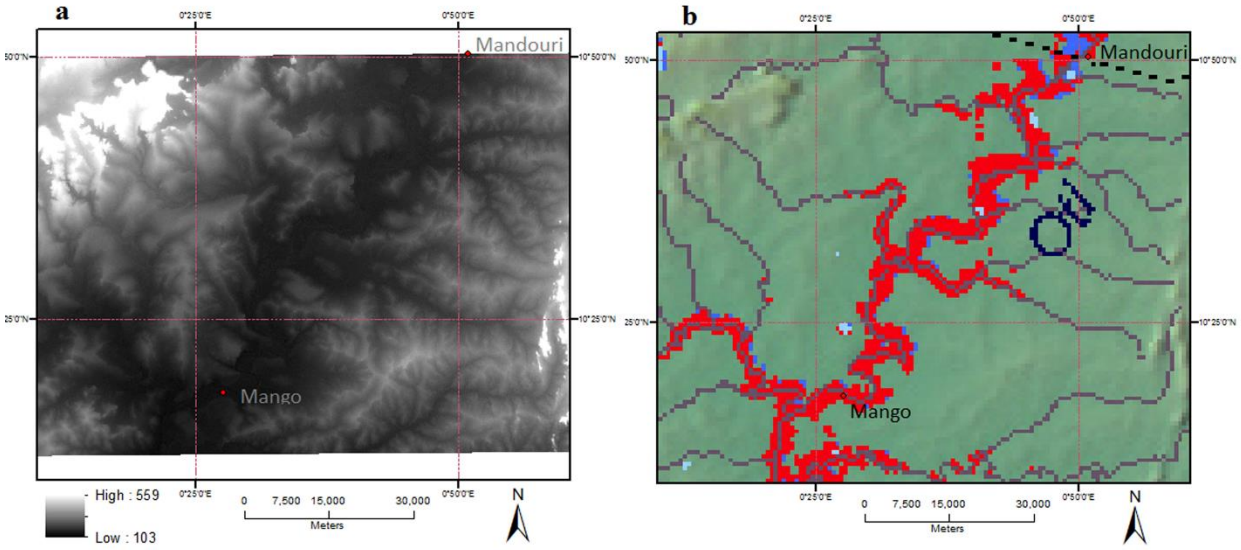


*Figure 3. 6.(a) Digital elevation model of the study site from SRTM and (b) Observed flood extent of the 2007 flood from NASA data (http://www.floodobervatory.colorado.edu) in red.*

The area of investigation for the community-based flood risk analysis (see Figure 1.4) refers to seven (7) communities of the Oti River Basin in Togo (Figure 3.7). The climate of this area is tropical semi-arid and is characterized by a rainy season starting from April to October with a mean annual rainfall between 900 and 1,100 mm and a dry season from November to

March. The livelihoods of the majority of the population in this study area are derived from subsistence farming livestock rearing and informal labor, all of which are threatened by the impacts of climate change. Most of the dwellings in the studied area are informal self-housing units, poorly planned and made of mud walls, wooden doors and windows. Consequently, many buildings collapsed from the force of the flood water. Despite the grave consequences of the 2007 flood in this area, people are still settling in the flood prone areas. With a poverty rate of more than 90 % (Table 3.3), these communities are the poorest in the country.

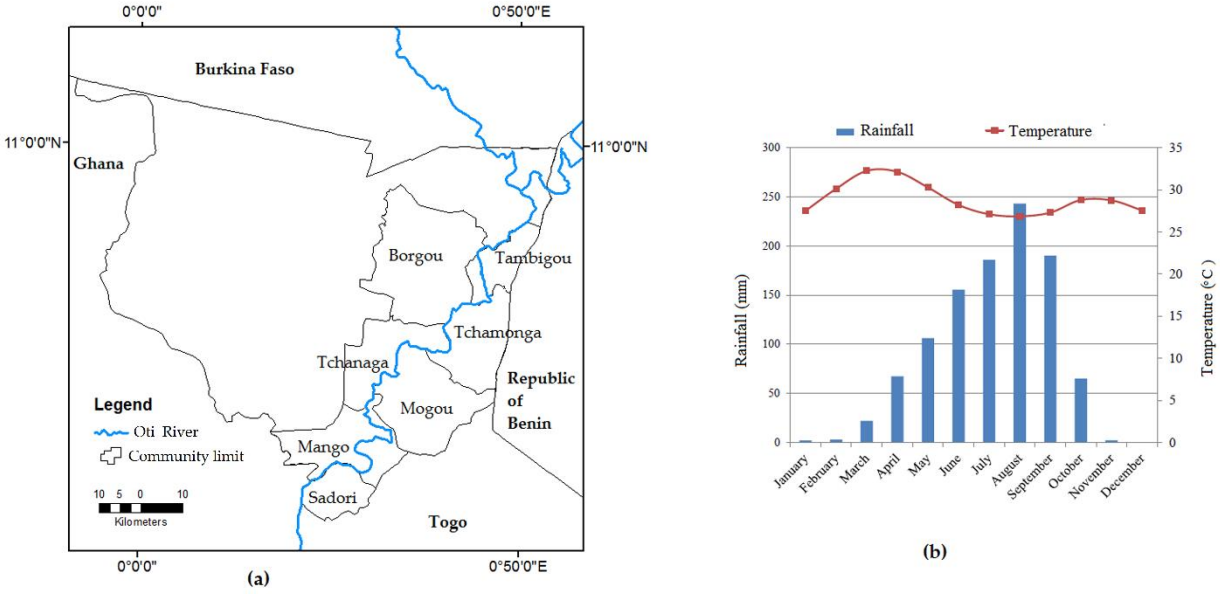


*Figure 3. 7.Location of the study area used in the community-based flood risk assessment.*

*Table 3. 3.Socio-economic characteristics of the selected communities.*

| Characteristics | Tambigou | Borgou | Tchamonga | Tchanaga | Mango | Mogou | Sadori |
|---|---|---|---|---|---|---|---|
| Density [1] (habitants per $km^2$) | 16 | 17 | 11 | 8 | 29 | 17 | 12 |
| Area ($km^2$) | 164 | 630 | 298 | 267 | 342 | 432 | 156 |
| Literacy level (%)[2a] | 25 | 21 | 18 | 31 | 81 | 22 | 31 |
| Poverty level (%)[1] | 96.7 | 96.3 | 95.9 | 95.8 | 40.8 | 96.2 | 96.5 |
| Area under forest (% of total area) | 21 | 9 | 8 | 24 | 30 | 18 | 71 |
| Rate of access to safe drinking water (%)[1] | 7.8 | 10.8 | 42.6 | 1.5 | 84.1 | 39.1 | 2.3 |
| Area prone to flood (% of total area) | 25 | 12 | 19 | 24 | 29 | 18 | 38 |
| Number of housing units[1] | 818 | 3,441 | 1,031 | 582 | 2,808 | 2,309 | 459 |

## 3.2. Methods

In this study, four (4) main methods were used, including regional flood frequency analysis, hydrological modelling, flood hazard mapping and integrated flood risk assessment.

### 3.2.1. Regional flood frequency analysis

#### 3.2.1.1. L-moment approach

L-moments are improvements over ordinary product moments of characterizing the shape of a frequency distribution and estimating the parameters of this distribution, especially for small size of environmental data. L-moments were developed by Hosking (1990) to facilitate the

[1] Source: DGSCN, 2010
[2] Source: Coulombe et al., (2011).
**a :** literacy level is defined as the percentage of adult population that can read and write.

estimation process in frequency analysis. According to the author, they are able to characterize a large number of distributions and are more robust to the presence of outliers in the data and are less biased for short streamflow data. Basically, L-moments are defined as a linear function of the probability weighted moments (PWMs) which were introduced by Greenwood et al. (1979). A PWM of a frequency distribution is given by Equation 3.1:

$$\beta_r = E[x\{F(x)\}^r] \quad (3.1)$$

where $\beta_r$ is the $r^{th}$ PWM , F($x$) is the cumulative distribution function of the random variable $x$, and $r$ =0,1,2,… is a positive integer. L-moments are a linear combination of PWMs (Hosking, 1990) and the $(r + 1)^{th}$ L-moment of a distribution ($\lambda_{r+1}$ ) is defined as shown in Equation 3.2:

$$\lambda_{r+1} = \sum_{k=0}^{r} P_{r,k}^{*} \ \beta_k \quad (3.2).$$

With $P_{r,k}^{*}$ given by equation (3.3):

$$P_{r,k}^{*} = (-1)^{r-k}\binom{r}{k}\binom{r+k}{k} \quad (3.3)$$

In the case where r=0, $\lambda_1$ is the mean of the distribution. When r=1, $\lambda_2$ is the scale measure of the distribution while $\lambda_3$ and $\lambda_4$ are measures of skewness and kurtosis for r equal to 2 and 3 respectively. In RFFA based on L-moments, L-moment ratios of a distribution are defined by $\tau_r = \lambda_r/\lambda_2$ and can be estimated by $t_r = l_r/l_2$ (Hosking, 1990); $t_r$ is the $r^{th}$ sample L-moment ratio while the L-moments of a sample are given by Equation 3.4:

$$l_{r+1} = \sum_{k=0}^{r} P_{r,k}^{*} \ b_k \quad (3.4)$$

$b_r$ is given by Equation 3.5:

$$b_r = n^{-1} \sum_{j=1}^{n} \frac{(j-1)(j-2)\ldots(j-r)}{(n-1)(n-2)\ldots(n-r)} x_j \quad (3.5)$$

where $x_j$, for $j$ = 1,. . . , $n$ is the ordered sample and $n$ is the sample size. Specifically, the sample L-coefficient of variation (L-cv) is t =$l_2/l_1$ while the sample L- coefficient of skewness (L-skew)

is $t_3 = l_3/l_2$ and the sample L-coefficient of kurtosis (L-kur) is $t_4 = l_4/l_2$ (Hosking and Wallis, 1997).

#### 3.2.1.2.Data screening

In order to check for errors in the data, outliers and trends, discordancy measure $(D_i)$ for a site $i$ as shown in Equation 3.6 was applied to AMAX series of 23 gauge stations in the Volta Basin. The critical value of $D_i$ depends on the number of sites (N). For N≥15, $D_i$ must be less than or equal to 3.0 for the site to be considered in the regional frequency analysis. Otherwise, it is deleted from the dataset (Hosking and Wallis, 1997).

$$D_i = \frac{1}{3} N(U_i - \overline{U})^T [(U_i - \overline{U})(U_i - \overline{U})^T]^{-1}(U_i - \overline{U}) \quad (3.6)$$

Where U is the vector of L-moments and N is the number of sites. $\overline{U}$ is an average of U .

#### 3.2.1.3.Identification of homogeneous groups

##### *3.2.1.3.1. Formation of clusters*

The aim of the cluster analysis is to partition data into clusters in a way that sites belonging to the same cluster are similar regarding their climatic/physiographic characteristics. In this study, Ward's algorithm (Ward, 1963) was used to form clusters with respect to the mean slope and drainage area of the basins because this method is able to produce homogeneous clusters which have approximatively the same size. Ward's method is a hierarchical clustering which uses the increase in the total within-group sum of squares as a result of joining groups. The application of the hierarchical clustering was based on the standardized Euclidean distance (d) which is given by Equation 3.7 (Ouarda et al., 2007):

$$d^2(p,q) = (x_p - x_q) D^{-1} (x_p - x_q)^T \quad (3.7)$$

Where $x_p$ and $x_q$ are the coordinates of sites $p$ and $q$ in the physiographic space, $D^{-1}$is a diagonal matrix. Since the variables are expressed in different units, each coordinate in the sum of squares is inverse weighted by the sample variance of that coordinate in order to eliminate the scale effects between the variables (Ouarda et al., 2007). In addition, the within-group sum of squares (GSS) of a cluster is defined as the sum of the distance between all objects in the cluster and its center of gravity. It can be expressed by Equation 3.8 (Ouarda et al., 2007):

$$GSS_r = \sum_{i=1}^{n_r} d^2(x_{ri} - \overline{x}_r) \quad (3.8)$$

Where $n_r$ and $\overline{x}_r$ are respectively the size and the centroid of cluster *r*.

According to Hosking and Wallis (1997), the results from the cluster analysis need not, and usually should not, be final. Many kinds of subjective adjustment of groups may be useful to improve the homogeneity of the clusters. In this study, a few sites were moved from one cluster to another and one site was deleted after the cluster analysis in order to improve the homogeneity of the groups.

#### 3.2.1.3.2. *Homogeneity test*

To identify the homogeneous groups, a homogeneity test was first applied to the Volta River Basin as a single region and secondly to clusters. The principle of the homogeneity test is to compare the observed variations in L-moments ratios for the sites in each region with the ones that would be expected for a homogeneous region (Hosking and Wallis, 1997). The variations in L-moments are computed as the standard deviation of at site L-cv weighted proportionally to the data length at each site. In order to ascertain what would be the variation in L-moments ratios for

a homogeneous region, the four parameter kappa distribution was fitted to the regional average L-moment ratios to generate a large number (greater than or equal to 500) of Monte Carlo simulations. The kappa distribution was chosen because it is a generalized distribution that produces many distributions as particular cases of the parameter values (Hosking and Wallis, 1997). The heterogeneity measure, $H_j$ (j=1, 2, 3) is given by Equation 3.9:

$$H_j = \frac{V_{j-}\mu_{v_j}}{\sigma_{v_j}} \tag{3.9}$$

Where $H_1$ is the heterogeneity measure based on observed $V_1$ which is the weighted standard deviation of t values, $H_2$ is the heterogeneity measure based on observed $V_2$ which is the weighted standard deviation of ($t/t_3$) distance, $H_3$ is the heterogeneity measure based on observed $V_3$ which is the weighted standard deviation of ($t_3/t_4$) distance, $\mu_{v_j}$ and $\sigma_{v_j}$ are mean and standard deviation of the simulated values of $V_j$. According to Hosking and Wallis (1997), a group is "acceptably homogeneous" if $H_j$ <1, "possibly heterogeneous" if 1≤ $H_j$ <2 and "definitely heterogeneous" if $H_j \geq 2$.

#### 3.2.1.4. Selection of appropriate distributions

The next step after the formation of homogeneous groups is to choose the best distribution for each homogeneous group. The selection of the distribution that will yield the accurate quantiles was thus carried out in this work by first applying the L-moment diagram methods to the homogeneous groups. Secondly, a numerical goodness of fit test and quantile-quantile plots were used to validate the choice. Five three-parameter distributions namely the Generalized Logistic distribution (GLO), the Generalized Extreme Value distribution (GEV), the

Generalized Pareto distribution (GPA), the Generalized Normal distribution (GNO) and the Pearson type III distribution (PE3) were considered in this study.

#### *3.2.1.4.1. L-moment ratio diagrams*

L-moment ratio diagrams were used to choose the suitable flood frequency distribution. In L-moment ratio diagrams, the sample L-skewness versus the sample L-kurtosis are plotted on a graph with the theoretical L-moment ratios of the candidate distributions. On these diagrams, a three- parameter distribution is plotted as a line and the best distribution is the one whose line is closer to the majority of the sample data. Nevertheless, the graph may not have a good power of discrimination when many probability distributions are suitable for the sample data in L-moment ratio diagrams. For this reason, a numerical test called Z-statistic was further applied to choose the best frequency distributions

#### *3.2.1.4.2. Z-statistic*

The Z-statistic, developed by Hosking and Wallis (1997) was used to select the best frequency distributions. This test is based on the comparison between sample L-kurtosis and population L-kurtosis for the selected theoretical distributions. The test statistic called $Z^{Dist}$, is defined in Equation 3.10 as follows:

$$Z^{Dist} = \left(\tau_4^{Dist} - t_4^R + B_4\right)/\sigma_4 \tag{3.10}$$

Where $D_{ist}$ refers to a particular distribution, $\tau_4^{Dist}$is the L-kurtosis of the selected distribution, $t_4^R$ is the regional weighted average of sample L-kurtosis, $B_4$ and $\sigma_4$ are respectively the bias of $t_4^R$ and the standard deviation of sample L-kurtosis. (Hosking and Wallis, 1997). For each of the groups, a kappa distribution with its parameters estimated from the fitting of the

distribution to theregional average L-moments ratios was used to simulate a large number of realizations for the same region. The frequency distribution which has the smallest absolute $Z^{Dist}$ is chosen as the best among other possible frequency distributions. At a confidence level of 90 %, the critical value of absolute $Z^{Dist}$ is 1.64 (Hosking and Wallis, 1997).

#### *3.2.1.4.3. Quantile-quantile plot*

In order to check the validity of the estimates provided by a fitted theoretical distribution, quantile-quantile plots were used to compare the estimated quantiles and the observed flood values. The empirical estimates were obtained using Gringorten formula shown in Equation 3.11 because it is considered as the best formula in use among the plotting position formulae (Shaw et al., 2011)

$$F = \frac{(\mathrm{j}-0.44)}{(\mathrm{N}+0.12)} \qquad (3.11)$$

Where F is the non-exceedance probability, j is the rank (1, 2, 3…..N) and N is the total number of data points.

### 3.2.1.5.Development of regional growth curves

In a regional flood frequency analysis using the index flood approach, a relationship is established between a flood quantile of a given return period ($Q_T$), and an index flood (taken as the mean AMAX series, $Q_m$ ) by introducing a regional growth curve ( $q_R$ ). This relationship is shown in Equation 3.12:

$$Q_T = q_{R*}Q_m \qquad (3.12)$$

T is the return period. Moreover, $q_R$ depends only on the parameters of the frequency distribution and the return periods. For instance, $q_R$ for the GPA distribution is given in Equations 3.13 and 3.14 while Equations 3.15 and 3.16 show the expressions of $q_R$ for the GEV distribution.

$$q_R = \varepsilon + \frac{\alpha}{k}\left[1 - \left(\frac{1}{T}\right)^k\right] \text{ for } k \neq 0 \quad (3.13)$$

And

$$q_R = \varepsilon - \alpha log\left(\frac{1}{T}\right) \text{ for } k = 0 \quad (3.14)$$

$$q_R = \varepsilon + \frac{\alpha}{k}\left\{1 - \left[-log\left(\frac{T-1}{T}\right)\right]^k\right\} \quad \text{for } k \neq 0 \quad (3.15)$$

$$q_R = \varepsilon - \alpha\left\{log\left[-log\left(\frac{T-1}{T}\right)\right]\right\} \quad \text{for } k = 0 \quad (3.16)$$

Where, $\alpha, \varepsilon, k$ are respectively the scale, location and shape parameters of the distributions.

#### 3.2.1.6.Development of prediction equations for the mean annual flood

In order to estimate the flood quantile for a given return period, the value of the index flood ($Q_m$) is needed. Because of the dearth of observed discharges at the ungauged basin, $Q_m$ cannot be calculated. In this case, a regression model between $Q_m$ and physiographic or climatic basin descriptors such as the drainage area, slope, altitude, mean annual precipitation (depending on data availability) is often used to estimate the index flood at ungauged sites. Usually, the study area is split into regions which are not necessarily homogeneous (Rosbjerg et al., 2013). In this study, regression models were estimated separately for the White and Black Volta Basins and the Oti Basin. Furthermore, a stepwise multi regression with the forward selection method has been used to choose the best regression model. This method adds one

independent variable at a time which increases the coefficient of determination ($R^2$) value of the regression. The drainage area (A), the slope (S) and the mean annual rainfall (P) were considered in this study (Appendix 3.1).

### 3.2.2. Hydrological modelling for flood prediction

#### 3.2.2.1.Description of LISFLOOD hydrological model

LISFLOOD is a distributed hydrological model which is developed by the Joint Research Center of the European Commission (Van der Knijff and De Roo, 2008). Apart from the hydrological processes, the model simulates flood, climate and land use changes impacts in large river basins. LISFLOOD is designed to be run at any temporal and spatial resolution but the authors recommend its application at a spatial resolution comprised between 100 m and 10 km (Van der Knijff and De Roo, 2008). In addition, the model is implemented in the PCRaster environmental modelling language (Van Deursen and Wessling, 2009) and wrapped in Python based interface. Figure 3.8 gives an overview of the structure of LISFLOOD model. One can note that, at the surface the important processes simulated by the model are interception and potential evapotranspiration. The rainfall intercepted by the vegetation is simulated through the method of Von Hoyningen-Huene for all land use except forests which are simulated using the method of Shuttleworth and Calder (Van der Knijff and De Roo, 2008). In the soil, LISFLOOD computes the vertical transport of water in two soil layers. The percolation to the groundwater, storage of groundwater and lateral subsurface flow are simulated by the model. Vertical transport of water in the two soil layers is simulated by the Richard's equation while the lateral flow and percolation to the groundwater store is calculated using the Darcy's method (Van der Knijff and De Roo, 2008). The main meteorological inputs of the model are represented by the precipitation

(P), the evapotranspiration rate of a closed canopy ($ET_0$), the evaporation rate from a bare soil surface (ES0) and potential evaporation rate from an open water surface (EW0)

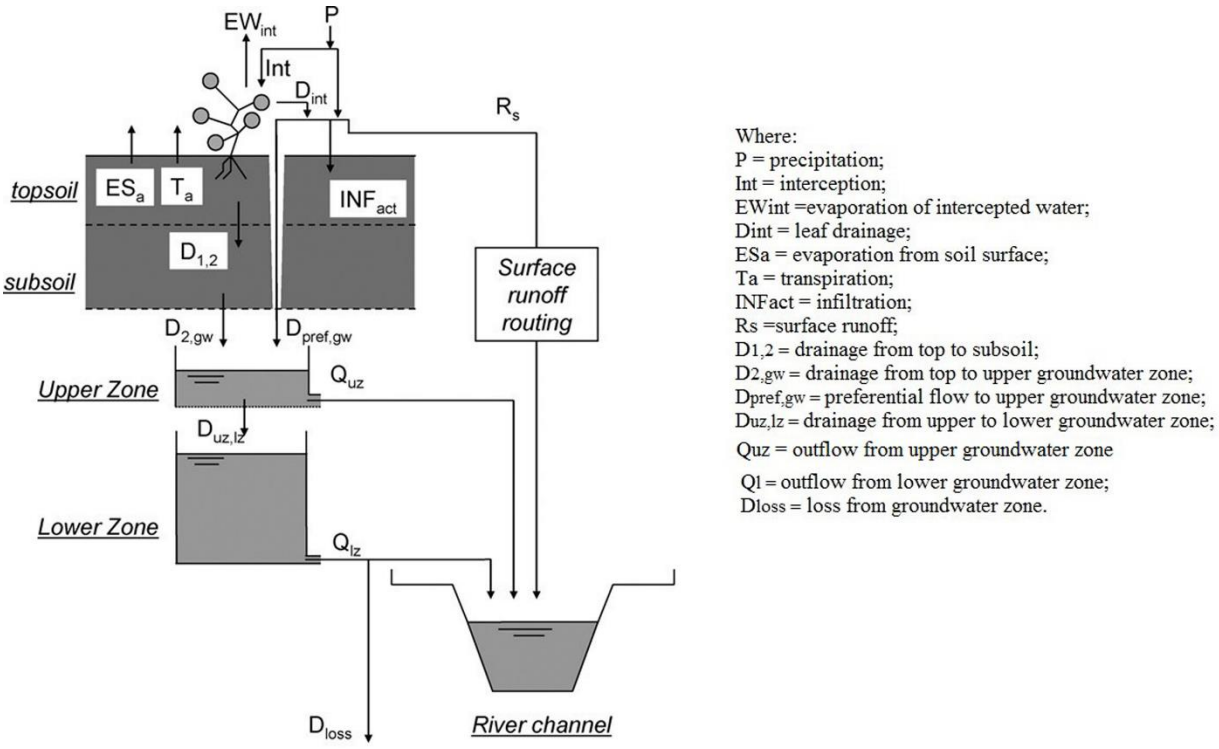


*Figure 3. 8.Schematic representation of LISFLOOD hydrological model (source: Van der Knijff and de Roo, 2008)*

#### 3.2.2.2.Data preprocessing

The input data used in LISFLOOD hydrological model are characterized by their spatial and temporal resolution, format and coordinate system. Apart from the soil and vegetation parameters, all the LISFLOOD input variables should be provided as PCraster maps. Hence, the input data were converted to PCraster maps with the same spatial (5km x 5 km) and temporal (daily) resolutions and a WGS 1984 UTM zone 31 N coordinate system. The following sections

describe the various techniques used in the data preparation. Detail information on PCraster can be obtained from Van Deursan and Wessling (2009).

#### *3.2.2.2.1. TRMM rainfall data processing*

Rainfall is the most important meteorological forcing in hydrological modelling. Rainfall can be estimated from rain gauges or radar. Even though rain gauge rainfalls are the most accurate data, they lack the appropriate spatial distribution to be used in a raster based distributed model. In this study, TRMM daily rainfall data were obtained on NetCDF format. Then, the TRMM NetCDF format files were extracted and converted to a text format files using 'R software' applications. In order to reduce volume errors during the simulation, corrections factors were first applied to the TRMM daily rainfall data. The correction factor ($C_F$) was computed as the ratio between the total rainfall ($P_i$) at meteorological stations and total TRMM rainfall ($R_i$) of the grids which correspond to each meteorological station. $C_F$ is given by Equation 3.17 (Hingray et al., 2009):

$$C_F = \sum_i^n P_i / \sum_i^n R_i \qquad (3.17)$$

Where *n* is the number of meteorological stations and *i* the station.

After correcting the satellite rainfall data, they were interpolated to 5 km resolution and converted to PCraster format using an inverse distance weighting method implemented in a geostatistical module of PCraster software. The following command syntax (Pebesma, 2014) was used:

1. *data (Rainfall): 'Rainfall.txt' ,x=1, y=2, v=3;*
2. *mask: 'maskOti.map';*
3. *predictions (Rainfall): 'Rainfall.map';*

The first line defines the data that is read for the variable *Rainfall*. The second line indicates the location map where the interpolation will be made. The third line generates the output PCraster map of the interpolated *Rainfall*.

#### *3.2.2.2.2. Potential evapotranspiration data processing*

Potential evapotranspiration is another component of catchment water balance. In the approach of LISFLOOD hydrological model, three types of potential evaporation are considered: (i) reference evapotranspiration (ETo), (ii) potential evaporation from a bare soil surface (ES0) and (iii) potential evaporation of open water surface (EW0). Reference evapotranspiration is 'the rate of evapotranspiration of a hypothetical reference crop with an assumed crop height of 1.2 m, a fixed surface resistance of 70 $sm^{-1}$ and an albedo of 0.23, closely resembling the evapotranspiration from an extensive surface of green grass of uniform height, actively growing, well-watered and completely shading the ground '( Allen et al., 1998). Due to the lack of the required weather data to compute ETo ($mm.day^{-1}$) using the Penman-Monteith equation (classical method to estimate ETo), the reference evapotranspiration was estimated in this study using the Hargreaves equation shown in Equation 3.18:

$$ET_o = 0.0023\ (T_{mean} + 17.8)(T_{max} - T_{min})^{0.5}\ R_a \qquad (3.18)$$

With respectively the daily mean temperature, the daily maximum temperature, daily minimum temperature and extraterrestrial radiation. The ETo values were further interpolated and converted to input PCraster maps using the command syntax described in section 3.2.2.2.1. In this research, EW0 ($mm.day^{-1}$) was estimated using the concept of pan evaporation which is linked to the reference evapotranspiration by a pan coefficient (Maidment, 1992). Taking EW0 as the pan evaporation, the evaporation from open water surface is given by Equation 3.19:

$$EW0 = {ET_o}/{K_{pan}} \quad (3.19)$$

Where ETo and $K_{pan}$ are respectively the reference evapotranspiration and the pan coefficient. The value of depends on the relative humidity and the wind speed of the study area. It is equal to 0.85 when the relative humidity is between 40-70 % and the wind speed is in the range of 2 -5 m/s (Allen et al., 1998). These characteristics apply to the Oti River Basin which has a wind speed and relative humidity respectively between 2 -4 m/s and 40-80% (Moniod et al., 1977). In this study, the potential evaporation from a bare soil was estimated using an empirical relation between ES0 and ETo suggested by Allen et al. (1998) and shown in Equation 3.20:

$$ESO = K_e \, ETo \quad (3.20)$$

Where ES0 is the potential evaporation from bare soil and $K_e$ the soil evaporation coefficient. The value of $K_e$ depends on the soil moisture. When the topsoil is wet, following rain or irrigation, $K_e$ is maximal and evaporation from the soil occurs at the maximum rate. When the soil surface is dry, $K_e$ is small and even zero when no water remains near the soil surface for evaporation (Allen et al., 1998). Based on examples given by Allen et al. (1998), the values of 0.17 and 0.81 were used respectively for the dry and wet seasons of the year.

#### *3.2.2.2.3. Creation of leaf area index PCraster maps*

Leaf Area Index (LAI) is an essential input for LISFLOOD hydrological model. It is used in the estimation of evaporation of intercepted water and evapotranspiration. In this study, monthly LAI values of the study area were obtained from SAF (http://Landsaf.meteo.pt), interpolated to 5 km spatial resolution and converted to PCraster maps.

#### 3.2.2.2.4. Creation of elevation input maps

The SRTM DEM of approximately 90 m spatial resolution was first resampled to 5km spatial resolution and converted to ASCII files using ArcGIS software. Then, a PCraster map of the DEM was created using the PCraster function "asc2map". In addition, a mask map, local drain direction map and channel geometry maps (channel bottom width map, channel side slope map, channel gradient map, channel length map, channel Manning's roughness coefficient and channel bank full depth map) were created using appropriate functions in PCraster application

#### *3.2.2.2.5. Creation of land use, soil classes and soil depth PCraster maps*

The input PCraster maps of land use (land cover, urban fraction, forest fraction) were produced after resampling the collected land cover map and reclassifying it via ArcGIS according to the Corine land cover 2000 classification (Bodis et al., 2009). Input PCraster maps related to soil texture was created using the Harmonized World Soil Database (HWSD) and numeric codes applied to soil type in LISFLOOD. The soil depth PCraster map was obtained using the Equation 3.21 as suggested by De Roo and Schmuck (2002) in cases where accurate soil depth data are not available for the study area.

$$SD.map = \max (300 - S.map * 290 - Dem.map /7, 30) \quad (3.21)$$

Where SD. map is the soil depth map, S. map is the mean slope map and Dem. map is the elevation map. Finally, tables of soil and vegetation parameters were created.

#### *3.2.2.2.6. Tables of soil and vegetation parameters*

Parameters of each soil class (saturated and volumetric soil moisture content, pore size index and saturated hydraulic conductivity) were computed from Maidment (1992) and HWSD (Viewer version 1.2). The Manning's roughness coefficient, crop group number, and routing depth for each land cover classes were taken respectively from Kalyanapu et al. (2009), Maidment (1992) and Allen et al. (1998)

### 3.2.2.3. Model setup

The setup of LISFLOOD hydrological model includes the organization of the input files (PCraster maps and tables) and output files, preparation of the setting file and initialization of the model. The classification of the input PCraster maps and tables are shown in Appendix 3.2. According to Van der Knijff and De Roo (2008), all the files in the hydrological model are organized by default as follow:

- all maps are in one directory (e.g. maps);
- all tables are in one directory (e.g. tables)
- all meteorological inputs maps are in one directory (e.g. meteo);
- all LAI maps are in one directory (e.g. lai);
- all the outputs are saved in one directory (e.g. outs).

#### *3.2.2.3.1. The settings file*

The settings file is an XML (Extensible Mark-up Language) file in which all input files and parameters required by LISLOOD are specified. The aim of the settings file is to connect variables and parameters in the model to input/output files and numerical values. The settings file can also be used to specify many options in the modelling process (Van der Knijff and De

Roo, 2008). In this study, the settings file was created by editing the template provided with LISFLOOD package.

#### *3.2.2.3.2. Initialisation of the model*

During the simulation, LISFLOOD requires some estimates of the initial state variables. In this study, the state of the soil at the beginning of the simulation is not known. So, a 'warm-up' period of one year prior to each simulation was applied. In addition, and as suggested by Van der Knijff and De Roo (2008), the initial amount of water on the soil surface, interception storage and storage in the upper groundwater zone were set to zero at the start of the simulation. For the remaining state variables (initial soil moisture content of topsoil and subsoil, initial water in lower groundwater zone and initial cross-sectional area of water in channels) , LISFLOOD hydrological model provides the possibility to initialize them internally by setting each of the variables to a value of '-9999'.

### 3.2.2.4.Calibration and validation of the model

Model calibration is the process of adjusting the model parameters in order to reduce the errors between model output and observed data. According to Van der Knijff and De Roo (2008), LISFLOOD hydrological model has five parameters that are used for calibration (Table 3.4). In the present work, the calibration was manually performed using a trial and error method and for the years 2001, 2002 and 2003. The model validation took place after the calibration to test if the model performs well on another portion of data which were not used in calibration. The LISFLOOD hydrological model was verified for the years 2005, 2006 and 2007.

*Table 3. 4.Calibration parameters of the LISFLOOD hydrological model (Van der Knijff and De Roo., 2008).*

| Parameter | Description | Lower bound | Upper bound |
|---|---|---|---|
| Upper Zone Time Constant (UZTC) | Time constant for water in upper zone [days] | 1 | 50 |
| Lower Zone Time Constant (LZTC) | Time constant for water in lower zone [days] | 50 | 5000 |
| Ground Water Percolation Value (GWPV) | Maximum rate of percolation going from the Upper to the Lower Zone [mm/day] | 0 | 1.5 |
| Xinanjiang parameter b (Xb) | Parameter in infiltration equation [-] | 0.1 | 1 |
| Power preferential Flow (PPF) | Parameter in preferential flow equation [-] | 1 | 6 |

Furthermore, the evaluation of the calibration results requires the comparison of observations and model simulations. Various objective functions are used for this purpose. In this work, we selected three objective functions for performance and uncertainty assessment of LISFLOOD model namely the Nash-Sutcliffe coefficient (NSE), the Root Mean Square Error (RMSE) and the percentage deviation (PD). The Nash-Sutcliffe coefficient of efficiency is commonly used to assess the performance of hydrological models. It is defined by Equation 3.22:

$$NSE = 1 - \frac{\sum_{i=1}^{n}\left(Q_{obs,i} - Q_{model,i}\right)^2}{\sum_{i=1}^{n}\left(Q_{obs,i} - Q_{obs,mean}\right)^2} \quad (3.22)$$

Where $Q_{obs}$ is observed discharges, $Q_{model}$ is simulated discharges at time/place $i$ and $Q_{obs,mean}$ is the mean of the observed discharges. The Nash-Sutcliffe coefficients range from -∞ to 1. A value of 1 corresponds to the best match between model and observation. A value of 0 shows that the model predictions are as accurate as the mean of the observed data, whereas a value less than zero (-∞ < NS< 0) indicates that the observed mean is a better predictor than the model.

The Root Mean Square Error (RMSE) is another measure of the difference between values predicted by a model and the values observed from the system which is modelled. The Root Mean Square Error serves to aggregate them into a single measure of model performance. The RMSE is defined as the square root of the mean squared error (Equation 3.23):

$$RMSE = \sqrt{\frac{\sum_{i=1}^{n}(Q_{obs,i}-Q_{model,i})^2}{n}} \quad (3.23)$$

The percentage deviation (PD) of observed and simulated quantity is computed using Equation 3.24:

$$PD = \frac{\sum_{i=1}^{n}(Q_{obs,i}-Q_{model,i})}{\sum_{i=1}^{n}Q_{obs,i}} \times 100 \quad (3.24)$$

A value of PD close to zero shows a best match between model and observation. A negative value of PD indicates an overestimation and a positive value of PD indicates an underestimation.

### 3.2.3. Flood hazard mapping

#### 3.2.3.1.Description of the flood inundation model

In this study, LISFLOOD-FP version 6.0.4 (Bates et al., 2013) was used to model flood extent of the Oti River. LISFLOOD-FP is a raster based hydraulic model developed at the University of Bristol (United Kingdom). The hydraulic model solves numerically the local inertial (Neal et al., 2012), diffusive (Trigg et al., 2009) or kinematic (Bates and De Roo, 2000)

approximations to the 1D shallow water equations given in Equations 3.25 and 3.26 (Bates et al., 2013) in order to simulate the propagation of the flood wave through the river channel.

$$\frac{\partial Q_x}{\partial t} + \frac{\partial}{\partial x}\left(\frac{Q_x^2}{A}\right) + gA\frac{\partial (h+z)}{\partial x} + \frac{gn^2 Q_x^2}{R^{4/3}A} = 0 \quad \text{(Momentum equation)} \qquad (3.25)$$

$$\frac{\partial A}{\partial x} + \frac{\partial Q_x}{\partial x} = 0 \quad \text{(Continuity equation)} \qquad (3.26)$$

where $Q_x$ is volumetric flow rate in the *x* Cartesian direction, A the cross sectional area of flow, *h* the water depth, *z* the bed elevation, *g* gravity, n the Manning's coefficient of friction, R the hydraulic radius, *t* time and *x* the distance in the *x* Cartesian direction.

In this model, the river channel is represented using the local inertial approximation implemented at sub-grid scale (Neal et al., 2012) and required data layer of channel widths were manually measured from Google maps to define the channel location. The section of the river channel was considered to be rectangular.

The performance of LISFLOOD-FP to predict flood inundation extent has been widely tested using observed flood extent maps from satellite (Di Baldasssare et al., 2009). The model has given good results in flood inundation modelling not only in Europe (Bates et al., 2010) but also in West Africa (Neal et al., 2012), Southern Africa (Schumann et al., 2013) and North Africa (Yan et al., 2014).

### 3.2.3.2. Application of the LISFLOOD-FP model

#### *3.2.3.2.1. Model setup*

A coupled 1D-2D LISFLOOD-FP model was set up for a 140 km reach of the Oti River using the sub-grid solver as described by Neal et al. (2012). The sub-grid model was chosen for

this study because of its ability to be applied in poor data environment. The application of the sub-grid solver of LISFLOOD-FP requires the specification of the streamlines of the river, floodplain topography, river widths, river bank elevation, inflow hydrographs and downstream boundary conditions along with model friction and channel depth parameters. The centrelines were derived from the digital elevation model using a flow accumulation process in ArcMap GIS software. Apart from the inflow hydrographs and the model friction parameters, all the input data were created in ArcMap GIS software and projected in a Cartesian coordinate systems (UTM zone 31 N). These raster data sets were exported as text files (asci raster) to be read by LISFLOOD-FP.

In addition, a DEM (≈30 m horizontal resolution) for the study area was obtained from the SRTM data set. No elevation correction for vegetation height was made because the floodplain and the river banks of the Oti River are situated in a semi-arid region with a sparse savanna vegetation, therefore, errors in the SRTM elevation values due to vegetation cover are not expected to be significant in this area (Baugh et al., 2013). Starting from the original 30 m resolution, five other raster grids (60m, 120m, 240m, 480m and 960m) were created by aggregating mean values in order to test the accuracy of the model at the different resolutions and assess the sensitivity of the model outputs to floodplain DEM resolution.

The river widths were measured from satellite imagery (Google earth) acquired in February 2015. In this period, it is easy to identify the channel width because the river is within its banks. Moreover the river bank elevation was estimated from the DEM by extracting the elevation of the floodplain cells that are adjacent to the river and smoothing these along river over a distance of 1 km using a moving window filter. A free boundary condition which specified that the valley slope and water surface slope were equivalent at the boundary was

applied to the downstream end of the model to allow water to leave the model domain. Since the study site is characterized by a lack of recent observed hydrological data, the LISFLOOD rainfall-runoff model was used to simulate input discharge data. The hydrograph of the reach outlet was then used as the input at the upstream end of the model to ensure all lateral inflows over the reach were accounted for in the hydrodynamic modelling.

Finally, the sub grid channel solver of LISFLOOD-FP has four parameters namely the Manning's friction coefficient separately for channel and floodplain, the exponent (*p*), and coefficient (*r*) of the hydraulic geometry. Manning's friction coefficient is a parameter that characterizes flow resistance for both the river channel and the floodplain. This coefficient can be distributed in space but the model is typically set up with one component for the floodplain ($n_{fp}$) and another component for the river channel ( $n_c$) where only limited data for the river is available. According to Chow (1959), Manning's friction coefficient for channel varies from 0.03 (clean) to 0.1 (very weedy reaches) and Manning's friction coefficient for floodplain from 0.03 (pasture and short grass) to 0.120 (heavy stand of timber and a few down trees). The hydraulic geometry coefficient affects the area and hydraulic radius of the channel bankfull cross-section (Neal et al., 2012) and can be estimated from hydraulic geometry relationships proposed by Leopold and Maddock (1953) and rearranged by Neal et al. (2012) to obtain the following expression shown in Equation 3.27:

$$d = rw^p \tag{3.27}$$

Where *d* and *w* are the reach averaged depth and the reach averaged width respectively whilst *r* and *p* are the hydraulic geometry parameters. Due to the lack of data in the study area, the initial values of the four parameters (*p*, *r*, $n_{fp}$ and $n_c$) where obtained from Chow (1959) and Leopold and Maddock (1953).

#### 3.2.3.2.2. Sensitivity tests

Three sets of sensitivity test were undertaken with the finished model, sensitivity to: (i) channel friction, (ii) channel geometry, (iii) floodplain DEM resolution. First, the aim of the channel friction simulations was to test the sensitivity of the model results to different values of Manning's friction coefficient of the channel ( $n_c$) ranging from 0.02 to 0.05 in 0.001 increment. For each simulation, the values of the other parameters were set constant. Other applications of LISFLOOD-FP (e.g. Horrit, 2005; Di Baldassarre et al., 2009) have shown that the model sensitivity to the floodplain friction parameter is often negligible or at least much lower than the sensitivity to channel friction. Therefore, it was not considered in the sensitivity analysis. Second, the sensitivity of the flood inundation extent to the river channel geometry was tested by running the model for different values of the coefficient of the hydraulic geometry ($r$ ) ranging from 0.035 to 0.175 in 0.005 increment. This is in effect a scaling of the channel depth, with reach averaged depth increasing with *r*. For each simulation, the values of the other parameters were set constant. Finally, to test floodplain DEM resolution, the model was run using the six different resolutions of the floodplain DEM outlined above.

#### 3.2.3.2.3. Simulation of the 2007 flood events

To consider the damaging flooding of September 2007, which was estimated to have a return period of ≅ 175 years at the Sabari gauge on the Oti River (Komi et al., 2016), the model simulated the extent of 2007 flood event for a period between 1st May 2007 and 30 November 2007. The simulated inundation extent was compared with the satellite observation produced on September 21, 2007 while a simple index of fit measure (Bates and De Roo, 2000) was used to

compare quantitatively the simulated extent to the satellite image. The performance measure (F) is given in Equation 3.28:

$$F(\%) = \frac{A \cap B}{A \cup B} \times 100 \quad (3.28)$$

where A is the observed inundated area, and B the inundated area predicted by the model. In order to calculate F, an inundation boundary vector was first created from the observed satellite image, as the original MODIS raster analysis was not obtainable. The boundary vector was converted to a wet and dry raster, resampled to the same resolution as the model simulation. The same wet and dry classification was applied to the simulation results. In order to calibrate the model, we consider only the Manning's friction coefficient for channel and the hydraulic geometry coefficient which were sampled in the range of the intervals given in Section 3.2.3.2.2 above.

#### 3.2.3.3. Flood hazard mapping

In order to delineate flood hazard maps for the selected reach, flood flow magnitudes for different return periods are used to drive the hydraulic model. In this study, the regional flood frequency analysis was used to estimate the design floods.

### 3.2.4. Integrated flood risk assessment

#### 3.2.4.1.Conceptual framework

This study draws from the CBDRI which was developed by the German Technical Cooperation Agency (GTZ) to strengthen the capacity of communities and local government for disaster risk management (GTZ, 2003). The CBDRI method characterizes the risk of natural

disaster via four (4) factors namely hazard, exposure, vulnerability, as well as capacity and measures. Figure 3.9 gives an overview of the conceptual framework of the CBDRI system.

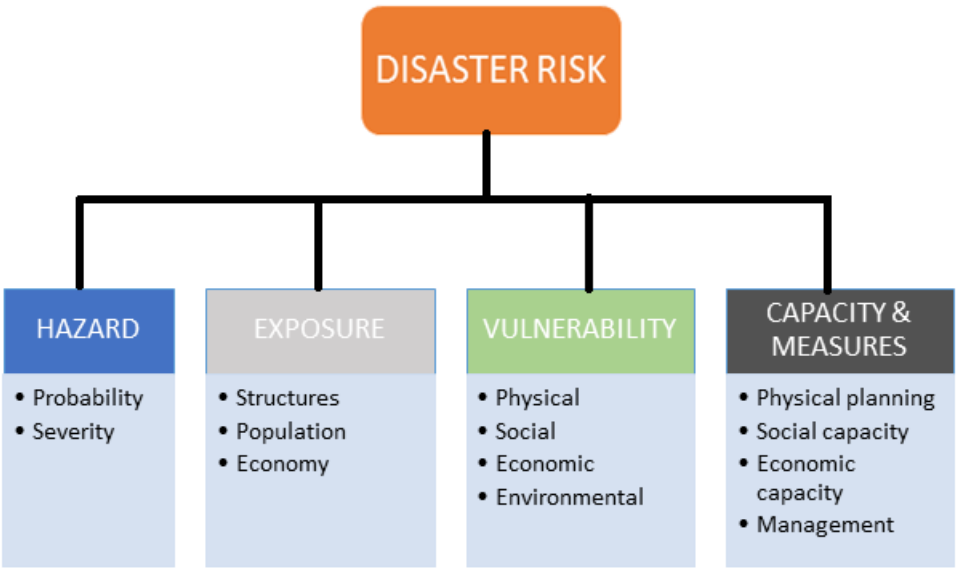


*Figure 3. 9. Schematic representation of the conceptual framework (modified from Bollin et al., 2003).*

In this study, a set of 37 indicators were used to quantify the risk index for a given community (Table 3.5). All indicators for each of the four factors (hazard, exposure, vulnerability and capacities and measures) are integrated into one index (e.g. hazard index). As it is shown in Figure 3.9, the indicators selected to measure hazard focus on two (2) different characteristics: probability and severity while the exposure factor is characterized by structures, population and economy. The indicators used to quantify vulnerability focus on the physical, social, economic and environmental vulnerabilities. Physical planning, social capacity, economic capacity and management are used to measure capacity and measures factor.

*Table 3. 5.Set of community-based disaster risk indicators (source: Bollin et al., 2003)*

| Factor component | Indicator Name | Indicator |
|---|---|---|
| **HAZARD** | | |
| Probability | (H1) Occurrence (experienced events)<br>(H2) Occurrence (possible events) | Frequency of events in the past 30 years<br>Probability of possible events. Chances per year |
| Severity | (H3) Intensity (experienced events)<br>(H4) Intensity (possible events) | Intensity of the worst event in the past 30 years<br>Expected intensity of possible events |
| **EXPOSURE** | | |
| Structures | (E1) Number of housing units<br>(E2) Lifelines | Number of housing units (Living quarter)<br>% of homes with piped drinking water |
| Economy | (E3) Local gross domestic product | Total locally generated GDP in constant currency |
| Population | (E4) Total resident population | Total resident population |
| **VULNERABILITY** | | |
| Physical/ Demographic | (V1) Density<br>(V2) Demographic pressure<br>(V3) Unsafe settlement<br>(V4) Access to basic services | People per $km^2$<br>Population growth rate<br>Homes in hazard prone area (ravines, river banks, etc)<br>% of homes with piped drinking water |
| Social | (V5) Poverty level<br>(V6) Literacy rate<br>(V7) Attitude<br>(V8) Decentralisation<br>(V9) Community participation | % of population below poverty level<br>% of adult population that can read and write<br>Priority of a population to protect against a hazard<br>Portion of self-generated revenues of the total budget<br>% of voter turnout at last commune election |
| Economic | (V10) Local resource base<br>(V11) Diversification<br>(V12) Stability<br>(V13) Accessibility | Total available local budget in USS<br>Economic sector mix for employees<br>% of businesses with fewer than 20 employees<br>Number of interruption of road access in last 5 years |
| Environmental | (V14) Area under forest | % Area of the commune covered with forest |
| **CAPACITY AND MEASURES** | | |
| Physical planning and engineering | (C1) Land use planning<br>(C2) Preventive structure<br>(C3) Environmental management | Enforced land use plan or zoning regulation<br>Expected effect of impact-limiting structures<br>Measures that promote and enforce nature preservation |
| Societal capacity | (C4) Public awareness programs<br>(C5) School curricula<br>(C6) Public participation | Frequency of public awareness programmes<br>Scope of relevant topics taught at school<br>Emergency committee with public representatives |
| Economic capacity | (C7) Access to local emergency funds<br>(C8) Access to international emergency funds<br>(C9) Insurance market | Release period of national emergency funds<br>Access to international emergency funds<br>Availability of insurance for buildings |
| Management and institutional capacity | (C10) Risk management committee<br>(C11) Risk map<br>(C12) Emergency plan<br>(C13) Early warning system<br>(C14) Institutional capacity building<br>(C15) Communication | Meeting frequency of a commune committee<br>Availability and circulation of risk maps<br>Availability and circulation of emergency plans<br>Effectiveness of early warning system<br>Frequency of training for local institutions<br>Frequency of contact with district level risk institutions |

Finally, four (4) indicators (H1, H2, H3 and H4) were selected to assess the hazard factor, four (4) indicators (E1, E2, E3 and E4) were used to measure the exposure factor, 14 indicators (V1, V2….V14) were chosen to assess the vulnerability factor and 15 indicators (C1, C2…C15) were used to quantify the capacity and measures factor which is about measures of prevention, mitigation and response (Table 3.5).

#### 3.2.4.2.Data sources and sampling procedure.

The application of CBDRI method requires a questionnaire (Appendix 3.3) to be administrated at the commune level. The four (4) factors of the risk index comprise various indicators but consideration of all for risk assessment is difficult due to the lack of data. Hence, 'degraded land' and 'overused land' were not considered in the present study, whereas 'total gross domestic product' , 'unsafe settlements' and percentage of home with piped drinking water were respectively replaced by average income per year, flood-prone areas and rate of access to safe drinking water. In total, seven (7) communities namely Sadori, Mango, Mogou, Tchamonga, Tchanaga, Tambigou and Borgou in the Oti and Kpendal prefectures of Togo were selected for this study because of their proximity to the Oti River. Mandouri was initially considered for the flood risk assessment but it was further removed due to difficulty of access during the field work and lack of data. In each community, one questionnaire was completed. In order to get reliable information, only knowledgeable people (member of the local development committee, formal community leader, teacher, etc.) were contacted to fill the questionnaire and the information is further verified from secondary sources when possible. However, some data such as population density (V1), population growth rate (V2), number of housing units (E1) access to basic services (V4) and literacy levels (V6) cannot be obtained from administering the questionnaire and were obtained from the 2010 Population and Housing Census data (DGCSN, 2010) and literature.

In addition, the percentage of forested area for each community area and flood prone areas were respectively derived from FAO (Food and Agriculture Organisation) land cover database (FAO, 2013) and NASA MODIS data.

#### 3.2.4.3. Estimation of the vulnerability, exposure and capacity and measure indices

To assess the vulnerability, exposure as well as capacity and measures indices of a risk index for a given community, many steps were followed. The first step consisted of making the different measurements of each indicator (e.g. 10,000 residents, 10% literacy level) comparable using a scale. The scaling was done by assigning a score (S) of 1, 2 or 3 according to the achieved class of low, medium or high (Appendix 3.3). A zero value was given if the indicator does not apply for a commune. In a second step, the scores were multiplied by a specific weight (W) of each indicator. The CBDRI model was developed in such a way that the total sum of weights for each of the four factors is equal to 3, so that the factor indices range between 0 and 10. Finally, separate indices were calculated for each factor using the following linear Equations (3.29, 3.30, 3.31 and 3.32):

$$V = W_{V1}S_{V1} + W_{V2}S_{V2} + W_{V3}S_{V3} + ... + W_{V14}S_{V14} \quad (3.29)$$

$$E = W_{E1}S_{E1} + W_{E2}S_{E2} + W_{E4}S_{E4}. \quad (3.30)$$

$$C = W_{C1}S_{C1} + W_{C2}S_{C2} + ... + W_{C15}S_{C15.} \quad (3.31)$$

$$H = W_{H1}S_{H1} + W_{H2}S_{H2} + W_{H3}S_{H3} + W_{H4}S_{H4} \quad (3.32)$$

where V, E, C and H are the values of the vulnerability, exposure , capacity and measures indices and hazard respectively; $S_i$ refer to the scaled value of the indicator , $W_i$ is the weight and *i* the indicator.

### 3.2.4.4.Estimation of the indicator weights

In the present study, the analytical hierarchy process (AHP) method was employed to compute weights for the different indicators considered in the CBDRI model. The AHP method which was developed by Saaty (1977), is a multi-criteria, mathematically based method which uses a set of pair-wise comparison matrices to estimate the relative importance of different criteria and alternatives among which the best decision is made. The Saaty's AHP model has attracted the interest of many researchers (e.g. Marinoni, 2004; Omkarprasad and Sushil, 2006 and Bathrellos et al., 2016) because it has the advantage of incorporating a test for checking the consistency of a choice, thus reducing the uncertainty in the evaluation process.

In order to compute the weights for each indicator, the AHP starts creating a pair-wise comparison matrix $M = (B_{ij})$. Each numerical value $B_{ij}$ of $M$ represents the relative importance of the *i*th indicator in comparison with the *j*th indicator. If $B_{ij}$>1, then the *i*th indicator is more important than the *j*th indicator, whereas if $B_{ij}$ < 1, then the *i*th indicator is less important than the *j*th indicator. If two indicators have the same importance, then $B_{ij}$=1. The numerical values satisfy the condition given in Equation 3.33 (Saaty, 1977).

$$B_{ij} * B_{ji} = 1 \qquad (3.33)$$

Moreover, the relative importance between two criteria was measured based on a numerical scale from 1 to 9 as follows: 1= *i* and *j* are equally important, 3 = *i* is slightly more important than *j*, 5 = *i* is strongly important than *j*, 7 = *i* is very strongly more important than *j*, 9 = *i* is extremely more important *j* and 2, 4, 6, 8 are intermediate values between the previous scales (Saaty, 1977).

After building the matrix *M*, a normalized pair-wise comparison matrix was derived by dividing each value $B_{ij}$ by the sum of all values of that column. Finally, the relative weight ($W_{AHP}$) vector was estimated by averaging the values on each row of the normalized pair-wise comparison matrix. The AHP method requires all indicator weights to satisfy the condition shown in Equation 3.34:

$$\sum_{i=1}^{n} W_{AHP} = 1 \quad (3.34)$$

The AHP method provides the possibility to check the consistency of the estimated weights. This is done with the consistency ratio (CR) which is shown in Equation 3.35 (Saaty, 2008):

$$\mathrm{CR} = \mathrm{CI}/\mathrm{RI} \quad (3.35)$$

Where CI is the consistency index which is obtained by first computing the scalar $\lambda_{max}$ as the average of the elements of the vector whose *i*th element is the ratio of the *i*th element of the vector ($M$*$W_{AHP}$) to the corresponding element of the vector $W_{AHP}$ (Saaty, 2008). Then, CI is calculated using the Equation 3.36:

$$CI = \frac{\lambda_{max} - n}{n-1} \quad (3.36)$$

where $\lambda_{max}$ is the largest eigenvalue of the matrix and *n* is the number of indicators. RI is a constant which depends on *n*. When CR < 0.1, the evaluation is consistent and reliable results can be expected from the AHP model (Saaty, 1977).

In this study, four pair-wise comparison matrices (Table 3.6, Table 3.7, Table 3.8 and Table 3.9) were constructed for the weight estimations of the different indicators used in the CBDRI model. Furthermore, $W_{AHP}$ was multiplied by 3 to get the final weights of each indicator.

*Table 3. 6.The weights estimated from the AHP model for the indicators of the hazard factor. For the definition of H1, H2, H3 and H4, see Table 6. 2. CR= 0.01 (< 0.1).*

| | H1 | H2 | H3 | H4 | $W_{AHP}$ | $W_{xi}$ |
|---|---|---|---|---|---|---|
| H1 | 1 | 1 | 1/3 | 2 | 0.2 | 0.6 |
| H2 | 1/2 | 1 | 1/3 | 2 | 0.18 | 0.54 |
| H3 | 3 | 3 | 1 | 2 | 0.47 | 1.41 |
| H4 | 1/2 | 1/2 | 1/2 | 1 | 0.15 | 0.45 |

*Table 3. 7.The weights estimated from the AHP model for the indicators of the vulnerability factor. For the definition of V1, V2 …V14, see Table 6.2. CR=0.01(<0.1)*

| | V1 | V2 | V3 | V4 | V5 | V6 | V7 | V8 | V9 | V10 | V11 | V12 | V13 | V14 | $W_{AHP}$ | $W_{xi}$ |
|---|---|---|---|---|---|---|---|---|---|---|---|---|---|---|---|---|
| V1 | 1 | 1 | 1/2 | 2 | 1/2 | 3 | 2 | 3 | 2 | 1 | 2 | 3 | 2 | 2 | 0.10 | 0.3 |
| 2 | | 1 | 1/2 | 2 | 1/2 | 3 | 2 | 3 | 2 | 1 | 2 | 3 | 2 | 2 | 0.10 | 0.3 |
| V3 | | | 1 | 3 | 2 | 5 | 3 | 5 | 3 | 2 | 3 | 5 | 3 | 3 | 0.17 | 0.51 |
| V4 | | | | 1 | 1/2 | 2 | 1 | 2 | 1 | 2 | 1 | 2 | 1 | 1 | 0.06 | 0.18 |
| V5 | | | | | 1 | 3 | 2 | 3 | 2 | 2 | 2 | 3 | 2 | 2 | 0.12 | 0.36 |
| V6 | | | | | | 1 | 1/2 | 1 | 1/2 | 1/3 | 1/2 | 1 | 1/2 | 1/2 | 0.03 | 0.09 |
| V7 | | | | | | | 1 | 2 | 1 | 1/2 | 1 | 2 | 1 | 1 | 0.05 | 0.15 |
| V8 | | | | | | | | 1 | 1 | 1/3 | 1/2 | 1 | 1/2 | 1/2 | 0.03 | 0.09 |
| V9 | | | | | | | | | 1 | 1/2 | 1 | 2 | 1 | 1 | 0.05 | 0.15 |
| V10 | | | | | | | | | | 1 | 2 | 3 | 2 | 2 | 0.09 | 0.27 |
| V11 | | | | | | | | | | | 1 | 2 | 1 | 1 | 0.05 | 0.15 |
| V12 | | | | | | | | | | | | 1 | 1/2 | 1/2 | 0.03 | 0.09 |
| V13 | | | | | | | | | | | | | 1 | 1 | 0.05 | 0.15 |
| V14 | | | | | | | | | | | | | | 1 | 0.05 | 0.15 |

*Table 3. 8.The weights estimated from the AHP model for the indicators of the exposure factor. For the definition of E1, E2, E3 and E4, see Table 6.2. CR=0.02 (<0.1).*

| | E1 | E2 | E3 | E4 | $W_{AHP}$ | $W_{xi}$ |
|---|---|---|---|---|---|---|
| E1 | 1 | 2 | 2 | 1/3 | 0.22 | 0.66 |
| E2 | 1/2 | 1 | 1/2 | 1/5 | 0.1 | 0.3 |
| E3 | 1/2 | 2 | 1 | 1/3 | 0.15 | 0.45 |
| E4 | 3 | 5 | 3 | 1 | 0.52 | 1.56 |

*Table 3. 9. The weights estimated from the AHP model for the indicators of the capacity and measure factor. For the definition of C1, C2…C15, see Table 6.2. CR=0 (<0.1).*

| | C1 | C2 | C3 | C4 | C5 | C6 | C7 | C8 | C9 | C10 | C11 | C12 | C13 | C14 | C15 | $W_{AHP}$ | $W_{xi}$ |
|---|---|---|---|---|---|---|---|---|---|---|---|---|---|---|---|---|---|
| C1 | 1 | 2 | 3 | 2 | 2 | 3 | 1 | 1 | 2 | 3 | 2 | 2 | 1/3 | 2 | 2 | 0.10 | 0.3 |
| C2 | | 1 | 2 | 1 | 2 | 2 | 1/2 | 1/2 | 1 | 2 | 1 | 1 | 1/3 | 1 | 1 | 0.06 | 0.18 |
| C3 | | | 1 | 1/2 | 1/2 | 1 | 1/3 | 1/3 | 1/2 | 1 | 1/2 | 1/2 | 1/5 | 1/2 | 1/2 | 0.03 | 0.09 |
| C4 | | | | 1 | 1 | 2 | 1/2 | 1/2 | 1 | 1/2 | 1 | 1 | 1/3 | 1 | 1 | 0.05 | 0.15 |
| C5 | | | | | 1 | 2 | 1/2 | 1/2 | 1 | 2 | 1 | 1 | 1/3 | 1 | 1 | 0.05 | 0.15 |
| C6 | | | | | | 1 | 1/3 | 1/3 | 1/2 | 1 | 1/2 | 1/2 | 1/5 | 1/2 | 1/2 | 0.03 | 0.09 |
| C7 | | | | | | | 1 | 1 | 2 | 3 | 2 | 2 | 1/3 | 2 | 2 | 0.10 | 0.3 |
| C8 | | | | | | | | 1 | 2 | 3 | 2 | 2 | 1/3 | 2 | 2 | 0.10 | 0.3 |
| C9 | | | | | | | | | 1 | 2 | 1 | 1 | 1/3 | 1 | 1 | 0.05 | 0.15 |
| C10 | | | | | | | | | | 1 | 1/2 | 1/2 | 1/5 | 1/2 | 1/2 | 0.03 | 0.09 |
| C11 | | | | | | | | | | | 1 | 1 | 1/3 | 1 | 1 | 0.05 | 0.15 |
| C12 | | | | | | | | | | | | 1 | 1/3 | 1 | 1 | 0.05 | 0.15 |
| C13 | | | | | | | | | | | | | 1 | 3 | 3 | 0.18 | 0.54 |
| C14 | | | | | | | | | | | | | | 1 | 1 | 0.05 | 0.15 |
| C15 | | | | | | | | | | | | | | | 1 | 0.05 | 0.15 |

### 3.2.4.5. Estimation of the flood hazard index

In the CBDRI system, the hazard factor has 2 components (see Table 3.5): the experienced hazard and the possible or expected hazard. Since the data regarding the hazard factor should be obtained from scientific sources (Bollin et al., 2003), the information on the experienced flood hazards was obtained from the literature (e.g. MERF, 2009; Paeth et al., 2011) while the probability and severity of the possible flood hazard (H2 and H4) were obtained through flood hazard mapping of the Oti River Basin. The regional flood frequency analysis and the calibrated flood inundation model were used to simulate the floodplain inundation depths of the 50 years. The 50-years flood was chosen because it provides a plausible measure of flood-affected populations (Hirabayashi and Kanae, 2009).

In addition, the flood hazard severity was estimated based on the categorization proposed by Dinh et al. (2012) as shown in Table 3.10.

*Table 3. 10.Categorization of flood hazard (source: Dinh et al., 2012).*

| Flood depth (m) | Hazard zone | Definition of hazard severity |
|---|---|---|
| 0-0.2 | Very low | This is the case in which the damage to property is expected to be very low |
| 0.2-0.5 | Low | This is the case in which the number of casualties due to floods, in terms of death or injuries, is insignificant, and the damage to property is expected to be relatively low |
| 0.5-1.0 | Medium | This is the case in which casualties, in terms of death and injuries are considerable, relative to the number of people living in the area under study. |
| 1.0-2.0 | High | This is the case in which damage to property is quiet extensive and the probability of having dead and injured people is high. |

Since, each community area has many flood severity classes (FC) with a particular extent; an average flood severity index (FSI) was used to estimate the average flood severity of a given community area. The FSI takes into account the areal extent of a flood depth and was calculated using Equation 3.37 (Adeloye et al., 2015). Then, the flood hazard index (H) was estimated using Equation 3.32.

$$FSI = \frac{\sum_{i=1}^{n} (FC)_i A_i}{\sum_{i=1}^{n} A_i} \quad (3.37)$$

Where $A_i$ is the areal extent of the flood severity class i, n is the number of flood severity classes. $(FC)_i$ was represented by the mean depth of the flood severity class (see Table 3.10)

### 3.2.4.6. Estimation of flood risk index

To calculate the overall flood risk index (R) in the community based system, Equation 3.38 was used. In this equation, a constant coefficient of 0.03 was multiplied by each factor in order to maintain the same scale between 0 and 10 as for the individual factor indices.

$$R = 0.03\{H * V * E[0.1(1-a)C + a]\} \quad (3.38).$$

In addition, the values of the risk index were grouped into five categories (very low, low, moderate, high and very high) as shown in Table 3.11

*Table 3. 11.Categorization of the flood risk index used in this study*

| Range of the flood risk index | Risk zone |
|---|---|
| 0-2 | Very low |
| 2-4 | Low |
| 4-6 | Moderate |
| 6-8 | High |
| 8-10 | Very high |

# RESULTS AND DISCUSSION

# 4. FLOOD FREQUENCY ANALYSIS

## 4.1. Data screening

Figure 4.1 gives the discordancy measures of the sites. It appears that only the site number 11 is discordant with a Di value of 3.36 and it was consequently deleted from the dataset. In addition, treating first the whole Volta Basin as a single region, the values of the different heterogeneity measures $H_1$, $H_2$ and $H_3$ obtained were respectively 4.11, 3.02 and 2.77. Therefore, the Volta Basin is "definitely heterogeneous "and homogeneous groups need to be formed.

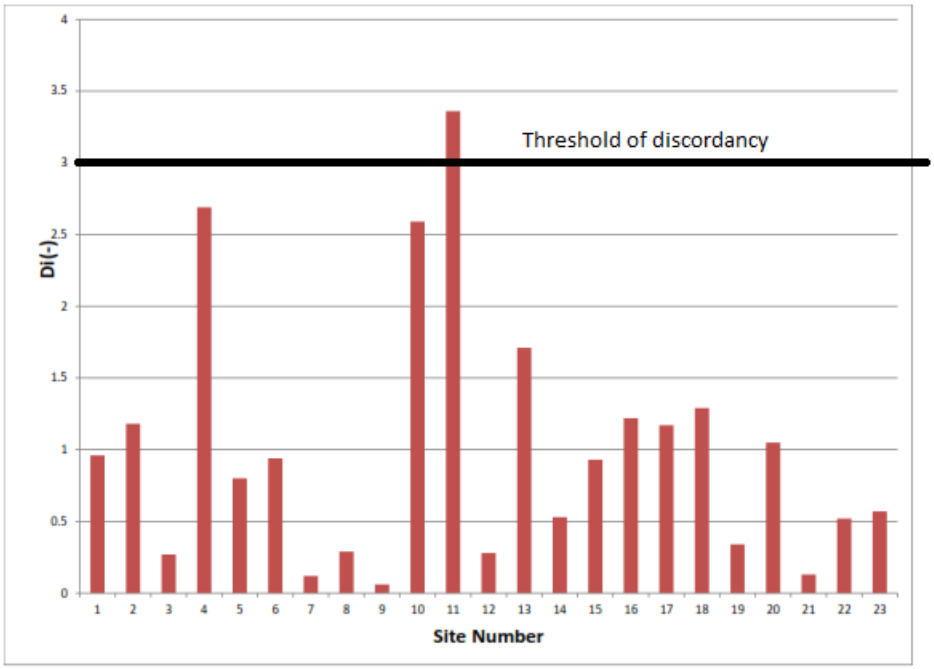


*Figure 4. 1.Discordancy measure (Di) of the different flow gauge sites*

## 4.2. Formation of homogeneous groups

Figure 4.2 and Table 4.1 show the results of the cluster analysis. . It can be seen from Table 4.1 that cluster 1 is "acceptably homogeneous" whereas clusters 2 and 3 are "definitively heterogeneous". Consequently, the clusters were adjusted to obtain the final groups shown in Table 4.2. It should be noted that the final groups are all "acceptably homogeneous".

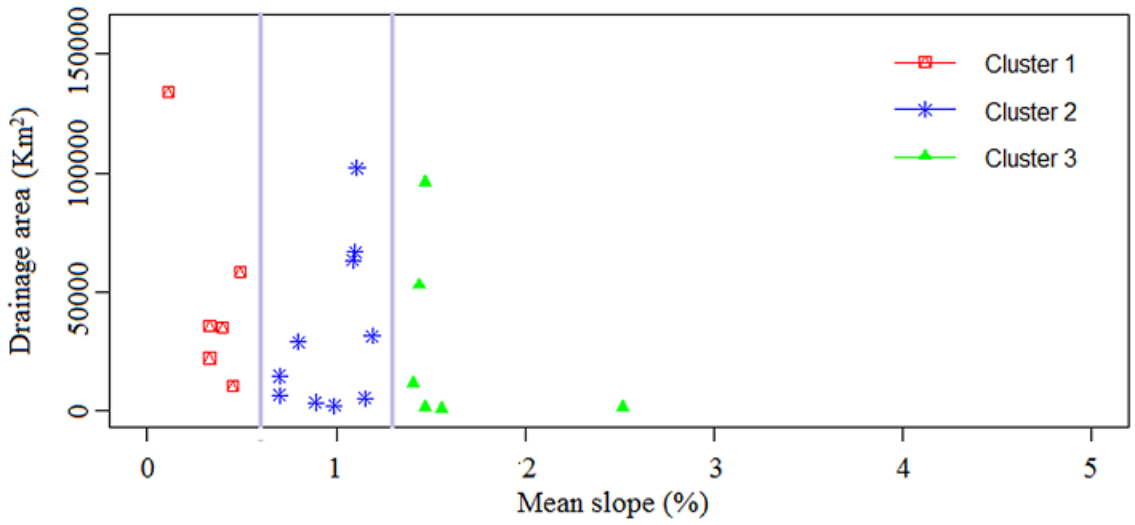


*Figure 4. 2.Formation of clusters through cluster analysis*

*Table 4. 1.Characteristics of the initial clusters.*

| Clusters | Number of sites | $H_1$ | $H_2$ | $H_3$ | Homogeneity |
|---|---|---|---|---|---|
| 1 | 6 | 0.44 | -0.32 | 0.39 | Homogeneous |
| 2 | 10 | 4.48 | 3.19 | 2.69 | Heterogeneous |
| 3 | 6 | 1.65 | 2.30 | 3.03 | Heterogeneous |

*Table 4. 2.Homogeneity measure of the final groups.*

| Groups | Number of sites | $H_1$ | $H_2$ | $H_3$ | Homogeneity |
|---|---|---|---|---|---|
| A | 7 | 0.12 | 0.29 | 0.43 | Homogeneous |
| B | 7 | -2.02 | 0.70 | 0.98 | Homogeneous |
| C | 7 | -0.21 | -1.34 | -0.37 | Homogeneous |

In addition, the location of the final homogeneous groups is shown in Figure 4.3. One can notice that all the sites of group A are situated in the Oti River Basin while those of group B are located in the White and Black Volta Basins. The sites of group C are scattered in the White Volta, Black Volta and Oti Basins. Similar results were found by Burn and Goel (2000) who confirmed that in regional flood frequency analysis, the catchments of a given homogeneous region may not be geographically contiguous but similar in terms of their flood generation processes.

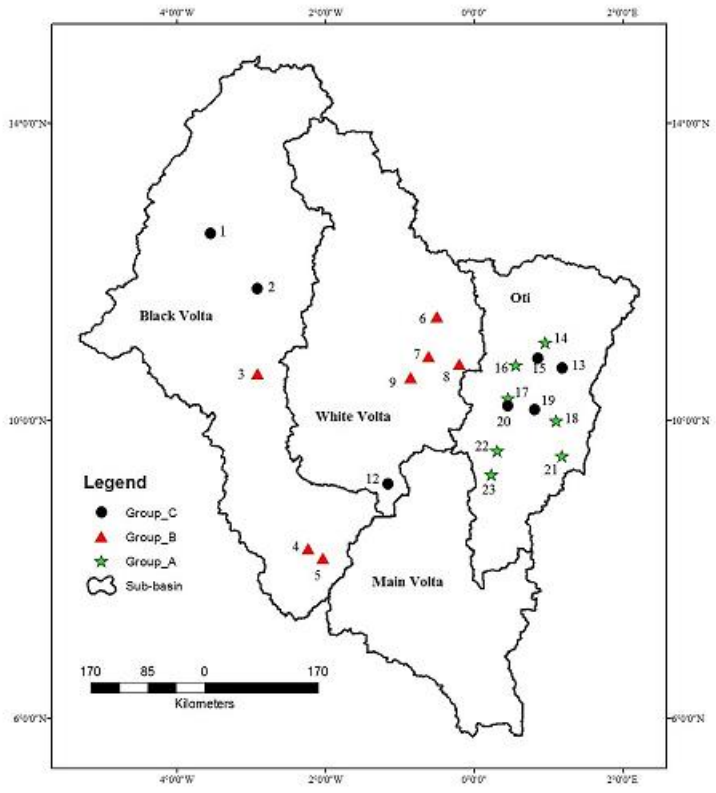


*Figure 4. 3. Location of the final homogeneous groups.*

## 4.3. Selection of appropriate distributions

The choice of the appropriate distribution for each group was based on L-moment ratio diagrams, Z-statistic, test and quantile-quantile plots. First, Figure 4.4 shows the L-moment ratio diagrams for the homogeneous groups. It can be noted that the maximum of sample sites lie close to the GPA distribution line for the group A whereas the sample sites are closer to the GEV and GPA distribution for both group B and group C. Secondly, Table 4.3 summarizes the Z-statistic values of the appropriate candidate distributions for the homogeneous groups. In this table, it is observed that only the GPA distribution has the absolute value of Z-statistic less than 1.64 for the group A and GEV distribution has the lowest absolute value of Z-statistic which is less than 1.64 for both group B and group C. Hence, the GPA distribution can be considered as regional distribution for the group A while the GEV distribution is acceptable for both groups B and C. These results are confirmed by the quantile-quantile plots on which the points lie approximately on the 1:1 line (Figure 4.5)

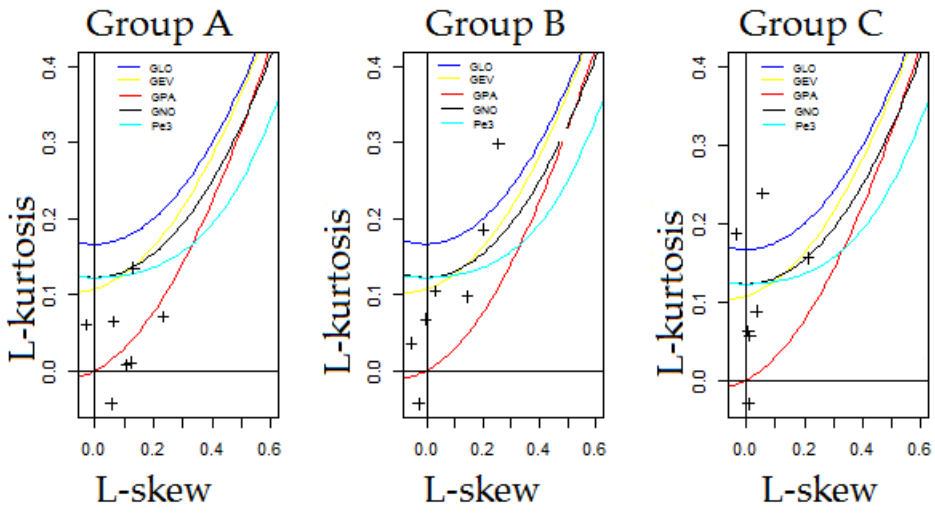


*Figure 4. 4.L-moment ratio diagrams for the homogeneous groups*

*Table 4. 3. Z-statistic values of the homogeneous groups.*

| Distribution | Group A | Group B | Group C |
|---|---|---|---|
| GPA | **0.55** | -2.57 | -3.57 |
| GEV | 4.29 | **0.39** | **0.15** |
| PE3 | 4.20 | 0.40 | 0.55 |
| GNO | 4.45 | 0.52 | 0.56 |
| GLO | 6.67 | 1.87 | 2.04 |

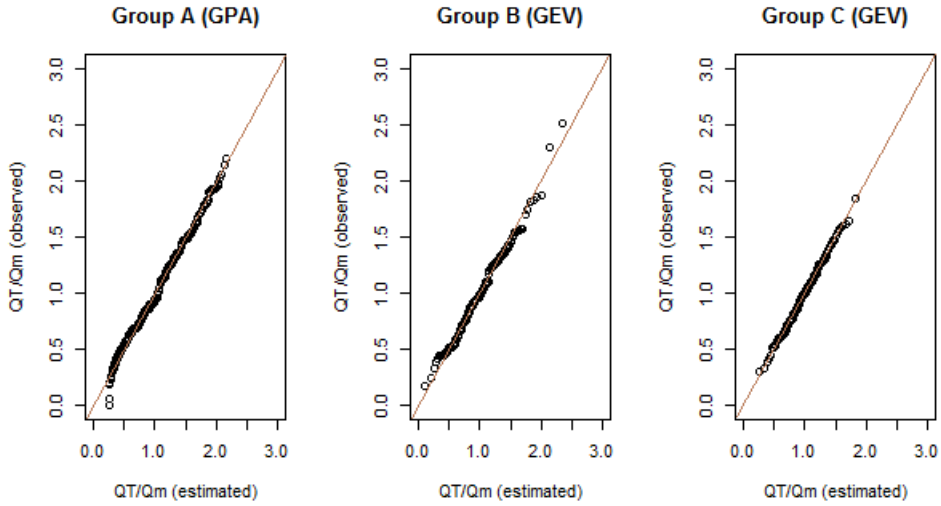


*Figure 4. 5. Quantile-quantile plots of the fitted frequency distributions*

## 4.4. Flood frequency relationships

### 4.4.1. Growth curves

The relationship between the normalized flood quantiles and their return periods (growth curve) is shown in Table 4.4 and Figure 4.6. Table 4.4 shows also the fitted parameters to the distributions selected. In order to estimate the flood quantile for a given return period, Equation 3.12 is used. For the ungauged sites where observed discharge data are not available to compute the index flood ($Q_m$), the values of $Q_m$ is computed via a multi regression model. It can be seen from the Figure 4.6 that the regional flood frequency curves for the different groups in the Volta

Basin are relatively flat. This result confirms the findings of Meigh et al. (1997) who showed that regional curves in West Africa and some regions affected by monsoon are "fairly flat". Moreover, Sutcliffe and Farquharson (1996) cited in Meigh et al. (1997) noted that a feature of many basins with flat curves is that floods appear to be due to the accumulation of rainfall over a distinct wet season or monsoon, and that the date of the annual maximum flood is relatively constant from year to year. This means that peak flows is more likely to be related to the annual total rainfall which is less variable than storm rainfall (Meigh et al., 1997).

*Table 4. 4. Quantile functions of the homogeneous groups.*

| Group | Distributions and their parameters | Growth curve |
|---|---|---|
| A | GPA : ε= 0.25; α = 1.22; k= 0.62 | $q_R$=0.25 +1.97*$\left\{1-\left(\frac{1}{T}\right)^{0.62}\right\}$ |
| B | GEV :ε=0.82; α=0.38; k=0.12; | $q_R$=0.82+3.17*$\left\{1-\left[-ln\left(\frac{T-1}{T}\right)\right]^{0.12}\right\}$ |
| C | GEV: ε= 0.88; α=0.30;k=0.23 | $q_R$=0.88+1.30*$\left\{1-\left[-ln\left(\frac{T-1}{T}\right)\right]^{0.23}\right\}$ |

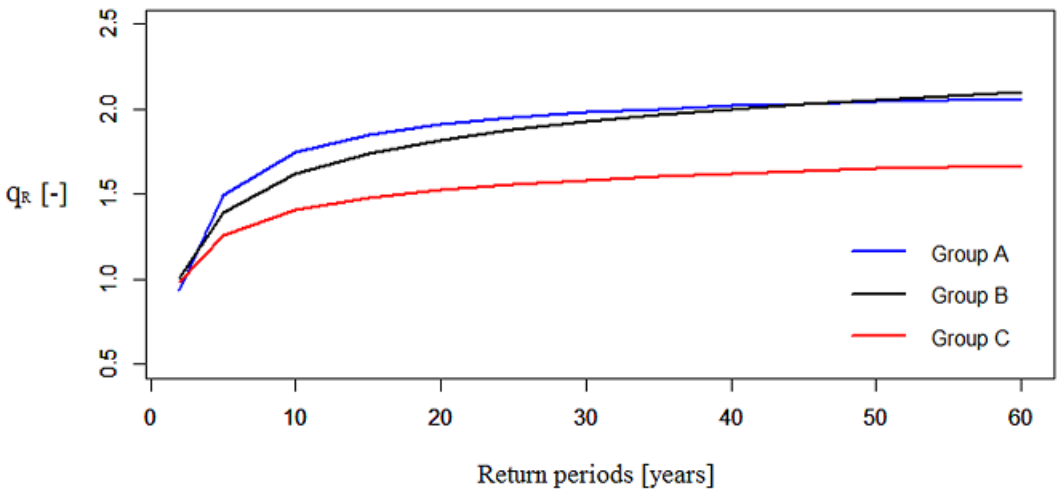


*Figure 4. 6.Regional growth curves of the different groups*

### 4.4.2. Multi-regression models for the index floods

Table 4.5 and Figure 4.7 show respectively the best regression models and the comparison between estimated quantiles and the observed values of $Q_m$ . The powers associated to the area (0.61 and 0.8) are comparable with findings of other similar studies such as Noto et al. (2009) and Lim et al. (2003). Also, these values (0.61 and 0.8) are reasonable because they show that the mean specific discharge ($Q_m/A$) decreases with the area (Hingray et al., 2009).

*Table 4. 5. Regression models for the estimation of the index flood at ungauged sites.*

| Groups | Regression models | $R^2$ |
|---|---|---|
| Oti River Basin | $Q_m = 10^{-7} * S^{0.41} * A^{0.61} * P^{2.42}$ | 0.96 |
| White Volta and Black Volta | $Q_m = 3 * 10^{-6} * S^{0.28} * A^{0.8} * P^{1.52}$ | 0.91 |

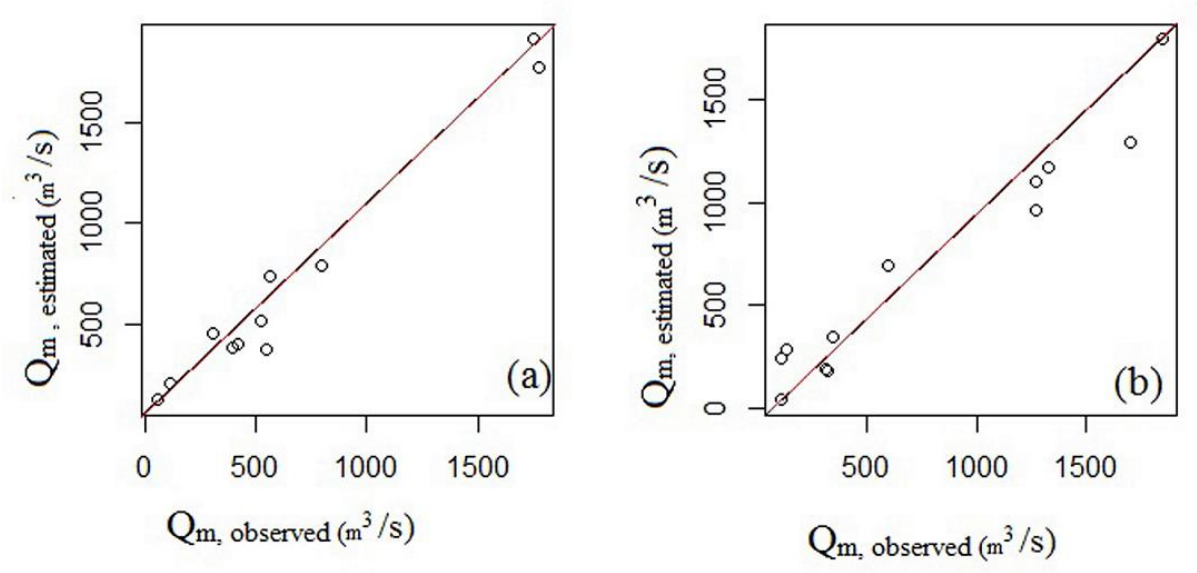


*Figure 4. 7. Diagnostic plots of the best regression models: (a) for the Oti River Basin and (b) for the White Volta and Black Volta. The 1:1 line is plotted for reference.*

In addition, Pandey and Nguyen (1999) have shown that non-linear optimization model is the best method for estimating the power-form flood regionalization model when compared with linear regression models. The same authors conclude that in terms of flood quantile prediction

and parameter uncertainty, the non-linear optimization model is the most robust when compared with linear regression methods. Consequently, the regression models obtained are suitable to estimate index floods for regional flood estimation in the Volta River Basin.

# 5. HYDROLOGICAL MODELLING FOR FLOOD PREDICTION

## 5.1. Data preprocessing

A total of 2, 211 PCraster maps were manually created for the purpose of this work. Figure 5.1 shows some examples of rainfall and reference evapotranspiration maps which were created using PCraster functions and used as input meteorological data for the raster based distributed hydrological model. One can observe the spatial variation of the daily rainfall and ETo which characterizes the input data of distributed hydrological models.

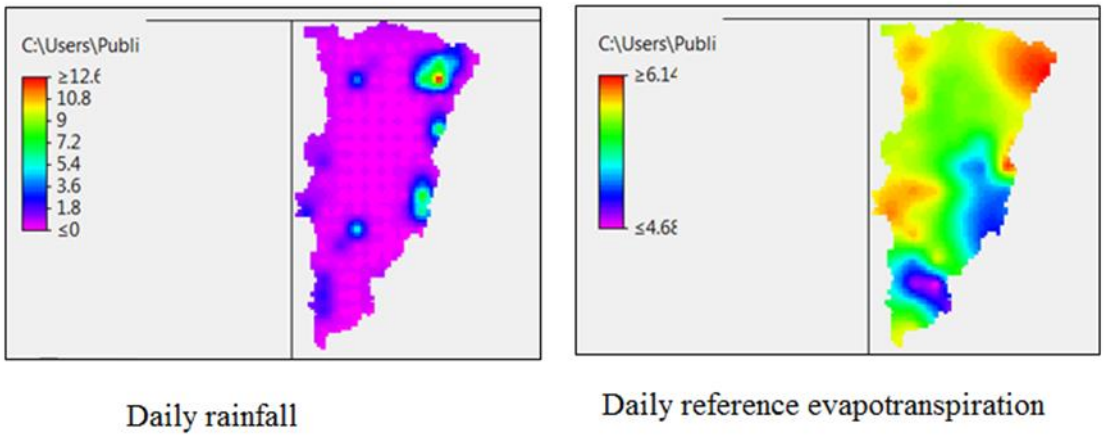


*Figure 5.1. Examples of the daily input PCRaster maps created using PCRaster functions*

Table 5.1 shows the cumulated rainfall of selected stations, cumulated TRMM rainfall of the corresponding grid and the applied correction factors. It can be seen that TRMM rainfalls underestimate slightly the rainfall for 2001, 2002, 2004 and 2006 whereas, the TRMM rainfall is higher than the observed rainfall at meteorological stations for 2000, 2003, 2005 and 2007)

*Table 5.1.Correction factors applied in this study*

| Year | Cumulated rainfall of selected stations and grids (mm) | | Correction Factor (Station/TRMM) |
|---|---|---|---|
| | Station | TRMM | |
| 2000 | 3911.3 | 4210.07 | 0.93 |
| 2001 | 5105.8 | 4947.62 | 1.03 |
| 2002 | 6269.11 | 5515.25 | 1.13 |
| 2003 | 5225.8 | 5512.22 | 0.95 |
| 2004 | 5410 | 4845.54 | 1.12 |
| 2005 | 4143 | 4501.39 | 0.92 |
| 2006 | 5251 | 4869.22 | 1.08 |
| 2007 | 5984 | 6262 | 0.95 |

## 5.2. Sensitivity analysis

Sensitivity of the five calibration parameters (UZTC, LZTC, GWPV, Xb and PPF) of LISFLOOD hydrological model was analyzed using five different values for each parameter which are highlighted in blue (Table 5.2). The sensitivity analysis was done by changing one parameter at a time while other parameters remained constant. The parameter values and objective functions (NSE and RMSE) are shown in Table 5.2. In this table, the combinations of parameters which gave the best objective function values are shown in bold.

*Table 5.2. Parameters and objective functions used in the sensitivity analysis*

| Runs | Parameters | | | | | Objective functions | |
|---|---|---|---|---|---|---|---|
| | UZTC | LZTC | GWPV | Xb | PPF | NSE | RMSE |
| | days | [days] | $[mmday^{-1}]$ | [-] | [-] | [-] | $[m^3s^{-1}]$ |
| 1 | 1 | 1 756.37 | 0.11 | 0.99 | 4.9 | 0.38 | 527.71 |
| 2 | 3 | 1 756.37 | 0.11 | 0.99 | 4.9 | 0.55 | 449.47 |
| 3 | 6 | 1 756.37 | 0.11 | 0.99 | 4.9 | 0.63 | 404.06 |
| 4 | 8 | 1 756.37 | 0.11 | 0.99 | 4.9 | 0.67 | 383.71 |
| 5 | **10** | **1 756.37** | **0.11** | **0.99** | **4.9** | **0.70** | **365.17** |
| 6 | 10 | 50 | 0.11 | 0.99 | 4.9 | 0.70 | 366.83 |
| 7 | 10 | 500 | 0.11 | 0.99 | 4.9 | 0.70 | 367.12 |
| 8 | **10** | **1 300** | **0.11** | **0.99** | **4.9** | **0.70** | **364.98** |
| 9 | 10 | 2 500 | 0.11 | 0.99 | 4.9 | 0.70 | 365.34 |
| 10 | 10 | 3 000 | 0.11 | 0.99 | 4.9 | 0.70 | 365.45 |
| 11 | 10 | 1 300 | 0.00 | 0.99 | 4.9 | 0.69 | 370.72 |
| 12 | 10 | 1 300 | 0.05 | 0.99 | 4.9 | 0.70 | 367.42 |
| 13 | **10** | **1 300** | **0.1** | **0.99** | **4.9** | **0.70** | **365.34** |
| 14 | 10 | 1 300 | 0.5 | 0.99 | 4.9 | 0.69 | 373.13 |
| 15 | 10 | 1 300 | 1 | 0.99 | 4.9 | 0.63 | 404.02 |
| 16 | 10 | 1 300 | 0.1 | 0.1 | 4.9 | 0.84 | 261.54 |
| 17 | 10 | 1 300 | 0.1 | 0.2 | 4.9 | 0.85 | 258.43 |
| 18 | **10** | **1 300** | **0.1** | **0.3** | **4.9** | **0.85** | **253.62** |
| 19 | 10 | 1 300 | 0.1 | 0.5 | 4.9 | 0.81 | 270.30 |
| 20 | 10 | 1 300 | 0.1 | 0.7 | 4.9 | 0.76 | 312.89 |
| 21 | 10 | 1 300 | 0.1 | 0.3 | 1 | 0.49 | 479 |
| 22 | **10** | **1 300** | **0.1** | **0.3** | **2** | **0.87** | **237.46** |
| 23 | 10 | 1 300 | 0.1 | 0.3 | 3 | 0.87 | 238.32 |
| 24 | 10 | 1 300 | 0.1 | 0.3 | 4 | 0.81 | 288.01 |
| 25 | 10 | 1 300 | 0.1 | 0.3 | 5 | 0.63 | 406.24 |

### 5.2.1. Effects of the upper zone time constant parameter

The Upper Zone Time Constant (UZTC) parameter reflects the residence time of water in the upper groundwater reservoir. As shown in Figure 5.2, when the value of UZTC parameter

increases, the peak discharge decreases and the slope of the falling limb becomes less steep. For this study, a value of '10' gave the best objective functions.

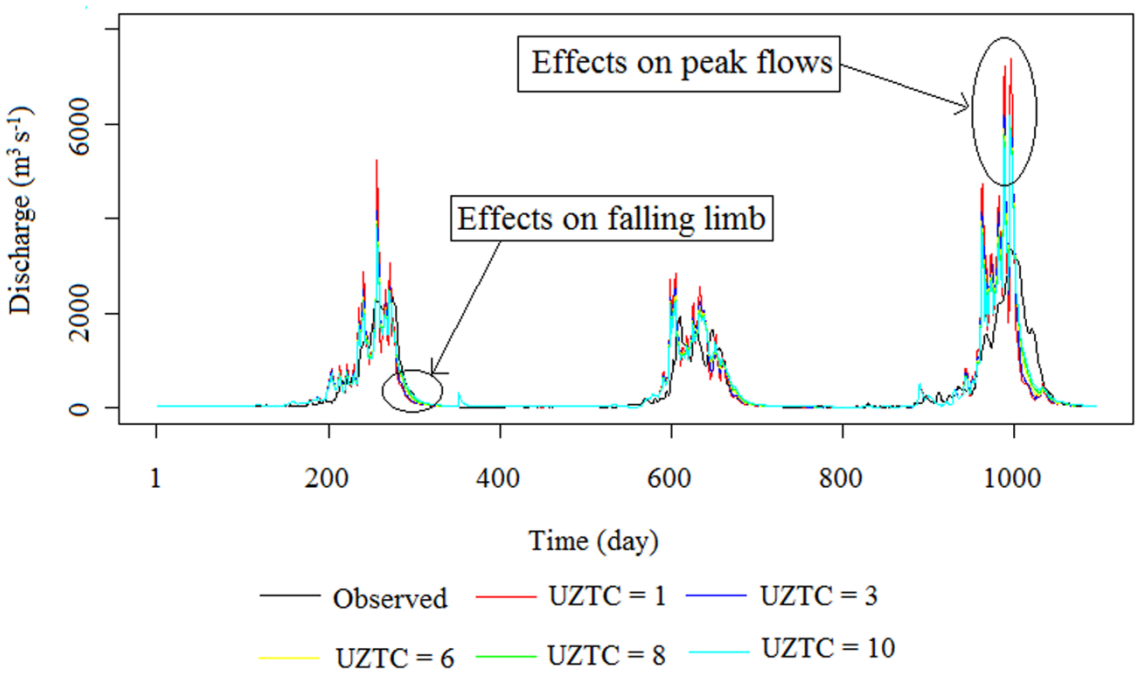


*Figure 5.2. Sensitivity of LISFLOOD hydrological model to change in the UZTC parameter.*

### 5.2.2. Effects of the lower zone time constant parameter

The Lower Zone Time Constant (LZTC) parameter indicates the residence time of water in the lower groundwater reservoir. According to the developers of the model, this parameter controls the base flow response of the hydrograph (Van der Knijff and De Roo., 2008). However, in this case study, the hydrological model was not sensitive to change in the value of this parameter (Table 5.2).

### 5.2.3. Effects of the groundwater percolation value parameter

The GroundWater Percolation Value (GWPV) parameter controls the movement of water from the upper to lower groundwater zone. An increase in this parameter value leads to an increase of the base flow during the dry season (Figure 5.3). The GWPV value that gave the best objective functions in this study was '0.1'.

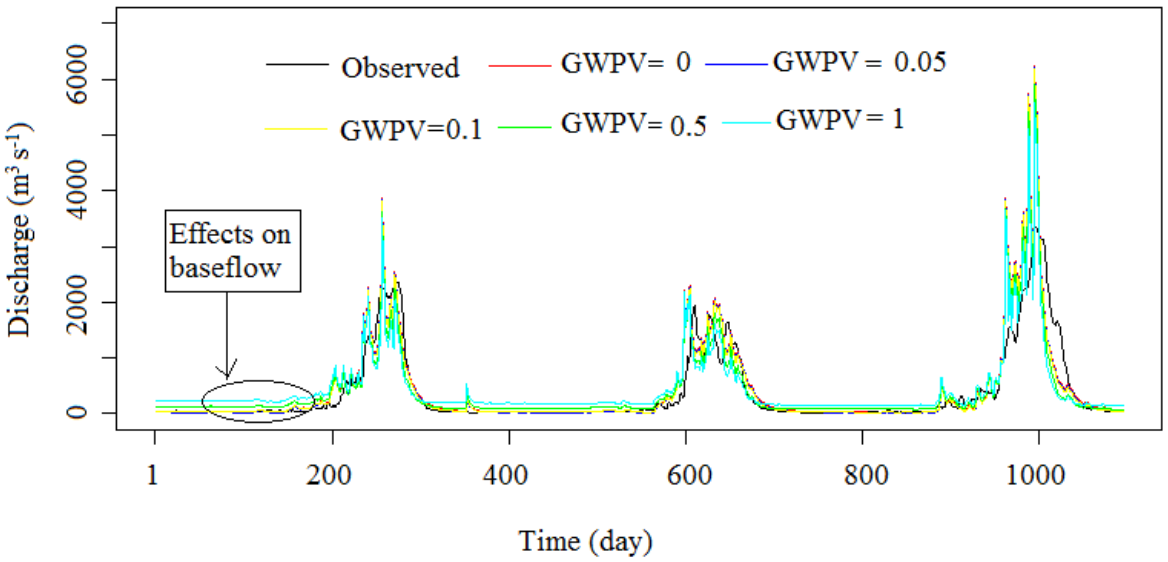


*Figure 5.3. Sensitivity of the hydrological model to change in the GWPV parameter value.*

### 5.2.4. Effects of the Xinanjiang parameter b (Xb)

Xb parameter controls the fraction of saturated area within a grid cell that is contributing to runoff and is inversely related to infiltration (Van der Knijff and De Roo., 2008). An increase in Xb parameter value resulted in an increase of the peak discharge as a consequence of a decrease in infiltration (Figure 5.4). For this study, Xb value of '0.3' gave the best goodness of fit measures as shown in Table 5.2.

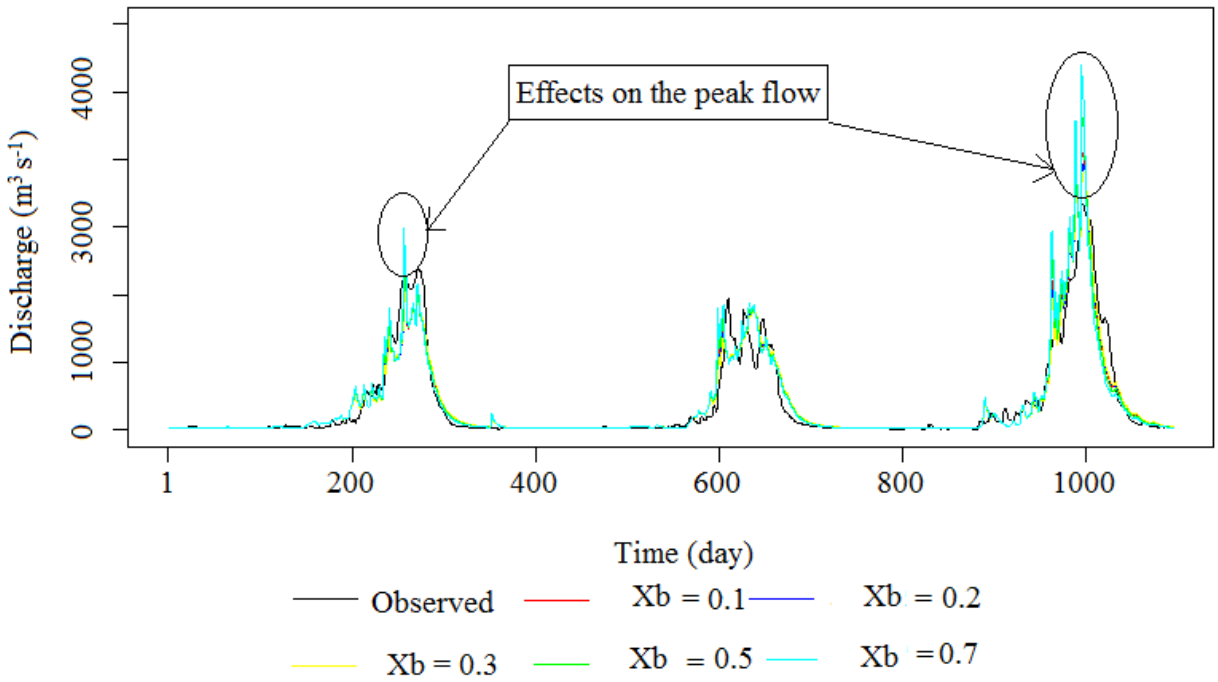


*Figure 5.4.Sensitivity of the hydrological model to change in the Xb parameter value*

### 5.2.5. Effects of the power preferential flow parameter.

The Power Preferential Flow (PPF) parameter is used as a power function relating preferential flow with the relative saturation of the soil (Van der Knijff and De Roo., 2008). The sensitivity analysis results showed that LISFLOOD hydrological model is very sensitive to PPF parameter. Both the rising limb and peak discharge decrease as the value of PPF increased (Figure 5.5). PPF value of '2' gave the best performance measure as shown in Table 5.2

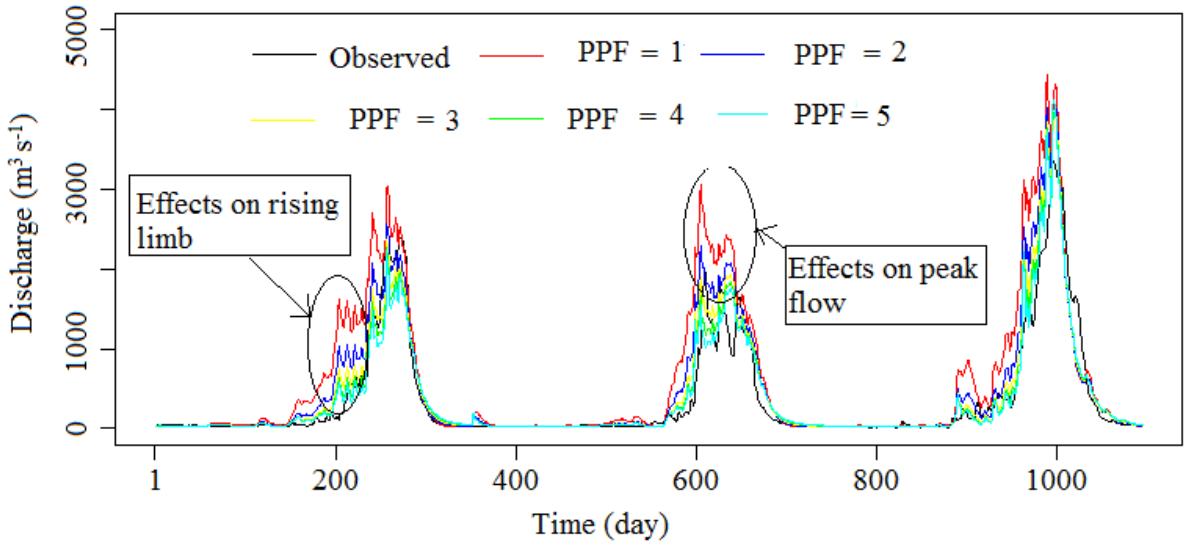


*Figure 5.5.Sensitivity of the hydrological model to change in the PPF parameter value*

### 5.2.6. Calibration and validation results

The calibration of the hydrological model using data from 2001 to 2003 resulted in NSE and RMSE values of 0.87 and 237 $m^3/s$ while the model validation using data from 2005 to 2007 produced better performance measures (NSE=0.94 and RMSE= 179 $m^3/s$). The values of the final calibration parameters are shown in Table 5.3.

*Table 5.3. Values of the calibrated parameters using trial and error method*

| Parameter | Optimal values | Lower bound | Upper bound |
|---|---|---|---|
| Upper zone time constant | 10 | 1 | 50 |
| Lower zone time constant | 1300 | 50 | 5000 |
| Ground water percolation value | 0.1 | 0 | 1.5 |
| Xinanjiang parameter b | 0.3 | 0.1 | 1 |
| Power preferential flow | 2 | 1 | 6 |

Generally, the goodness of-fit measures for calibration are better than for validation (e.g. Sintondji, 2005; Bormann and Diekkrüger, 2003) since the calibration process seeks to minimize the differences between the observed and simulated time series. In this case study, the goodness-of-fit measures are actually better for validation than calibration. This would suggest that variability from the norm in the calibration data set is greater than in the validation data set. The same behavior of LISFLOOD hydrological model was observed by Thiemig et al. (2015) for the Olifants River at Loskop North (15, 000 $km^2$ ) in South Africa: the modified version of the Kling-Gupta Efficiency (KGE') values obtained by these Authors were better for validation (KGE'= 0.56) than calibration (KGE'=0.34). Also, the performance measures of the same hydrological model obtained by Koriche (2012) for the upper and middle Awash River Basin (Ethiopia) were better for validation (NSE=0.82 and RMSE= 29.37 $m^3 s^{-1}$) than calibration (NSE=0.72 and RMSE=55.29 $m^3 s^{-1}$). Moreover, the RMSE values for both the calibration and validation periods represent less than 10% of the mean annual peak flows and about 50 % of the mean stream flow values. These acceptable values of performance measures (NSE) prove that the calibration process compensate for some of the errors in the input data and LISFLOOD hydrological model can be used to predict flood in the Oti River. Also, the good NSE values of LISFLOOD hydrological model may be because it was primarily developed to predict flood discharges.

Furthermore, Figure 5.6 and Figure 5.7 show respectively the comparison between observed and simulated hydrographs during calibration and validation of the LISFLOOD hydrological model at Sabari gauge station (Ghana). In the year 2001, the observed peak flow is higher than the simulated peak flow, whereas in 2002, 2003, 2005, 2006 and 2007 the difference between the observed and simulated peak flows is low as shown by the values of PD which are

respectively 6.8 %, 0.5%, -2.7%, 2.6%, 1.3% and 0.7% for the years 2001, 2002, 2003, 2005, 2006 and 2007.

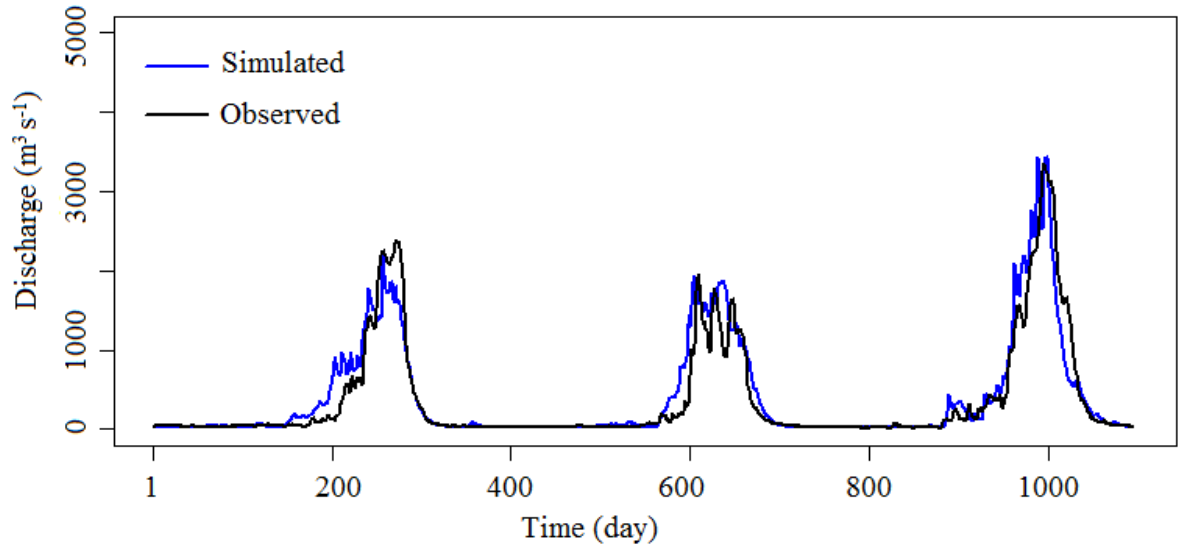


*Figure 5.6. Comparison between simulated (blue line) and observed (black line) hydrographs for the calibration at Sabari gauge station (Ghana)*

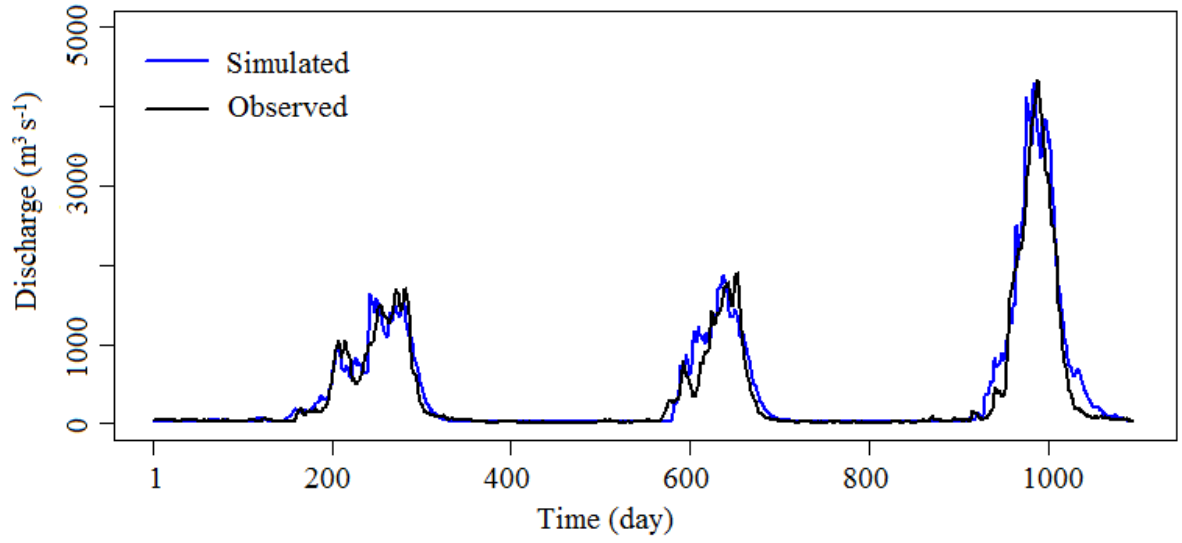


*Figure 5.7.Comparison between simulated (blue line) and observed (black line) hydrographs for the validation at Sabari gauge station (Ghana)*

It is worth to mention that parameter uncertainty analysis was not considered in the present study under the assumption that uncertainty from the data will dominate the hydrological modelling (He et al., 2009).

# 6. FLOOD HAZARD MAPPING

## 6.1. Input hydrographs

Due to the lack of observed input discharge to calibrate the flood inundation model, the calibrated hydrological model was used to simulate the input discharges. Figure 6.1 shows the comparison between the simulated hydrographs at the inlet (Mandouri with an area of 29,100 $km^2$) and outlet of the studied reach. It can be noted that the peak discharge at the outlet of the studied reach is about 31% higher than the peak flow at the inlet. This increase of discharge from the upstream boundary to the downstream end suggests some contributions of lateral inflow which need to be taken into account in the hydraulic modelling.

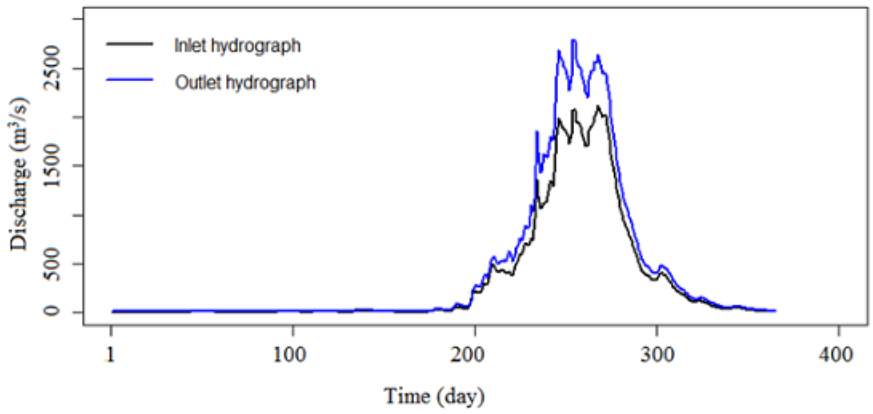


*Figure 6.1. Simulated hydrographs of the 2007 flood at inlet and outlet of the studied reach.*

## 6.2. Hydraulic modelling

### 6.2.1. Sensitivity analysis

Table 6.1 and Figure 6.2 show respectively the initial parameters of the model (obtained from Leopold and Maddock, 1953 and Chow, 1959) and the performance of the LISFLOOD-FP at 960 m DEM resolution with different Manning's friction coefficients for the channel (Figure 6a) and with different values of the hydraulic geometry coefficient *r* (Figure 6b).

*Table 6.1. Initial values of the hydraulic model (LISFLOOD-FP) parameters.*

| Parameters | $n_c$ | $n_{fp}$ | $p$ | $r$ |
|---|---|---|---|---|
| Initial values | 0.03 | 0.04 | 0.74 | 0.36 |

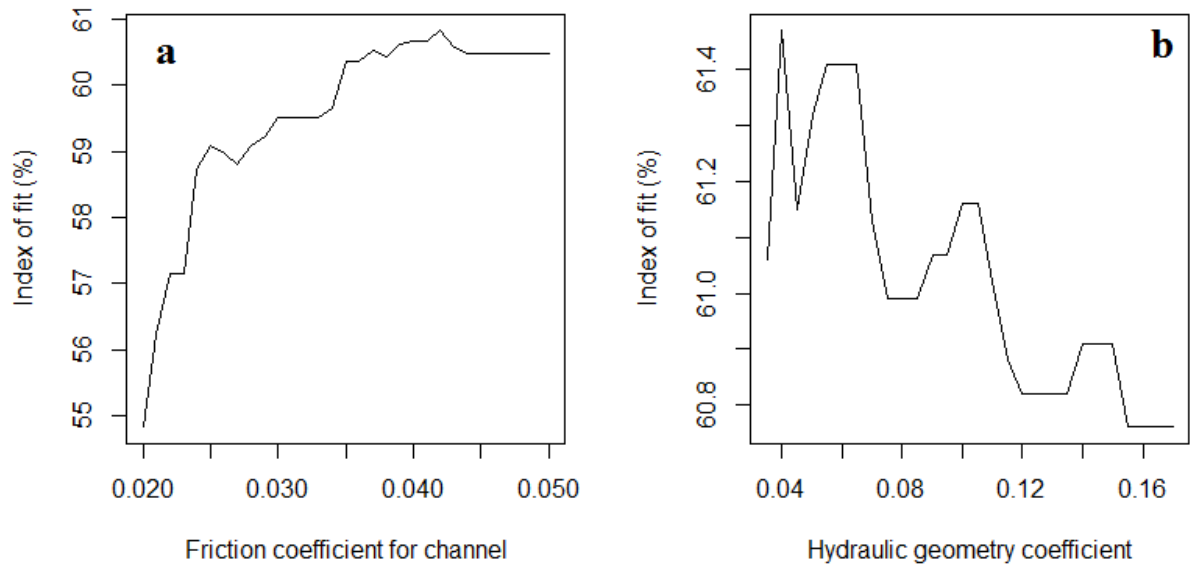


*Figure 6.2. Performance of the sub-grid model of LISFLOOD-FP with different Manning's friction coefficient for channel (a) and with different hydraulic geometry coefficient (b)*

One can note that the performance of the sub-grid model peaked at $n_c$ of 0.042 but decreased with further increase in the value of $n_c$. The model performance was less sensitive to Manning's *n* when the optimal *n* was exceeded. This behavior is commonly seen when large

flood events are assessed using spatial performance measures because the flood extent tends to increase only gradually with increased water depth once most of the floodplain valley is inundated. The maximum performance measure for *r* was obtained at 0.04. From these results, it is clear that both the friction coefficient for the channel and the hydraulic geometry coefficient could influence the inundation extent in this case study. However, the sensitivity of the model results to the hydraulic geometry coefficient was relatively low compared to friction coefficient for channel.

### 6.2.2. Effects of the DEM resolution on the simulation results

Figure 6.3 shows the simulations results for the different aggregated DEM resolutions. The simulated water surface elevations are almost the same for the different aggregated DEM resolutions with a slight difference at about 80 km of the reach where the water surface elevations from 480m and 960m DEM resolutions are over 1 m lower than the water surface elevations for 30m, 60m, 120 m and 240m DEM resolutions.

Generally, by changing the resolution of the floodplain DEM, other inputs to the model namely channel width and bank elevation must be aggregated as the resolution coarsens. This can locally affect the channel slope and simulated water surface elevations along with the differing topographies. However, the results of the present study show that the DEM resolution doesn't really affect the water surface elevation simulations in many locations, meaning that the changes in extent with resolution are essentially due to the detail of the DEM rather than any more complex hydraulic interaction between the DEM and river channel.

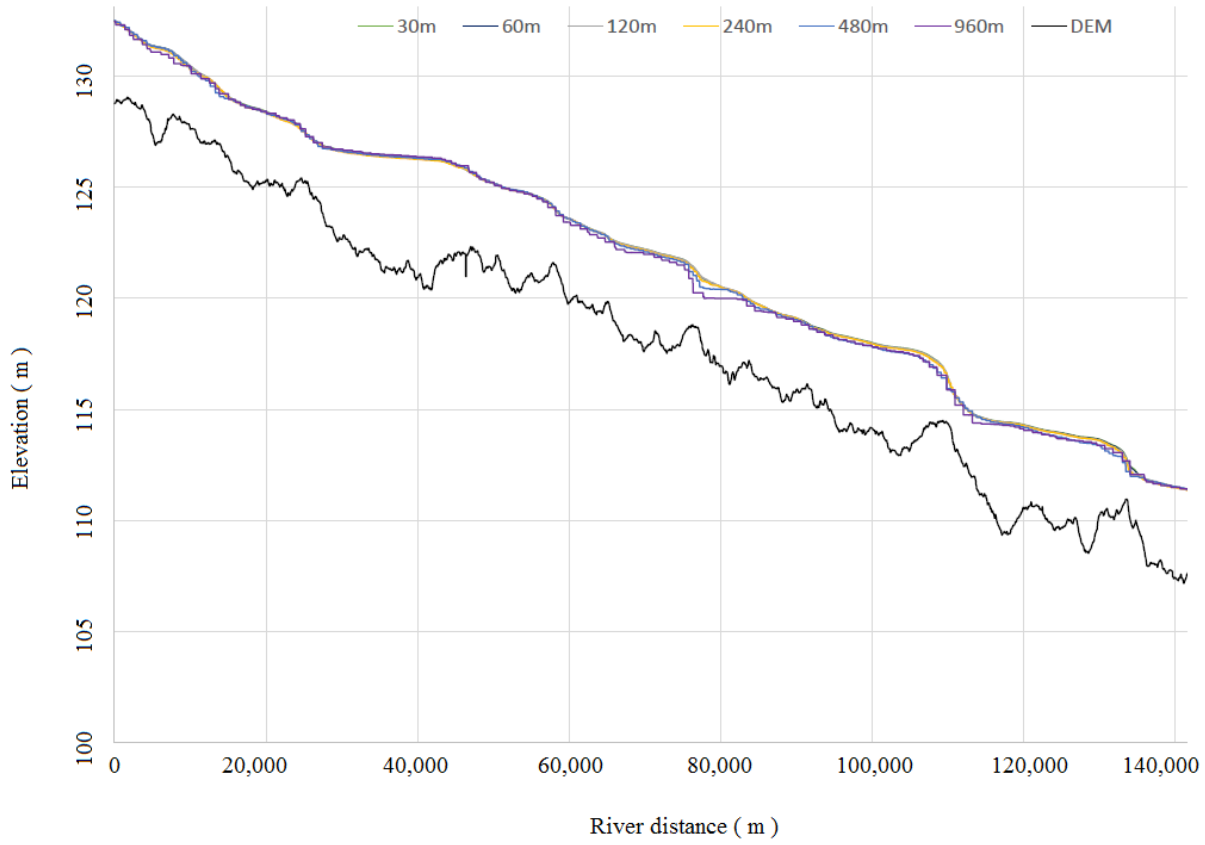


*Figure 6.3. Floodplain longitudinal profile (black and with 30 m DEM) and water surface elevations simulated by LISFLOOD-FP for different aggregated DEM resolutions.*

Moreover, Table 6.2 presents the variation of the performance in simulating the flood extent when the DEM resolution coarsens. This Table shows that the performance of the model actually increases when the resolution coarsens until the optimum resolution is exceeded and there could be a number of reasons for this. It might be that the local scale noise in the SRTM data is reducing the accuracy of the inundation simulation at finer resolution: for example, some smoothing of the DEM by aggregating to coarser resolution might be beneficial for the flood extent simulation in this case. Another factor is the validation data resolution. The model performs worse at finer resolutions than the model validation data and this might be expected given that the validation data cannot represent the finer scale detail in the inundation model.

Similar results were obtained by Dutta and Nakayama (2008) who conclude that there is a threshold resolution of DEM (100 m in their case) in the simulated surface inundation beyond which the model outcomes become arbitrary. For this case study, the threshold resolution could be 480 m.

*Table 6.2.Performance of the sub-grid model of LISFLOOD-FP for different DEM resolutions.*

| DEM resolutions (m) | 30 | 60 | 120 | 240 | 480 | 960 |
|---|---|---|---|---|---|---|
| Index of fit (%) | 52 | 53 | 56 | 59 | 60 | 59 |

### 6.2.3. Simulation of the 2007 flood event

The optimum parameters are given in Table 6.3 while Figure 6.4 shows the results of the calibration for the hydraulic model at 480 m DEM resolution as contour plots of measure of fit over the parameter range. The best fit of the sub-grid model of LISFLOOD-FP is characterized by a Manning's coefficient for channel ($n_c$) of around 0.045 $m^{1/3}s^{-1}$ and 0.05 for the coefficient of the hydraulic geometry ($r$). However, by analyzing Figure 4.18, one can observe that different combinations of optimum parameter values may fit the calibration data equally. This equifinality in flood inundation model has been well illustrated in the literature (Di Baldassarre, 2012; Bates et al., 2005; Romanowicz and Beven, 2003).

*Table 6.3. Models' parameters used for the flood inundation modelling.*

| Parameters | $n_c$ | $n_{fp}$ | $p$ | $r$ |
|---|---|---|---|---|
| Optimum parameters | 0.045 | 0.04 | 0.74 | 0.05 |

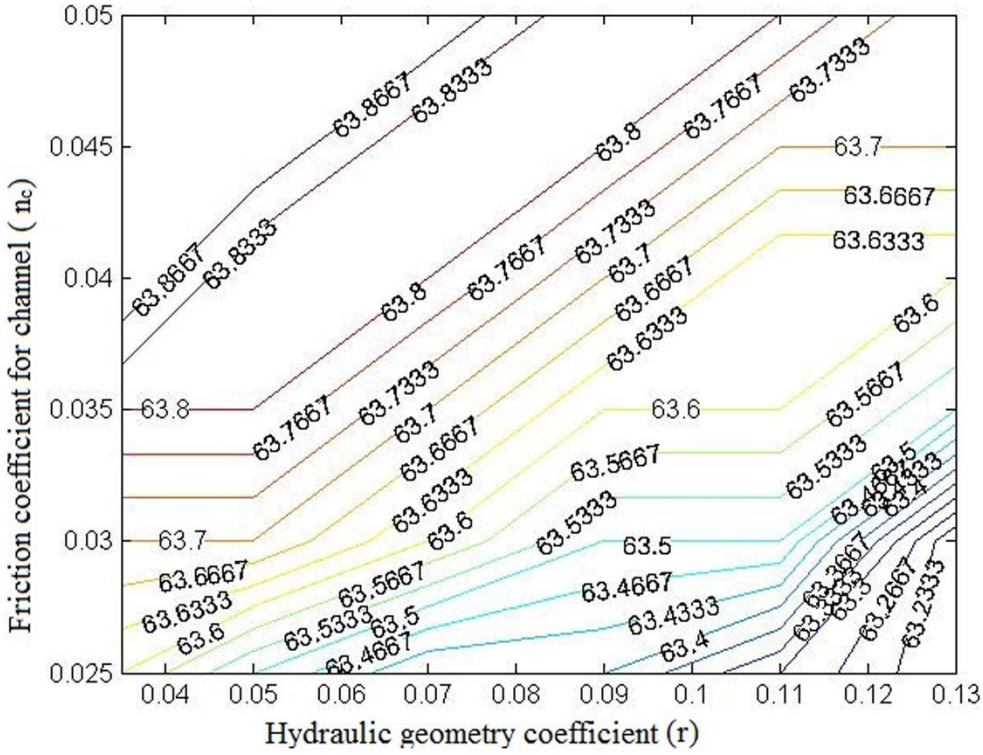


*Figure 6.4.Results of the calibration of the sub-grid model of LISFLOOD-FP showing measures of fit as a function of the hydraulic geometry coefficient and the Manning's friction coefficient for channel.*

In addition, Figure 6.5 shows that there is agreement between the simulated flood extent and the satellite observation in a maximum of flood areas along the main river channel. However, the hydraulic model suggested flooding in some areas where the satellite detected none. The disagreements between the observed and simulated flood extents occur where the centrelines derived from the DEM by flow accumulation do not correspond with observed river channel locations. Moreover, some of the flooding occurred on tributaries that we have not included in the model. Another possible reason for this disagreement is that the inundation at some areas did not last until the time when the satellite image was captured.

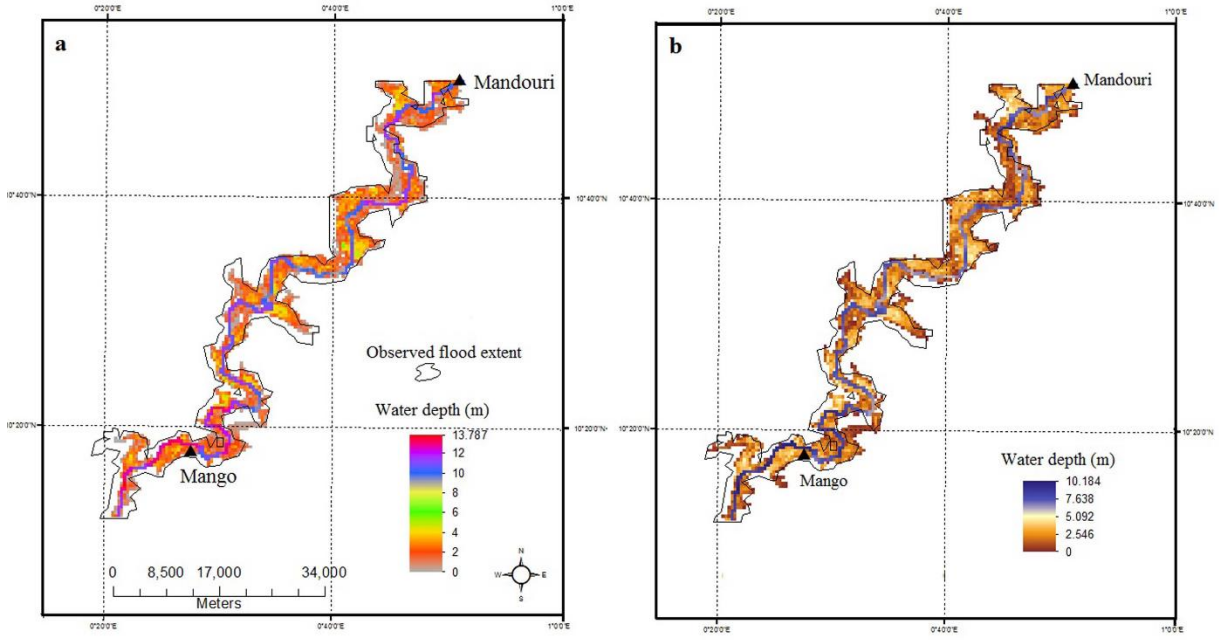


*Figure 6.5. Comparison of simulated flood extent (red) with satellite observation (black outline) before calibration (a) and after calibration (b) for the severe flood of September 2007.*

Finally, the performance measures of 60% and 64 % were achieved for the simulated flood extent respectively prior to the calibration (Figure 6.5a) and after the calibration (Figure 6.5b). The values of F found for this study are relatively low compared to previous studies where either high resolution topography data was available or the floodplain was many kilometers wide (e.g. Bates and De Roo, 2000; Horrit and Bates, 2001; Wilson et al., 2007) but high compared to the results from other data sparse areas such as Amarnath et al. (2015) who found 38 % for F and similar to the results of Sayama et al. (2012) who found 61% for F. However, the model simulation can be considered as an acceptable result because the majority of the flooded areas along the main reach was identified as shown visually in Figure 6.5b and other studies have obtained similar fits when SRTM data has been used.

### 6.2.4. Flood hazard mapping

Table 6.4 and Figure 6.6 shows respectively the design floods and the simulated flood hazard maps. It can be seen from Figure 4.20 that the differences between the inundation areas for the different return periods (10, 20, 30 and 50 years) is not significant while the maximum water depth increase slightly (from 9.53 m for the 10-year flood to 9.71m for the 50-year flood). This result can be explained by the fact that the flood frequency curve for the study site is relatively flat. In addition, depending on the thickness of the overbank sediments, the degree of relief on the floodplain surface and the width of the floodplain relative to the size of the river, floods of higher return periods or greater magnitude can be characterized by increased depths and velocities but do not usually affect a much wider area (Thompson and Clayton, 2002).

*Table 6.4. Design floods for the outlet of the channel reach*

| Return periods | Flood quantiles ($m^3/s$) | 95 % confidence interval |
|---|---|---|
| 5 | 1,363 | [1,359 ; 1,366 ] |
| 20 | 1,746 | [1,741 ; 1,750] |
| 30 | 1,808 | [1,803 ; 1,813] |
| 50 | 1,868 | [1,862 ; 1,873] |

The simulated flood hazard maps can provide additional information for efficient flood risk management in the Oti River Basin. However, it is worth noting that fluvial flood hazard mapping is affected by various sources of uncertainty including data and model parameter uncertainties. (Beven et al., 2011; Apel et al., 2008; Aronica et al., 2002). There are many methods for evaluating uncertainty in flood inundation modelling. However, classical uncertainty estimation is based on sampling methods (Monte Carlo, GLUE) which are computationally expensive. Thus, the parameter sensitivity analysis (instead of complete uncertainty analysis)

performed in this study can help in understanding the simulation uncertainty, as well as the behavior of the hydraulic model for different parameter values (Sayama et al., 2012).

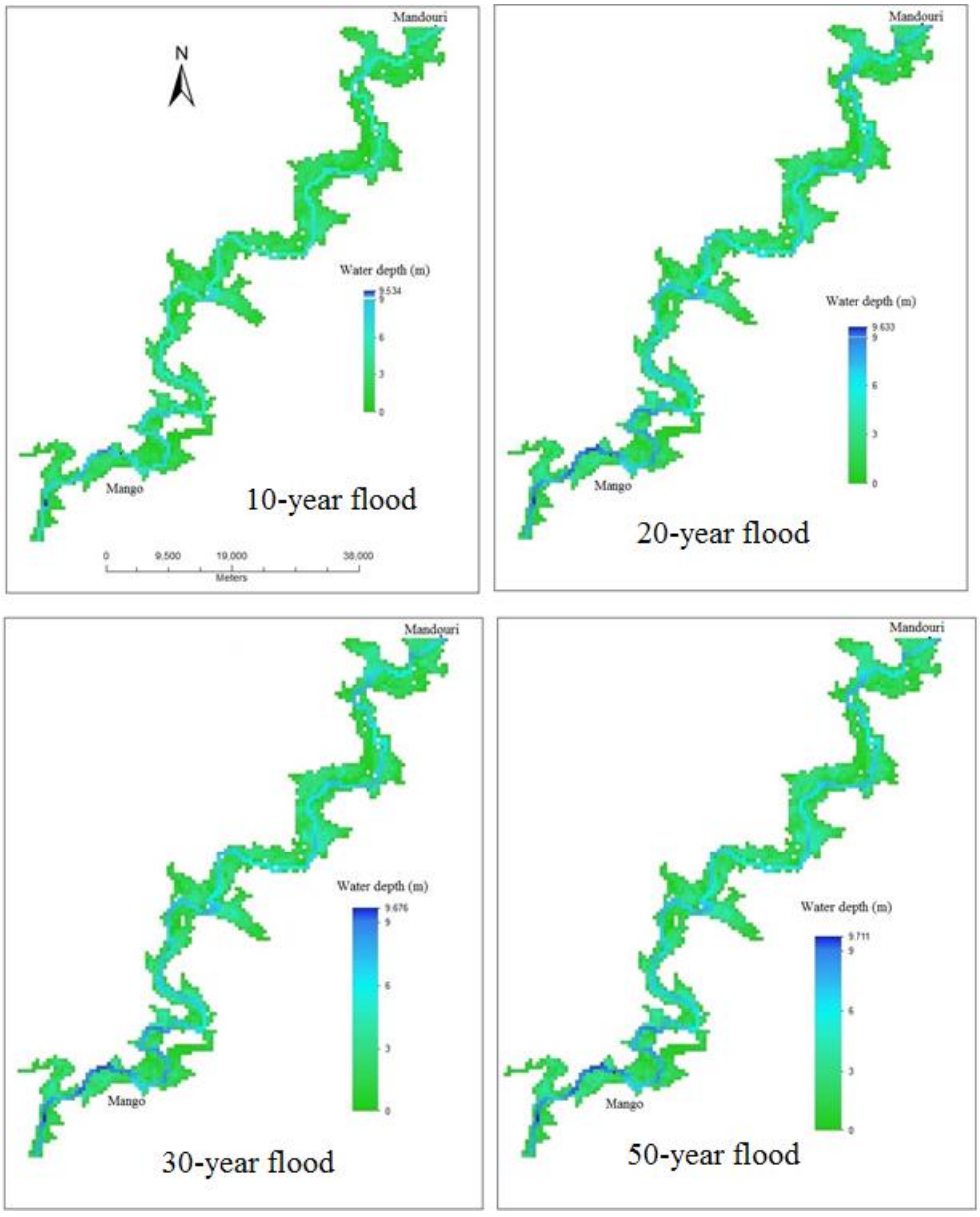


*Figure 6.6. Simulated flood hazard maps of the study area*

# 7. INTEGRATED FLOOD RISK ASSESSMENT

## 7.1. Scores

Table 7.1 shows the scores allocated by the communities and the associated weights. As it is expected, there are differences in the scores assigned to some of the indicators in this case study. For example, 57.15 %, 28.57 % and 14.29 % of the studied communities score respectively low, medium and high levels for 'lifelines' indicator and 14.29 %, 57.15% and 28.57 % of the communities score respectively low, medium and high levels for the 'area under forest indicator' (V14) However, these communities have almost the same scores for many indicators, for instance those which characterize the hazard as well as the social and economic vulnerability. Moreover, the scores obtained for most of the capacity and measures indicators are relatively low and consequently high for the vulnerability indicators. All of the communities score low level for many indicators of the 'capacities and measures' factor (e.g. C2, C7, C9,C10, C11 and C12) and high level for many indicators of the vulnerability factor such us poverty level and literacy rate. The low scores for the capacity and measures indicators highlight the insufficiency of social, economic and institutional capacities to cope with extreme floods in the Oti River Basin (Togo). For instance, the people interviewed pointed out the absence of flood risk management committee at the village level, non-access to local emergency fund and insurances for house owners. In addition, education and culture of flood risk management are not part of the school curricula. Apart from Sadori, Mango and Borgou, the investigated communities lack early warning systems and emergency plans for extreme floods.

*Table 7.1.Scores obtained by the communities: experienced hazard (a) and possible hazard (b)*

| Factor component | Indicator Name | Borgou | Tambigou | Tchanaga | Tchamoga | Mogou | Mango | Sadori |
|---|---|---|---|---|---|---|---|---|
| **HAZARD** | | **S** | **S** | **S** | **S** | **S** | **S** | **S** |
| Probability | **(**H1) Occurrence ( a) | 3 | 3 | 3 | 3 | 3 | 3 | 3 |
| | **(**H2) Occurrence (b) | 2 | 2 | 2 | 2 | 2 | 2 | 2 |
| Severity | (H3) Intensity (a) | 3 | 3 | 3 | 3 | 3 | 3 | 3 |
| | (H4) Intensity (b) | 3 | 3 | 3 | 3 | 3 | 3 | 3 |
| **EXPOSURE** | | | | | | | | |
| Structures | (E1) Number of houses | 1 | 1 | 1 | 1 | 1 | 1 | 1 |
| | (E2) Lifelines | 1 | 1 | 1 | 2 | 2 | 3 | 1 |
| Economy | (E3) Economy | 1 | 1 | 1 | 1 | 1 | 1 | 1 |
| Population | (E4) Population | 1 | 1 | 1 | 1 | 1 | 1 | 1 |
| **VULNERABILITY** | | | | | | | | |
| Physical | (V1) Density | 1 | 1 | 1 | 1 | 1 | 1 | 1 |
| | (V2) Demographic pressure | 2 | 2 | 2 | 2 | 2 | 2 | 2 |
| | (V3) Flood-prone areas | 2 | 2 | 2 | 2 | 2 | 2 | 3 |
| | (V4) Access to basic services. | 3 | 3 | 3 | 2 | 2 | 1 | 3 |
| Social | (V5) Poverty level | 3 | 3 | 3 | 3 | 3 | 3 | 3 |
| | (V6) Literacy | 3 | 3 | 3 | 3 | 3 | 1 | 3 |
| | (V7) Attitude | 2 | 2 | 2 | 2 | 2 | 3 | 2 |
| | (V8) Decentralization | 2 | 2 | 2 | 2 | 2 | 2 | 2 |
| | (V9) Participation | 3 | 3 | 3 | 3 | 3 | 3 | 3 |
| Economic | (V10) Local resource base | 3 | 3 | 3 | 3 | 3 | 3 | 3 |
| | (V11) Diversification | 3 | 3 | 3 | 3 | 3 | 2 | 3 |
| | (V12) Stability | 3 | 3 | 3 | 3 | 3 | 3 | 3 |
| | (V13) Accessibility | 2 | 2 | 2 | 2 | 2 | 2 | 2 |
| Environmental | (V14) Area under forest | 3 | 2 | 2 | 3 | 2 | 2 | 1 |
| **CAPACITIES AND MEASURES** | | | | | | | | |
| Physical capacity | (C1) Land use planning | 3 | 3 | 3 | 3 | 3 | 3 | 3 |
| | (C2) Preventive measures | 1 | 1 | 1 | 1 | 1 | 1 | 1 |
| | (C3) Environmental management | 2 | 2 | 2 | 2 | 2 | 2 | 2 |
| Societal capacity | (C4) Public awareness | 2 | 2 | 2 | 2 | 2 | 2 | 2 |
| | (C5) School curriculum | 0 | 0 | 0 | 0 | 0 | 0 | 0 |
| | (C6) Public participation | 3 | 3 | 3 | 3 | 3 | 3 | 3 |
| Economic capacity | (C7) Access to national fund | 1 | 1 | 1 | 1 | 1 | 1 | 1 |
| | (C8) Access to international fund | 3 | 3 | 3 | 3 | 3 | 3 | 3 |
| | (C9) Insurance market | 1 | 1 | 1 | 1 | 1 | 1 | 1 |
| Management and Institutional Capacity | (C10) Risk management/emergency | 1 | 1 | 1 | 1 | 1 | 1 | 1 |
| | (C11) Risk map | 1 | 1 | 1 | 1 | 1 | 1 | 1 |
| | (C12) Emergency plan | 1 | 0 | 0 | 0 | 0 | 1 | 1 |
| | (C13) Early warning system | 2 | 0 | 0 | 0 | 0 | 2 | 2 |
| | (C14) Institutional capacity | 1 | 1 | 1 | 1 | 1 | 1 | 1 |
| | (C15) Communication | 1 | 1 | 1 | 1 | 1 | 1 | 1 |

Consequently, decreasing vulnerability and increasing capacity of the communities to manage their own flood risk should be paramount in order to mitigate flood risk in the study area. For example, due to the high poverty level in the majority of the community areas, creating new income-generating opportunities could be essential to reduce the vulnerability of the local population. The results of this study showed the need for non-structural measures to reduce the negative consequences of floods in the study area. These measures include the implementation of early flood warning systems for all the flood-prone communes and public education about flood risk, real involvement of wide range of local actors in national efforts to manage flood risks so that they can contribute as much as possible to the reduction of flood risks in their own localities; and creation of culture of awareness in which the population realizes the negative impacts of floods on development. Moreover, actions to discourage settlements in flood-prone areas and building codes to make houses more resilient to flooding are useful to mitigate flood risk in the Oti River Basin.

## 7.2. Possible flood hazard severity

Figure 7.1 shows the 50-year flood hazard map simulated by the hydraulic modelling. This result is used to estimate the severity of the possible flood hazard. When the set of thresholds applied in Table 3.10 are considered, all the community areas fall in high flood severity. Sadori community has the highest flood depth while Mango community has the lowest flood depth (Table 7.2). The difference in simulated flood depth can be explained by the variability of both the local topography and soil properties of the studied villages. Also, it is worth to note that the flood depth at the communities may be higher than simulated, given that flooding from tributaries were not considered in this study.

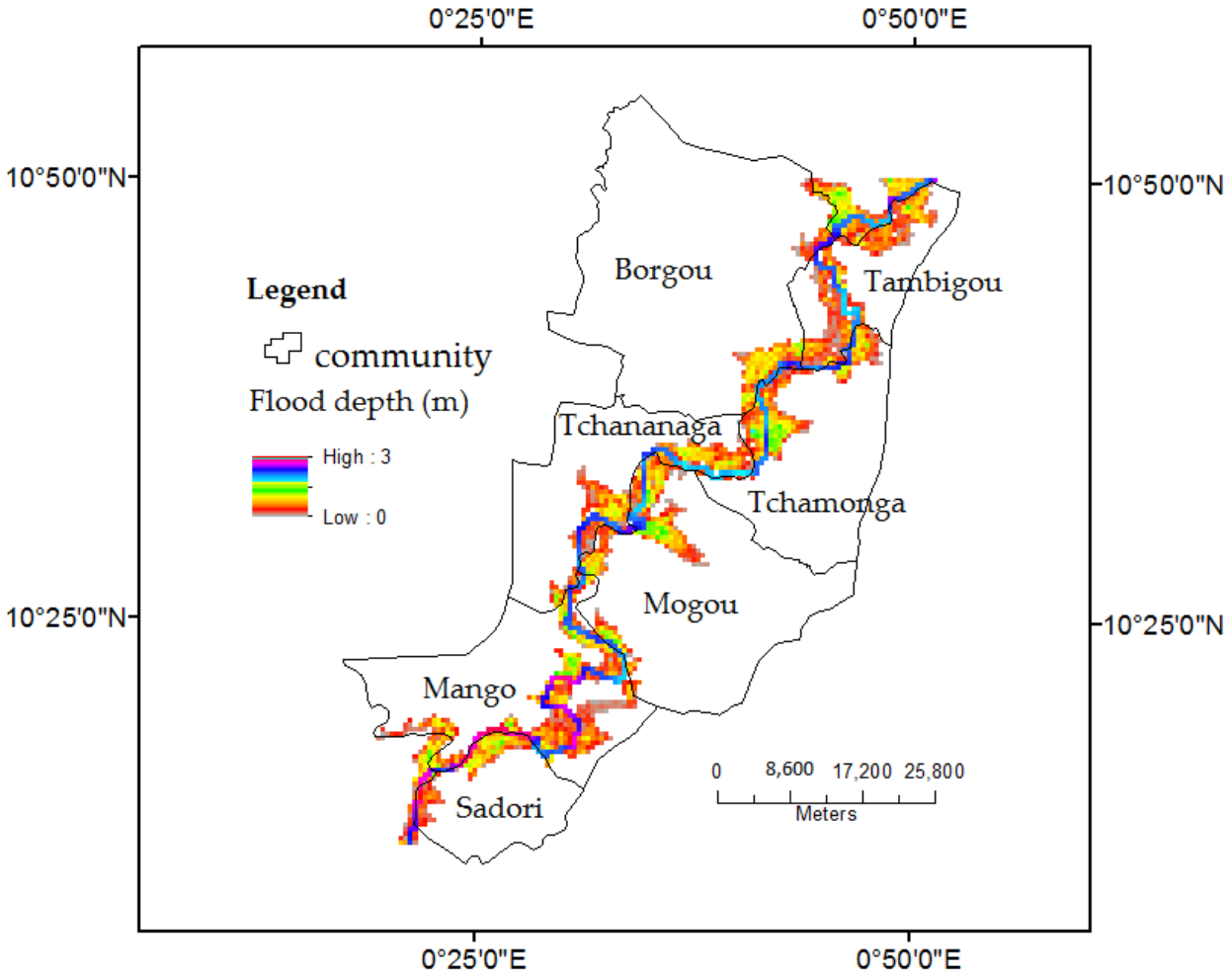


*Figure 7.1. Simulated 50-year flood map of the Oti River Basin in Togo*

*Table 7.2.Averaged simulated flood depth for the 50-year flood at the different communities in the Oti River Basin.*

| Community | Averaged flood depth (m) | Severity |
|---|---|---|
| Borgou | 1.57 | High |
| Tambigou | 1.53 | High |
| Tchanaga | 1.56 | High |
| Tchamonga | 1.54 | High |
| Mogou | 1.60 | High |
| Mango | 1.52 | High |
| Sadori | 1.62 | High |

## 7.3. Indices of the risk factors

Figure 7.2 shows the indices of the four factors that contribute to the risk in the CBDRI model. It is clear from this Figure that the hazard and vulnerability are the major factors that contribute to the overall flood risk in the communities selected for this study. The high level of hazard index (H) can be explained by the repeated and catastrophic floods that have impacted the communities of the Oti River Basin during the last two decades (1998, 2007, 2008 and 2010) and the high level of simulated flood depth, while the observed elevated vulnerability index (V) is mainly due the high poverty level of the communities and insufficiency of access to basic services such as safe drinking water. Furthermore, the relative homogeneity observed in the majority of the vulnerability and coping capacity is reasonable because the studied communities are almost similar in their social and economic profiles as shown by their poverty levels. In addition, their economic capacities for disaster risk management are also the same: all are funded by non-governmental organization in case of flood disaster. They are managed at the top by a central government (lack of decentralization). For this reason, large difference in vulnerability and capacities in the Oti River Basin at the village scale is unexpected.

## 7.4. Flood risk index

As it is shown in Table 7.3, flood risk in all the studied communities is moderate when we consider the classification shown in Table 3.11. This moderate level of flood risk is associated with a combination of high indices of flood hazard as well as vulnerability to flood and low indices of capacities and exposure. In addition Mango has the highest flood risk index (5.01) while the lowest flood risk index is estimated at Tambigou and Tchanaga (4.36). The small difference (0.65) between the highest and lowest flood risk indices is an indication of the relative homogeneity of flood risk across these communities.

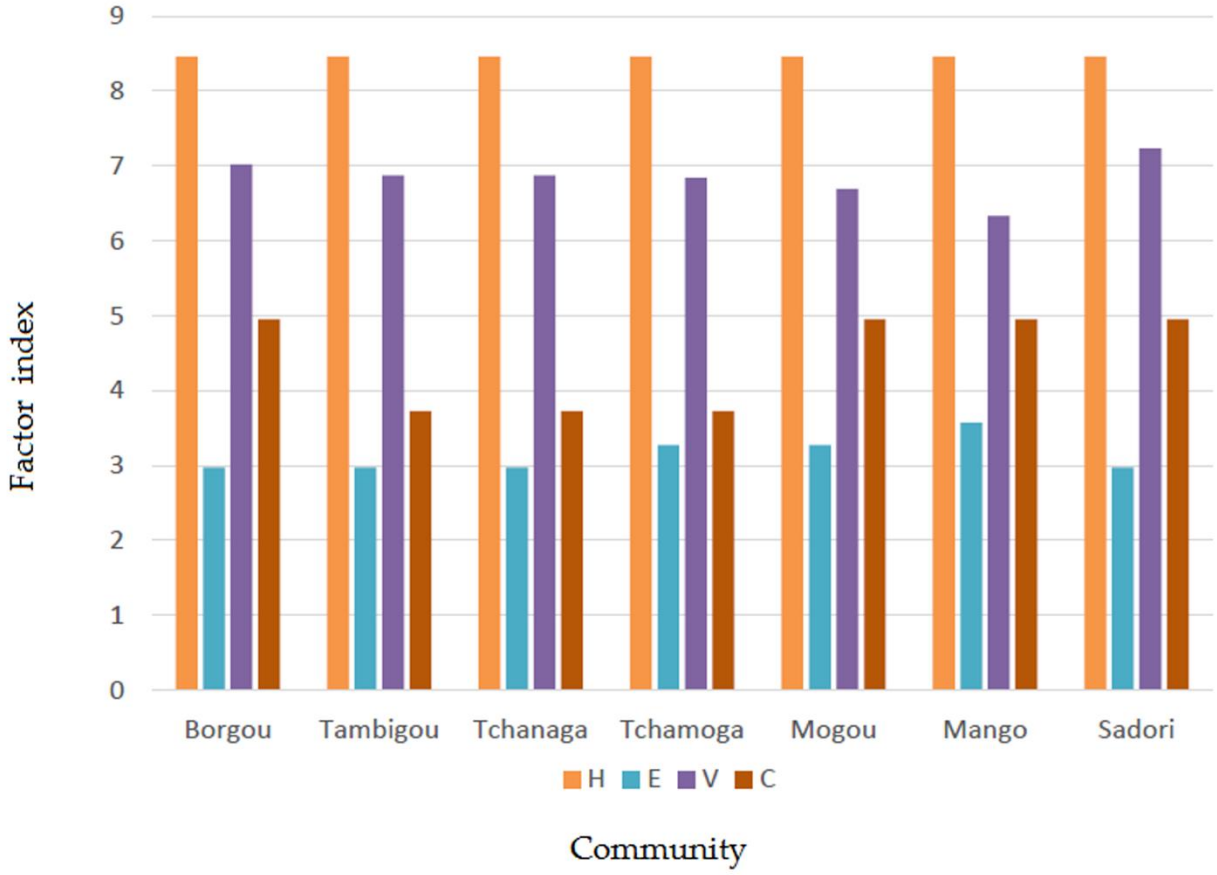


*Figure 7.2. Computed indices of the four risk factors for the different communities. C, H, V and E stand for capacities, hazard, vulnerability and exposure indices.*

*Table 7.3. Flood risk index of the different communities*

| Communities | Borgou | Tambigou | Tchanaga | Tchamoga | Mogou | Mango | Sadori |
|---|---|---|---|---|---|---|---|
| Risk index | *4.62* | *4.36* | *4.36* | *4.78* | *4.85* | *5.01* | *4.76* |

In this study, the estimated flood risk indices summarize complex information about flood risk in a simple way that is easy for non-experts to understand and use in flood risk management policies. However, the majority of some data were subjective as they were collected from selected local residents.

# 8. GENERAL CONCLUSIONS

## 8.1. Summary

The main objective of this study is to develop some methodologies for flood risk assessment in poorly gauged river basins taking the Oti River Basin as case study. Specifically, it focused on the identification of the suitable models for flood frequency estimation, the modelling of flood hazards and the analysis of the main factors that contribute to flood risk in the study area.

First, we have presented a flood estimation procedure for the Volta River Basin in West Africa using regional flood frequency analysis methods based on L-moments. This study represents a huge step forward in the local context towards improvement of design flood estimates. The selection of the appropriate frequency distributions was based on the identification of homogeneous regions using both clustering algorithm and statistical tests, L-moment ratio diagrams, quantile-quantile plots and a numerical goodness-of- fit test (Z-statistic). It was found that GPA and GEV distributions are the most robust flood frequency distributions among five candidates distribution with three parameters. In addition, the relatively flat shape of the flood frequency curves may suggest that flood in the Volta River Basin is caused by an accumulation of rainfall over the monsoon (rainy season) rather than by a storm rainfall.

Second, a methodology for simulating flood hazard maps at ungauged basins is presented. This methodology links hydrological modelling, regional flood frequency analysis and hydraulic modelling to simulate flood inundation maps. The performance of the hydraulic model was checked by an index of fit and we found that the sub-grid model of LISFLOOD-FP can be used to delineate flood inundation areas for the study area with an acceptable (given the DEM data available) index of fit of 64 %. However, there are many obstacles in modelling flood hazard in

the Oti River Basin because not enough data are available. In addition, although the DEM used in this study is the best available for this region, it is still considered very poor when compared to those from elsewhere like LiDAR elevation data used in many developed countries. The results from the sensitivity analysis indicates the importance of the DEM resolution, the Manning's friction and the hydraulic geometry of the river in flood inundation modelling. Finally, the study showed that changes in the flood extent with DEM resolution are mainly due to the detail of the DEM rather than the hydraulic interaction between the DEM and the river channel. The possibility to identify and predict flood prone areas at ungauged rivers is the major advantage of the proposed methodology. It is the first time that a flood hazard mapping is performed for the Oti River Basin and the outcomes of this study can contribute to an efficient flood risk management in this area. For instance, flood inundation maps can help in mitigating flood damages, establishing early flood warning systems and discouraging new settlements in flood-prone areas.

Third, we performed a comprehensive flood risk assessment of rural communities in the Oti River Basin of Togo and identified the relative contributions of hazard, exposure, vulnerability and lack of coping capacity factors to flood risk. In this work, while the flood risk for the rural communities studied is moderate, there were high levels of hazard, vulnerability and lack of capacity and measures, whereas the exposure is relatively low. The application of the CBDRI model showed that the model can be useful for an integrated flood risk assessment, particularly in data scarce environments of West Africa where the required data for conventional flood risk assessment are missing. In addition, the outcomes of this study provide community members as well as governments officials with empirical risks and vulnerabilities evidence. Consequently, the information provided by the community-based disaster risk index system can be used to

support decision- makers at local and national levels in order to analyze and understand the flood risk a community is exposed to. Also, periodic application of the proposed method can be a measure to examine the projects undertaken to manage flood risks. In order to reduce flood risk in the Oti River Basin, decreasing vulnerability through creation of income-generating opportunities and increasing capacity of communities to manage their own flood risk should be paramount.

## 8.2. Limits

The results of CBDRI model are dependent on the selected indicators, their categorization, as well as the set of thresholds and the spatial scale of application. The selected indicators are only simplification of key elements of flood risk and vulnerabilities that we wanted to measure; they are not real measures of these elements themselves. In addition, the return period associated to the simulated flood hazard severity is 50 years. Given the significant contribution of the hazard factor to the total flood risk, the results will differ if flood with lower or higher return period than 50 years is used.

In addition, due to the coarse resolution (30 m and 90 m) of the topography data, the need to use both simulated input hydrographs and remote sensing data and the lack of sufficient observed flood extent and discharge data to conventionally validate the flood inundation model for the study area, it is rather difficult to isolate sources of uncertainties in the predictions of the models.

## 8.3. Recommendations for policy

Based on the assessment of flood risk in the Oti River Basin presented in this study, the following recommendations have been suggested:

1) Necessity to implement functional flood early warning systems in floodplain areas as technical adaptation strategy to the effects of climate change. Currently, elementary early warning systems of flood are installed in some communities (Borgou, Mango and Sadori) but they should be extended and improved.

2) To be more effective, flood warning systems can be combined with a high level of community awareness: considering the presence of housing units in areas at high risk of flooding (Figure 7.2) and the flood damages during the past flood events, public awareness of flood should be systematically raised in the study area. Thus, the public is aware that there is a need to restrict uses of flood prone areas for housing, and industrial purposes in order to reduce the potential flood damages.

3) The incorporation of flood risk topics in school curricula and public programs are also crucial to the success of flood early warning systems.

4)Furthermore, public participation in decision making regarding flood risk management is important to improve the implementation of the measures and to give the community the opportunity to express their concerns.

5) Local emergency group to respond to flood events should be prepared in due time and maintained operational in flood prone areas.

6) The creation of new incomes-generating activities are important to reduce the economic vulnerability of the communities because of the high poverty level of the local population in the Togo part of the Oti River Basin.

7) Finally, the retention of excess water into natural and artificial flood retention areas (reservoirs) -which are adequately regulated- may be useful against extreme floods.

## 8.4. Perspectives

The following recommendations are suggested for further research in the Oti River Basin:

1) It is important to understand the future effects of both climate and land use changes on flood risk in the Oti River Basin, given that human activities (urbanization, agricultural practices and deforestation) and climate change will change considerably the situation of flood in river basins.

2) A functional flood forecasting model should be validated, introduced and regularly improved for the Oti River Basin.

3) Flow monitoring stations should be installed in the Togo part of the Oti River to provide continuous data on surface-water levels and discharges.

4) Further analyses are needed to understand the effects of climatic variables such as rainfall on the variability of L-moments of AMAX discharges in the context of the Oti River Basin.

5) It also is useful to perform statistical analyses of rainfall data in order to investigate any similarities with the flood frequency in the study area.

# APPENDICES

**Appendix 1a**

*hydrology*

MDPI

Article

# Regional Flood Frequency Analysis in the Volta River Basin, West Africa

**Kossi Komi [1,*], Barnabas A. Amisigo [2,†], Bernd Diekkrüger [3,†] and Fabien C. C. Hountondji [4]**

1 Graduate Research Program on Climate Change and Water Resources, West African Science Service Center on Climate Change and Adapted Land Use (WASCAL), University of Abomey-Calavi, Cotonou, Abomey-Calavi BP 2008, Benin
2 CSIR-Water Research Institute, Accra P.O. Box M 32, Ghana; barnyy2002@yahoo.co.uk
3 Department of Geography, University of Bonn, Bonn 53115, Germany; b.diekkrueger@uni-bonn.de
4 University of Parakou, BP 123 Parakou, Benin; fabienho@yahoo.com
* Correspondence: Kossik81@yahoo.fr; Tel.: +229-64-08-20-20
† These authors contributed equally to this work.

Academic Editor: Luca Brocca
Received: 9 November 2015; Accepted: 26 January 2016; Published: 6 February 2016

**Abstract:** In the Volta River Basin, flooding has been one of the most damaging natural hazards during the last few decades. Therefore, flood frequency estimates are important for disaster risk management. This study aims at improving knowledge of flood frequencies in the Volta River Basin using regional frequency analysis based on L-moments. Hence, three homogeneous groups have been identified based on cluster analysis and a homogeneity test. By using L-moment diagrams and goodness of fit tests, the generalized extreme value and the generalized Pareto distributions are found suitable to yield accurate flood quantiles in the Volta River Basin. Finally, regression models of the mean annual flood with the size of the drainage area, mean basin slope and mean annual rainfall are proposed to enable flood frequency estimation of ungauged sites within the study area.

**Keywords:** flood; Volta River Basin; regional frequency analysis; L-moments

## . 1. Introduction

Flood fatalities in Africa have increased dramatically over the past half-century [1]. In order to mitigate flood risk, efficient flood management is urgently needed. Flood management, and especially flood risk assessment, requires the estimation of the relation between flood magnitude and its probability of exceedance. The estimation of design floods for a site has been a common problem in some regions, and there is always great interest in this estimation process, particularly for ungauged basins or for sites characterized by a short sample length. For instance, the prediction of floods in ungauged or poorly-gauged basins is one of the main tasks of the PUB (Prediction in Ungauged Basins) initiative, which was launched from 2003–2012 by the International Association of Hydrological Sciences to engage the scientific community towards achieving major advances in the capacity to make reliable predictions in ungauged basins [2]. Two main methods are often used to solve the problem of the data scarcity. The first one is called regional flood frequency analysis (RFFA), which consist of using the spatial coherence of

hydrological variables to provide regional estimates of flood quantiles, which are superior to at-site estimates even in the presence of moderate heterogeneity [3]. The second approach is the use of paleo flood data to extend the dataset in time. Although the use of paleo flood data if available increases the length of the time series for a more accurate estimation of flood quantiles, paleo flood data may contain many errors and may represent other climate and land use conditions not comparable with the actual situations.

With regard to RFFA in Africa, few studies were carried out. For instance, a regional flood frequency analysis based on L-moments is performed in the KwaZulu-Natal province of South Africa [4]. Kachroo *et al.* [5] and Mkhandi *et al.* [6] proposed some methodologies to delineate homogeneous regions and identify regional distributions for RFFA in Southern Africa. Padi *et al.* [7] performed a large-scale analysis of flood data in Africa using probabilistic regional envelope curves (PRECs). However, it was the first time an index-flood method with L-moments together was applied in West Africa, particularly in the Volta River Basin (VRB), in order to identify the suitable flood frequency distributions.

Several approaches, such as the index flood method, the regional shape estimation procedure, the "region of influence approach", the hierarchical regions method, the fractional membership procedure, the Bayesian approach, PRECs and canonical correlation analysis, have been proposed for the purpose of RFFA. First, the index flood method was suggested by Dalrymple [8]. It assumes that sites within the same group are characterized by the same frequency distribution apart from a scaling factor called the index flood. In addition, the index flood method is based on the identification of homogeneous groups in which a relationship between the dimensionless flood and the return period is estimated. The homogeneous group is formed by basins, which are assumed to have similarities in meteorological and/or morphological characteristics. Secondly, the regional shape estimation method was proposed by Stedinger and Lu [9]. This method computes the location and scale parameters for each site, while the shape parameter is calculated by taking the average value in a group. Thirdly, the "region of influence" approach, developed by Burn [10], is based on the identification of a region of influence, which consists of sites with similar flood generation processes, and a weight must account for each site in the estimation of the quantiles. Another technique of regionalization is the hierarchical regions method [11], which defines first large regions wherein the coefficient of skewness is considered constant, and these regions are further divided into subgroups, wherein the coefficient of variation is supposed constant, as well. Then, a relationship is defined between the location parameter of the distribution and the climatic/physiographic characteristics. In the fractional membership method proposed by Wiltshire [12], the sites are assumed to have a fractional membership in many regions, rather than belonging to a particular region, and the parameters of the flood distribution can be estimated via a weighted average of the corresponding estimates for different regions. Bayesian methods have been applied to include regional information in flood frequency analysis [13,14,15]. In these methods, regional information is first used to define a prior distribution, which is further modified based on observed data at sites to provide a posterior distribution. PRECs were suggested by Castellarin [16] to estimate design floods at ungauged basins. In this approach, it is assumed that the flood frequency is homogeneous, and the flood quantiles are normalized by the drainage area (A) of the basin and then related to A by a double-logarithmic plot. Canonical correlation analysis (CCA) has been used for the purpose of regional flood frequency estimation [17,18]. CCA is a multivariate statistical method that permits establishing the interrelations that may exist between two groups of variables by identifying the linear combinations of the variables of the first group that are the most correlated to some linear combinations of the variables of the second group [18]. Table 1 summarizes the advantages and disadvantages of some procedures of RFFA.

In this study, a RFFA has been performed for the VRB, West Africa. This is important because accurate at-site frequency analysis for the majority of the sites in the VRB is actually a great challenge due to the lack of flow gauging stations on many rivers and the short length of the available daily discharge

data. More specifically, the paper applied the index flood methods based on L-moments [19].

The main aim of this study is to determine appropriate flood frequency distributions that enable adequate estimation of design floods in the VRB. Particularly, three research questions relevant to the development of a flood frequency model are investigated: (i) what are the best probability distributions of describing annual maximum discharges (AMAX) in the VRB context? (ii) What are the best multi-regression models that could be used for estimating AMAX, particularly at ungauged sites in the study area? (iii) What are the characteristics of AMAX in the VRB?

**Table 1**: Pros and cons of some regional flood frequency estimation methods. RFFA, flood frequency analysis.

| RFFA Methods | Advantages | Disadvantages |
|---|---|---|
| Index flood method | The multiplication of regional estimate with at-site statistic reduces the uncertainties associated with regionalization. | This method is sensitive to the homogeneity assumption and the formation of regions. |
| Regional shape estimation method | This method is more effective when higher-order L-moment ratios are equal at each site. | The conditions for good performance of this method are not physically plausible. |
| Region of influence method | The explicit construction of a region is not necessary. | It is difficult to define the appropriate weights |
| Hierarchical approach | This method uses more information to estimate the distribution parameters. | This method may produce abrupt changes in the parameters from one site to another. |
| Fractional membership approach | The explicit construction of a region is not necessary. | It is difficult to define the appropriate weights |
| Bayesian method | This model accounts for sources of uncertainty, and the homogeneity of the sites is not required. | The prior distributions of parameters are not precise and do not add more precision to the estimates [3] |
| Probability regional envelope curves | This method is more effective to estimate very high flood quantiles. | The logarithmic transformations may introduce biases in the estimates. |
| Canonical correlation analysis method | Possibility to predict multiple dependent variables from multiple independent variables. | One is constrained to identify linear relationship, which may not be reasonable. |

**2. Methodology**

In this study, we apply the index flood method based on L-moments, as reported by Hosking and Wallis [19]. The methods used in the present study are articulated in five steps: (i) screening of the data; (ii) identification of homogeneous groups; (iii) selection of the regional flood frequency distributions; (iv) development of regional growth curves; and (v) development of prediction equations for the mean annual flood.

## Appendix 1a

*2.1. Study Area and Data*

The present study is carried out in the Volta River Basin (VRB) of West Africa. Its geographic coordinates range from 5°30′W–2°00′E longitude–5°30′N–14°30′N latitude. The VRB covers a total area of about 400,000 km$^2$, and it is drained by four main rivers, namely the Black Volta, White Volta, Oti and Main Volta rivers (Figure 1). According to Amisigo [20], the mean annual discharge of the Black Volta River near its source is around 0.4 km$^3$; the mean annual discharge of the White Volta River is about 0.2 km$^3$ downstream of its source; and the Oti River joins the Main Volta with a flow of about 12.7 km$^3$/year. In addition, the actual study sites are located upstream of the large Volta Lake created by the Akosombo Dam in Ghana. Twenty three flow gauging stations were selected for this study and the main criteria used to choose the sites were based on the length of record periods (minimum of thirteen years) and continuity (no consecutive gaps). Specifically, the AMAX were obtained for the years 1950–1973 for the White Volta and Black Volta from Moniod *et al.* [21] and for the years 1959–1990 for the Oti River. The mean annual precipitation values (1956–1974) for the sites of the White and Black Volta sub-basins were obtained from Moniod *et al.* [21], while some mean annual precipitation values (1975–2007) for the Oti River sub-basin were computed based on observed daily rainfall data. Table 2 and Table 3 show respectively the inter-site correlation of the AMAX and characteristics of the sub-basins (sites) used in this study.

*2.2. L-Moment*

L-moments are improvements over ordinary product moments. They are used to characterize the shape of a frequency distribution and estimate the parameters of this distribution, especially for a small size of environmental data [19]. For a detail description of L-moments, the reader is referred to Hosking [22]. The sample L-moments can be estimated using Equation 1 [22]:

$$l_{r+1} = \sum_{k=0}^{r} P^*_{r,k}\ b_k \tag{1}$$

$P^*_{r,k}$ and $b_r$ are given in Equations 2 and 3, respectively. $l_{r+1}$ is the ($r$ + 1)-th L-moment of the sample.

$$P^*_{r,k} = (-1)^{r-k}\binom{r}{k}\binom{r+k}{k} \tag{2}$$

$$b_r = n^{-1}\sum_{j=1}^{n}\frac{(j-1)(j-2)\ldots.(j-r)}{(n-1)(n-2)\ldots.(n-r)}x_j \tag{3}$$

where $x_j$, for j = 1,…,$n$, is the ordered sample and $n$ is the sample size. Moreover, in RFFA based on L-moments, L-moments ratios of the sample are estimated using Equation 4:

$$t_r = \frac{l_r}{l_2} \tag{4}$$

where $t_r$ is the $r$-th sample L-moment ratio and $l_r$ is the $r$-th sample L-moment. Specifically, the sample L-coefficient of variation (L-cv) is t = $l_2/l_1$, while the sample L coefficient of skewness (L-skew) is $t_3 = l_3/l_2$, and the sample L-coefficient of kurtosis (L-kur) is $t_4 = l_4/l_2$ [22].

## Appendix 1a

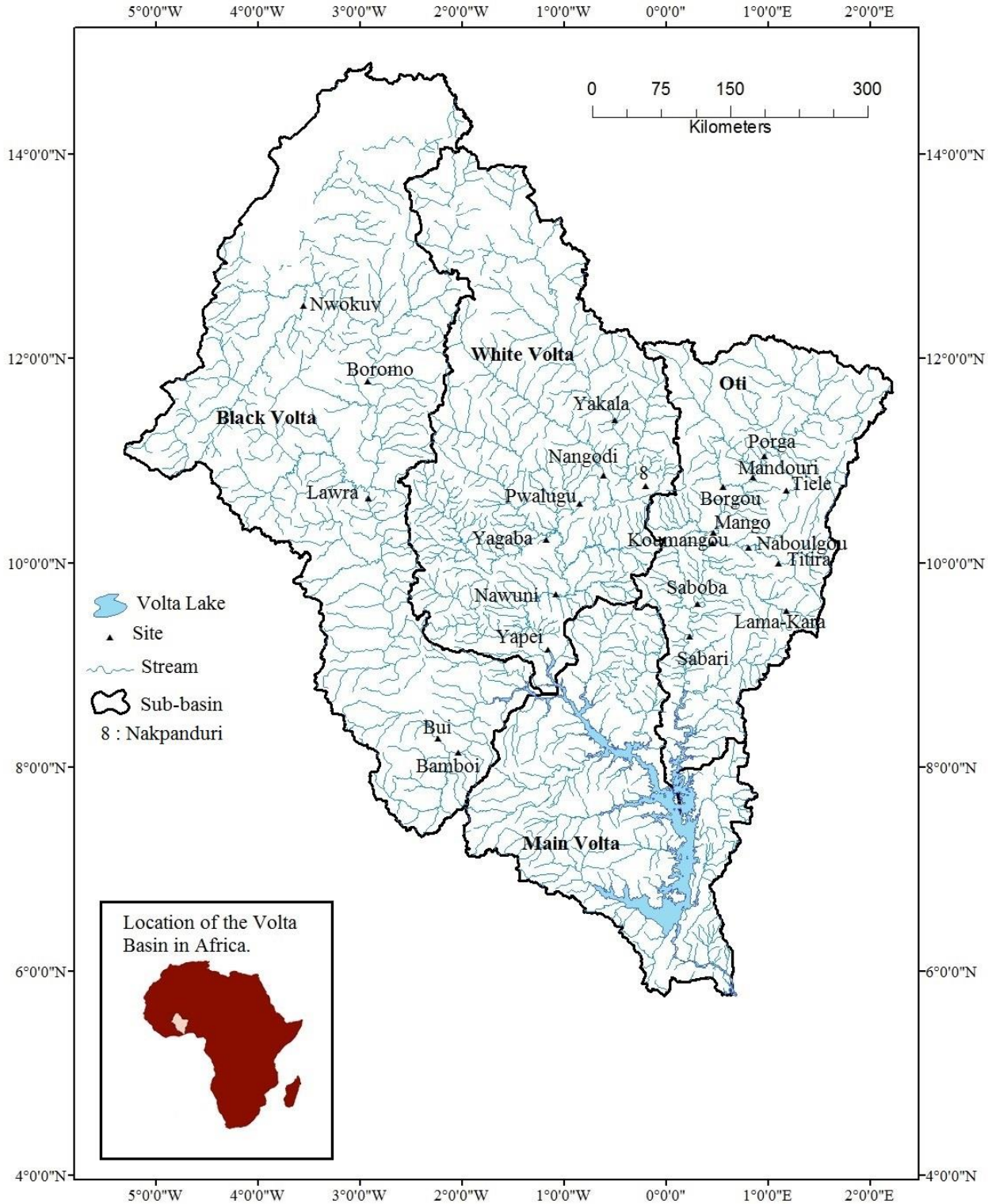


**Figure 1.** Location of the study area and the flow gauge stations.

## Appendix 1a

**Table 2.** Inter-site correlation of annual maximum discharges (AMAX) in the Volta River Basin

| Stations | Periods | Inter-Site Correlation Squared ($R^2$) |
|---|---|---|
| Nwokuy, Boromo | 1955–1973 | 0.19 |
| Boromo, Lawra | 1955–1973 | 0.06 |
| Lawra, Bui | 1954–1973 | 0.01 |
| Bui, Bamboi | 1954–1973 | 0.01 |
| Yakala, Nangodi | 1958–1973 | 0.10 |
| Nangodi, Nakpanduri | 1958–1972 | 0.37 |
| Nakpanduri, Pwalugu | 1958–1972 | 0.21 |
| Pwalugu, Yagaba | 1958–1973 | 0.00 |
| Yagaba, Nawuni | 1958–1973 | 0.00 |
| Nawuni, Yapei | 1953–1967 | 0.00 |
| Tiele, Porga | 1963–1973 | 0.21 |
| Porga, Mandouri | 1963–1979 | 0.00 |
| Mandouri, Borgou | 1960–1979 | 0.00 |
| Borgou, Mango | 1960–1987 | 0.00 |
| Mandouri, Mango | 1959–1979 | 0.01 |
| Mango, Titira | 1962–1987 | 0.11 |
| Titira, Naboulgou | 1962–1987 | 0.62 |
| Naboulgou, Koumangou | 1962–1987 | 0.00 |
| Koumangou, Lama-Kara | 1959–1987 | 0.03 |
| Lama-Kara, Saboba | 1959–1987 | 0.00 |
| Mango, Saboba | 1959–1989 | 0.00 |
| Saboba, Sabari | 1959–1990 | 0.71 |

*2.3. Data Screening*

In order to check for errors in the data, outliers and trends, the discordancy measure ($D_i$) for a site $i$ as shown in Equation 5 was applied to the AMAX series of the 23 gauge stations in the VRB. The critical value of $D_i$ depends on the number of sites ($N$). For $N \geq 15$, $D_i$ must be less than or equal to 3.0 for the site to be considered in the RFFA; otherwise, it is deleted from the dataset [19].

$$D_i = \frac{1}{3} N (U_i - \overline{U})^T [(U_i - \overline{U})(U_i - \overline{U})^T]^{-1} (U_i - \overline{U}) \quad (5)$$

where $U$ is the vector of L-moments and $N$ is the number of sites. $\overline{U}$ is an average of $U$.

## Appendix 1a

**Table 3.** Site characteristics used in the RFFA. L-cv, L-coefficient of variation; L-kur, L-coefficient of kurtosis.

| Number | Site Name | River | Area ($km^2$) | Main Slope (%) | Sample Length (year) | L-cv | L-skew | L-kur |
|---|---|---|---|---|---|---|---|---|
| 1 | Nwokuy | Black Volta | 14,800 | 0.70 | 20 | 0.20 | 0.06 | 0.24 |
| 2 | Boromo | Black Volta | 35,000 | 0.40 | 19 | 0.15 | 0.01 | 0.06 |
| 3 | Lawra | Black Volta | 66,820 | 1.10 | 23 | 0.23 | 0.15 | 0.10 |
| 4 | Bui | Black Volta | 96,000 | 1.47 | 20 | 0.26 | 0.25 | 0.30 |
| 5 | Bamboi | Black Volta | 134,200 | 0.11 | 24 | 0.25 | 0.20 | 0.19 |
| 6 | Yakala | White Volta | 31,680 | 1.19 | 18 | 0.22 | −0.03 | −0.04 |
| 7 | Nangodi | Red Volta | 11,570 | 1.41 | 16 | 0.25 | 0.03 | 0.10 |
| 8 | Nakpanduri | White Volta | 1530 | 1.47 | 15 | 0.23 | −0.05 | 0.04 |
| 9 | Pwalugu | White Volta | 63,350 | 1.09 | 16 | 0.22 | 0.00 | 0.07 |
| 10 | Yagaba | White Volta | 10,600 | 0.45 | 16 | 0.26 | −0.23 | 0.11 |
| 11 | Nawuni | White Volta | 92,950 | 1.05 | 21 | 0.13 | −0.31 | 0.20 |
| 12 | Yapei | White Volta | 102,170 | 1.11 | 17 | 0.19 | 0.04 | 0.09 |
| 13 | Tiele | Magou | 836 | 1.56 | 13 | 0.17 | 0.21 | 0.16 |
| 14 | Porga | Pendjari | 22,280 | 0.33 | 27 | 0.28 | 0.13 | 0.13 |
| 15 | Mandouri | Oti | 29,100 | 0.80 | 21 | 0.21 | 0.01 | −0.03 |
| 16 | Borgou | Sansargou | 2280 | 0.99 | 28 | 0.31 | −0.03 | 0.06 |
| 17 | Mango | Oti | 35,650 | 0.33 | 37 | 0.32 | 0.23 | 0.07 |
| 18 | Titira | Keran | 3695 | 0.89 | 26 | 0.31 | 0.06 | −0.04 |
| 19 | Naboulgou | Keran | 5470 | 1.153 | 26 | 0.19 | 0.01 | 0.06 |
| 20 | Koumangou | Koumangou | 6730 | 0.70 | 29 | 0.14 | −0.03 | 0.19 |
| 21 | Lama-Kara | Kara | 1560 | 2.52 | 34 | 0.26 | 0.06 | 0.06 |
| 22 | Saboba | Oti | 53,090 | 1.44 | 32 | 0.24 | 0.11 | 0.01 |
| 23 | Sabari | Oti | 58,670 | 0.49 | 32 | 0.28 | 0.10 | 0.01 |

*2.4. Identification of Homogeneous Groups*

2.4.1. Cluster Analysis

The aim of the cluster analysis is to partition data into clusters in a way that sites belonging to the same cluster are similar regarding their climatic/physiographic characteristics. In this study, Ward's algorithm [23] is used to form clusters with respect to the mean slope and drainage area of the basins, because this method is able to produce homogeneous clusters that have approximatively the same size.

Ward's method is a hierarchical clustering that uses the increase in the total within-group sum of squares as a result of joining groups. The application of the hierarchical clustering was based on the standardized Euclidean distance ($d$), which is given by Equation (6) [24]:

$$d^2(p,q) = \left(x_p - x_q\right) D^{-1} \left(x_p - x_q\right)^T \quad (6)$$

where $x_p$ and $x_q$ are the coordinate of sites $p$ and $q$ in the physiographic space and $D^{-1}$ is a diagonal matrix. Since the variables are expressed in different units, each coordinate in the sum of squares is

inverse weighted by the sample variance of that coordinate in order to eliminate the scale effects between the variables [24]. In addition, the within-group sum of squares (GSS) of a cluster is defined as the sum of the distance between all objects in the cluster and its center of gravity. It can be expressed by Equation (7) [24]:

$$GSS_r = \sum_{i=1}^{n_r} d^2(x_{ri} - \overline{x}_r) \quad (7)$$

where $n_r$ and $\overline{x}_r$ are respectively the size and the centroid of cluster *r*.

According to Hosking and Wallis [19], the results from the cluster analysis need not, and usually should not, be final. Many types of subjective adjustment of groups may be useful to improve the homogeneity of the clusters. In this study, a few sites were moved from one cluster to another, and one site was deleted after the cluster analysis in order to improve the homogeneity of the groups.

2.4.2. Homogeneity Test

To identify the homogeneous groups, a homogeneity test was first applied to the Volta River Basin as a single region and secondly to the clusters. The principle of the homogeneity test is to compare the observed variations in L-moments ratios for the sites in each region with the ones that would be expected for a homogeneous region [19]. The variations in L-moments are computed as the standard deviation of at site L-cv weighted proportionally to the data length at each site. In order to ascertain what would be the variation in L-moments ratios for a homogeneous region, the four-parameter kappa distribution is fitted to the regional average L-moment ratios to generate a large number (greater than or equal to 500) of Monte Carlo simulations. The kappa distribution is chosen because it is a generalized distribution that produces many distributions as particular cases of the parameter values [19]. The heterogeneity measure, $H_j$ (j = 1, 2, 3) is given by Equation 8:

$$H_j = \frac{V_j - \mu_{v_j}}{\sigma_{v_j}} \quad (8)$$

where $H_1$ is the heterogeneity measure based on observed $V_1$, which is the weighted standard deviation of t values, $H_2$ is the heterogeneity measure based on observed $V_2$, which is the weighted standard deviation of ($t/t_3$) distance, $H_3$ is the heterogeneity measure based on observed $V_3$, which is the weighted standard deviation of ($t_3/t_4$) distance, and $\mu_{v_j}$ and $\sigma_{v_j}$ are the mean and standard deviation of the simulated values of $V_j$. According to Hosking and Wallis [19], a group is "acceptably homogeneous" if $H_j$ <1, "possibly heterogeneous" if $1 \leq H_j$ <2 and "definitely heterogeneous" if $H_j \geq 2$.

*2.5. Selection of the Regional Flood Frequency Distribution*

The next step after the formation of homogeneous groups is to choose the best distribution for each homogeneous group. The selection of the distribution that will yield the accurate quantiles was thus carried out in this work by first applying the L-moment diagram method to the homogeneous groups. L-moment diagrams are useful for evaluating which distribution(s), among a suite of possible models, provides a satisfactory approximation to the distribution of a particular hydrologic variable in a region [25]. In L-moment ratio diagrams, the sample L-skewness *versus* the sample L-kurtosis is plotted on a graph with the theoretical L-moment ratios of the candidate distributions. On these diagrams, a three-parameter distribution is plotted as a line, and the best distribution is the one whose line is closer to the majority of the sample data. Nevertheless, the graph may not have a good power of discrimination when many probability distributions are suitable for the sample data in L-moment ratio diagrams. For this

reason, a numerical goodness of fit test, called the Z-statistic, is secondly applied to choose the best frequency distributions. This numerical test is based on the comparison between sample L-kurtosis and population L-kurtosis for the selected theoretical distributions. The test statistic, called $Z^{Dist}$, is defined in Equation 9 as follows:

$$Z^{Dist} = \left(\tau_4^{Dist} - t_4^R + B_4\right)/\sigma_4 \quad (9)$$

where $D_{ist}$ refers to a particular distribution, $\tau_4^{Dist}$ is the L-kurtosis of the selected distribution, $t_4^R$ is the regional weighted average of sample L-kurtosis and $B_4$ and $\sigma_4$ are respectively the bias of $t_4^R$ and the standard deviation of sample L-kurtosis. For each of the groups, a kappa distribution with its parameters estimated from the fitting of the distribution to the regional average L-moments ratios is used to simulate a large number of realizations for the same region. The frequency distribution that has the smallest absolute $Z^{Dist}$ is chosen as the best among other possible frequency distributions. At a confidence level of 90%, the critical value of absolute $Z^{Dist}$ is 1.64 [19]. Finally, quantile-quantile plots were used to compare the estimated quantiles and the observed flood values and to check the validity of the estimates provided by a fitted theoretical distribution. Five three-parameter theoretical distributions, namely the generalized logistic distribution (GLO), the generalized extreme value distribution (GEV), the generalized Pareto distribution (GPA), the generalized normal distribution (GNO) and the Pearson Type III distribution (PE3), were considered in this study.

*2.6. Development of Regional Growth Curves*

In an RFFA using the index flood approach, a relationship is established between a flood quantile of a given return period Q (T), and an index flood (taken as the mean AMAX series, $Q_m$) by introducing a regional growth curve, $q_R$ .This relationship is shown in Equation 10:

$$Q(T) = q_R{*}Q_m \quad (10)$$

T is the return period. Moreover, $q_R$ depends only on the parameters of the frequency distribution and the return periods. For instance, $q_R$ for the GPA distribution is given in Equations 11 and 12, while Equations 13 and 14 show the expressions of $q_R$ for the GEV distribution.

$$q_R = \varepsilon + \frac{\alpha}{k}\left[1 - \left(\frac{1}{T}\right)^k\right] \text{ for } k \neq 0 \quad (11)$$

$$q_R = \varepsilon - \alpha log\left(\frac{1}{T}\right) \text{ for } k = 0 \quad (12)$$

$$q_R = \varepsilon + \frac{\alpha}{k}\left\{1 - \left[-log\left(\frac{T-1}{T}\right)\right]^k\right\} \text{ for } k \neq 0 \quad (13)$$

$$q_R = \varepsilon - \alpha\left\{log\left[-log\left(\frac{T-1}{T}\right)\right]\right\} \text{ for } k = 0 \quad (14)$$

where $\alpha, \varepsilon$ and $k$ are, respectively, the scale, location and shape parameters of the distributions.

*2.7. Development of Regression Models*

In order to estimate the flood quantile for a given return period, the value of the index flood ($Q_m$) is needed. Because of the dearth of observed discharge data at the ungauged basins, $Q_m$ cannot be calculated. In this case, a regression model between $Q_m$ and physiographic or climatic basin descriptors, such as the drainage area, slope, altitude and mean annual precipitation (depending on data availability), is often used to estimate the index flood at ungauged sites, because the variation in flow discharges is

related to the variations in physiographic and climatic characteristics of the basin. Usually, the study area is split into regions that are not necessarily homogeneous [26]. In this study, regression models were estimated separately for the White and Black Volta basins and the Oti River Basin.

Furthermore, a stepwise multi-regression with the forward selection method has been used to choose the best regression models. This method adds one independent variable at a time, which increases the coefficient of determination ($R^2$) value of the regression. We started with the drainage area (A) of the basins in the equations. Then, other independent variables, such as mean slope (S), mean annual precipitation (P) and, elevation, are checked one at a time, and the most significant is added to the model at each stage. The procedure was terminated when all of the independent variables not in the equations have no significant effect on $R^2$.

**3. Results and Discussion**

Figure 2 gives the discordancy measures of the sites. It appears that only Site Number 11 is discordant with a Di value of 3.36, and it was consequently deleted from the dataset. In addition, treating first the whole VRB as a single region, the values of the different heterogeneity measures $H_1$, $H_2$ and $H_3$ obtained were respectively 4.11, 3.02 and 2.77. Therefore, the VRB is "definitely heterogeneous", and homogeneous groups need to be formed.

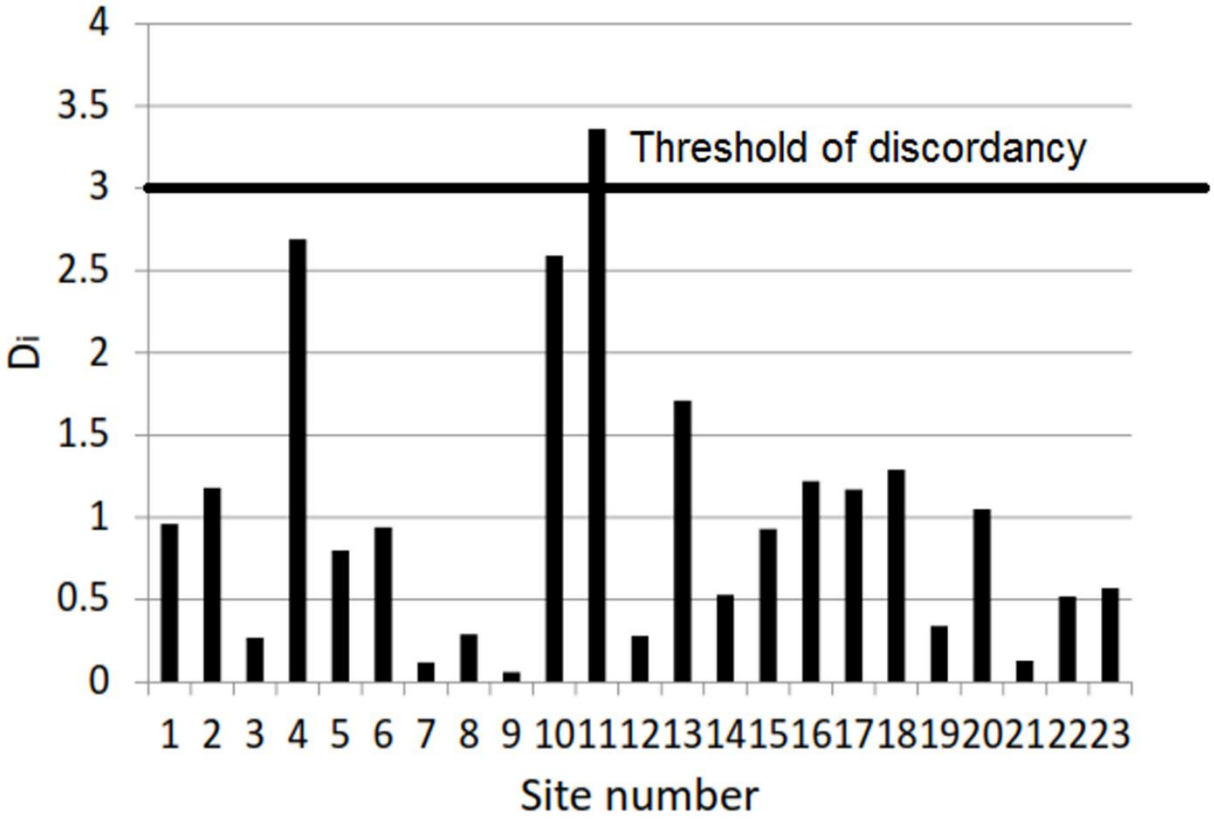


**Figure 2.** Discordancy measure (Di) of the different gauge sites

*3.1. Formation of Homogeneous Groups.*

## Appendix 1a

Figure 3 and Table 4 show the results of the cluster analysis. It can be seen from Table 4 that Cluster 1 is "acceptably homogeneous", whereas Clusters 2 and 3 are "definitively heterogeneous". Consequently, the clusters were adjusted to obtain the final groups shown in Table 5. It should be noted that the final groups are all "acceptably homogeneous".

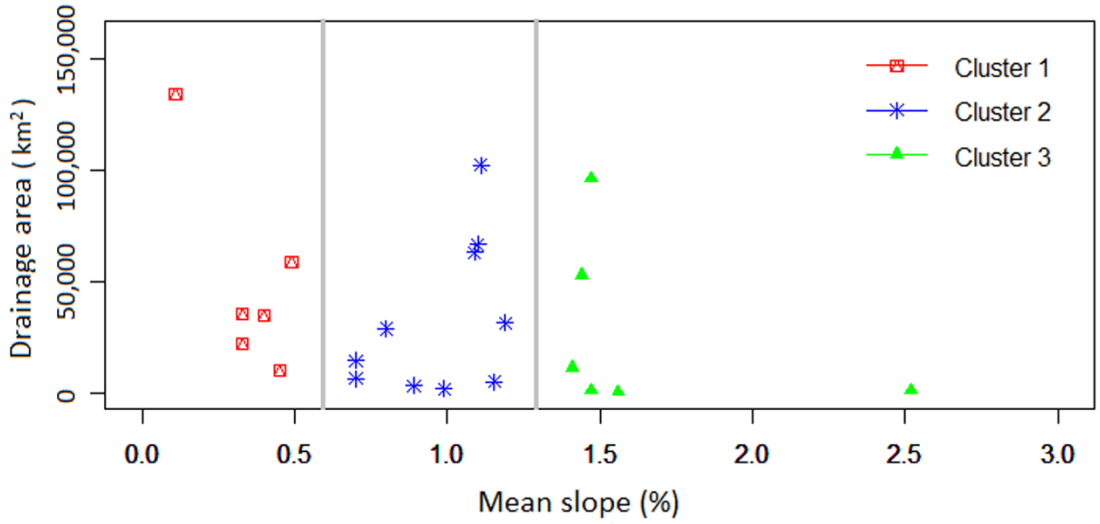


**Figure 3.** Formation of three groups through the cluster analysis.

**Table 4.** Characteristics of the initial clusters.

| Clusters | Number of Sites | $H_1$ | $H_2$ | $H_3$ | Homogeneity |
|---|---|---|---|---|---|
| 1 | 6 | 0.44 | −0.32 | 0.39 | Homogeneous |
| 2 | 10 | 4.48 | 3.19 | 2.69 | Heterogeneous |
| 3 | 6 | 1.65 | 2.30 | 3.03 | Heterogeneous |

**Table 5.** Homogeneity measure of the final groups.

| Groups | Number of Sites | $H_1$ | $H_2$ | $H_3$ | Homogeneity |
|---|---|---|---|---|---|
| A | 7 | 0.12 | 0.29 | 0.43 | Homogeneous |
| B | 7 | −2.02 | 0.70 | 0.98 | Homogeneous |
| C | 7 | −0.21 | −1.34 | −0.37 | Homogeneous |

In addition, the location of the final homogeneous groups is shown in Figure 4. One can notice that all the sites of Group A are situated in the Oti River Basin, while those of Group B are located in the White and Black Volta basins. The sites of Group C are scattered in the White Volta, Black Volta and Oti basins. Similar results were found by Burn and Goel [27], who confirmed that in RFFA, the catchments of a given homogeneous region may not be geographically contiguous, but similar in terms of their flood generation processes.

## Appendix 1a

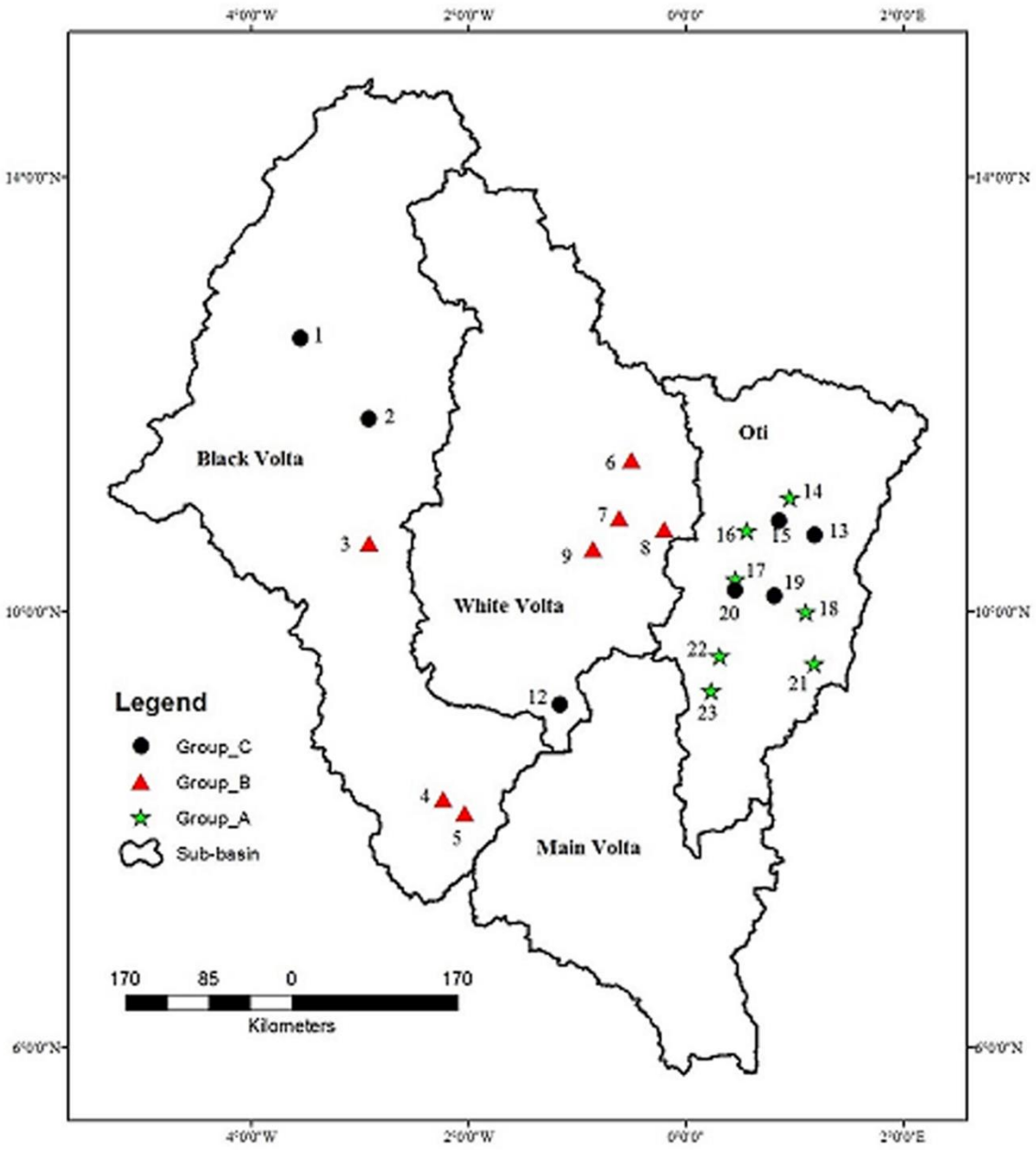


**Figure 4.** Location of the final homogeneous groups (for the site characteristics; please see Table 3)

*3.2. Selection of Appropriate Distributions*

The choice of the appropriate distribution for each group is based on L-moment ratio diagrams, Z-statistic tests and quantile-quantile plots. First, Figure 5 shows the L-moment ratio diagrams for the homogeneous groups. It may be noted that the maximum of sample sites lies close to the GPA distribution line for Group A, whereas the sample sites are closer to the GEV and GPA distribution for both group B and Group C. Secondly, Table 6 summarizes the Z-statistic values of the appropriate candidate distributions for the homogeneous groups. In this table, it is observed that only the GPA

distribution has the absolute value of the Z-statistic less than 1.64 for Group A and the GEV distribution has the lowest absolute value of the Z-statistic, which is less than 1.64, for both Group B and Group C. Hence, the GPA distribution can be considered as the regional distribution for Group A, while the GEV distribution is acceptable for both Groups B and C. These results are confirmed by the quantile-quantile plots for which the points lie approximately on the 1:1 line (Figure 6).

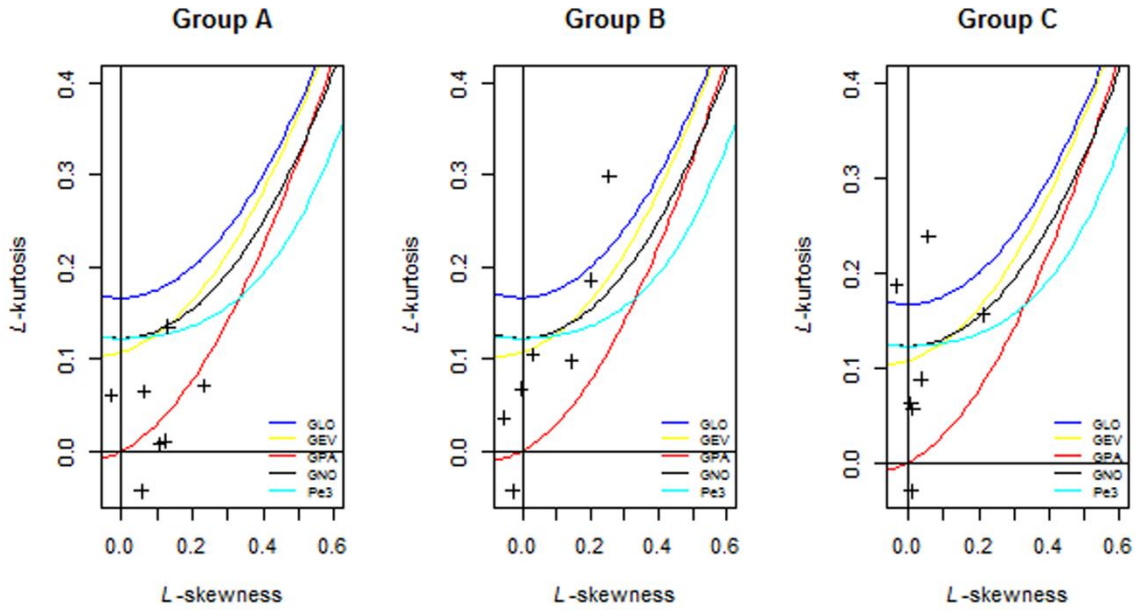


**Figure 5.** L-moment ratio diagrams for the homogeneous groups. GLO: generalized logistic distribution; GEV: generalized extreme value distribution; GPA: generalized Pareto distribution; GNO: generalized normal distribution; PE3: Pearson Type III distribution.

**Table 6.** Z-statistic values of the homogeneous groups.

| Distribution | Group A | Group B | Group C |
|---|---|---|---|
| Generalized Pareto distribution | 0.55 | −2.57 | −3.57 |
| Generalized extreme value distribution | 4.29 | 0.39 | 0.15 |
| Pearson Type III distribution | 4.20 | 0.40 | 0.55 |
| Generalized normal distribution | 4.45 | 0.52 | 0.56 |
| Generalized logistic distribution | 6.67 | 1.87 | 2.04 |

## Appendix 1a

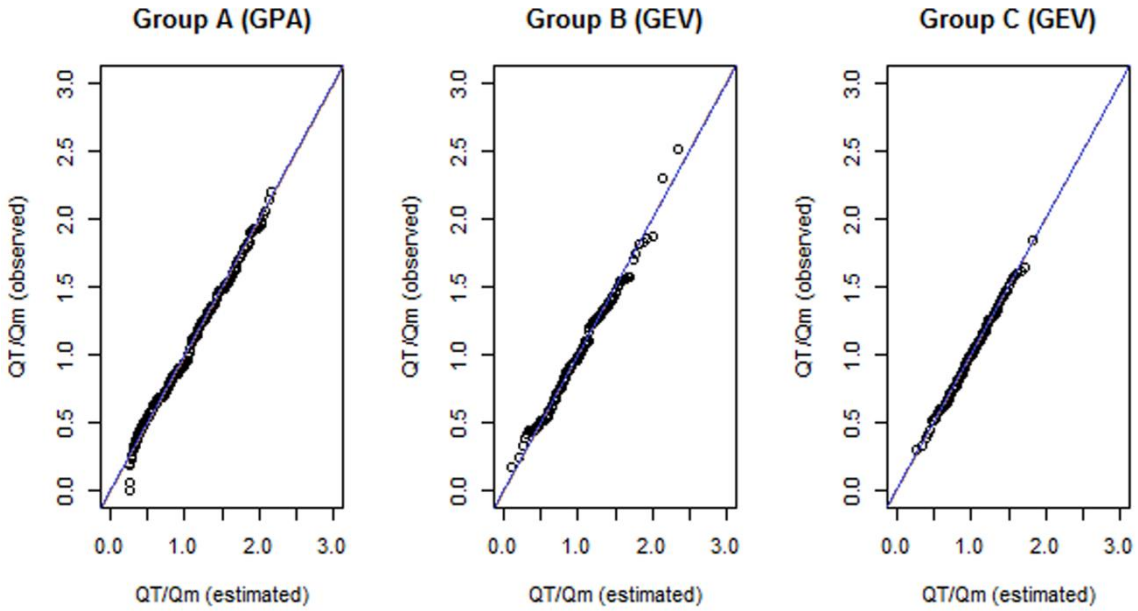


**Figure 6.** Quantile-quantile plots of the fitted frequency distributions for the three groups. GPA: generalized Pareto distribution; GEV: generalized extreme value distribution.

*3.3. Flood Frequency Relationships*

3.3.1. Regional Growth Curves

Table 7 and Figure 7 show respectively the quantile functions and the regional growth curves of the homogeneous groups. Table 7 shows also the fitted parameters to the distributions selected. In order to estimate the flood quantile for a given return period, Equation 10 is used. For the ungauged sites where observed discharge data are not available to compute the index flood ($Q_m$), the values of $Q_m$ are estimated via a multi-regression model.

**Table 7**. Quantile functions of the homogeneous groups.

| Group | Distributions and Their Parameters | Quantile Functions |
|---|---|---|
| A | GPA : ε = 0.25; $\alpha$ = 1.22; k = 0.62 | $q_R = 0.25 + 1.97\left\{1 - \left(\frac{1}{T}\right)^{0.62}\right\}$ |
| B | GEV :ε = 0.82; $\alpha$ = 0.38; k = 0.12; | $q_R = 0.82 + 3.17\left\{1 - \left[-ln\left(\frac{T-1}{T}\right)\right]^{0.12}\right\}$ |
| C | GEV: ε = 0.88; $\alpha$ = 0.30;k = 0.23 | $q_R = 0.88 + 1.30\left\{1 - \left[-ln\left(\frac{T-1}{T}\right)\right]^{0.23}\right\}$ |

## Appendix 1a

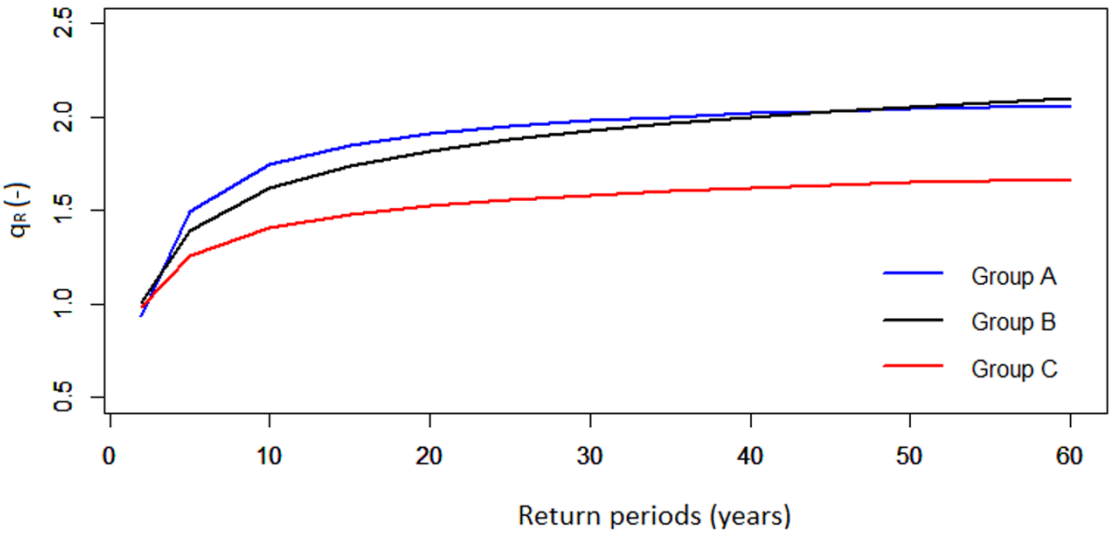


**Figure 7.** Regional growth curves of the homogeneous groups. $\boldsymbol{q_R = Q(T)/Q_m}$; with $\boldsymbol{Q_m}$, the index flood, and $\boldsymbol{Q(T)}$, the flood quantile of return period T.

It can be seen from Figure 7 that the regional flood frequency curves for the different groups in the Volta Basin are relatively flat. This result confirms the findings of Meigh *et al.* [28], who showed that regional curves in West Africa and some regions affected by monsoon are "fairly flat". Moreover, Sutcliffe and Farquharson [29], cited in Meigh *et al.*[28], noted that a feature of many basins with flat curves is that floods appear to be due to the accumulation of rainfall over a distinct wet season or monsoon and that the date of the annual maximum flood is relatively constant from year to year. This means that the peak flow is more likely to be related to the annual total rainfall, which is less variable than storm rainfall [28].

3.3.2. Regression Models

Table 8 and Figure 8 show respectively the best regression models and the comparison between estimated quantiles and the observed values of $Q_m$ (index flood). In these equations, A, P and S are respectively the drainage area, the mean annual precipitation and the mean slope of the basins. The powers associated with the area (0.61 and 0.8) are comparable to the findings of other similar studies, such as Lim *et al.* [30] and Noto *et al.* [31]. These values (0.61 and 0.8) are also reasonable because they show that the mean specific discharge ($Q_m/A$) decreases with the area [32].

**Table 8.** Regression models for the estimation of the index flood at ungauged sites.

| Sub-Basins | Regression Models | $R^2$ |
|---|---|---|
| Oti River | $Q_m = 10^{-7} S^{0.41} A^{0.61} P^{2.42}$ | 0.96 |
| White Volta and Black Volta | $Q_m = 3 \times 10^{-6} S^{0.28}\, A^{0.8} P^{1.52}$ | 0.91 |

## Appendix 1a

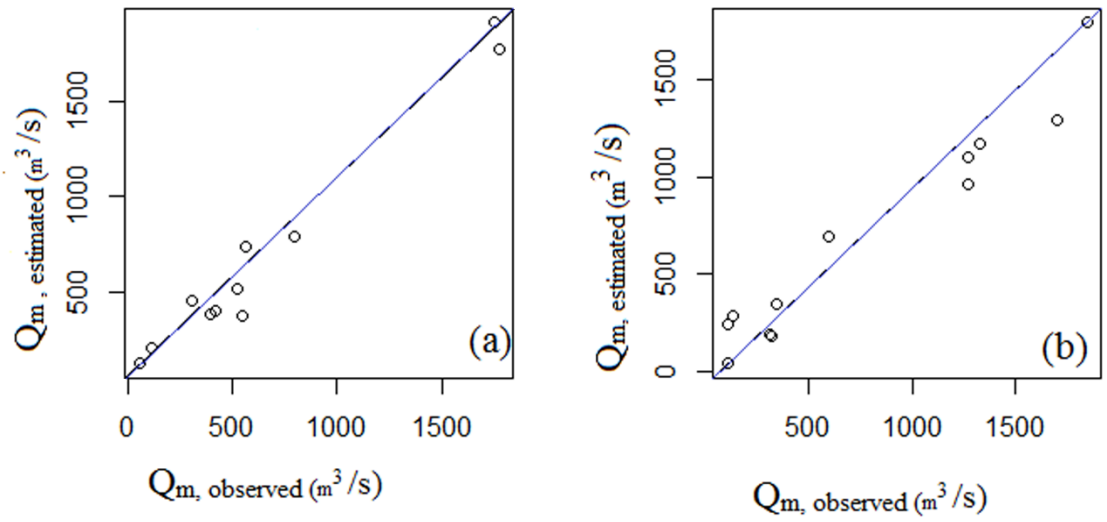


**Figure 8.** Diagnostic plots of the best regression models: (**a**) for the Oti River Basin and (**b**) for the White Volta and Black Volta basins. The 1:1 line is the plot for reference.

In addition, Pandey and Nguyen [33] have shown that the non-linear optimization model is the best method for estimating the power-form flood regionalization model when compared to linear regression models. The same authors conclude that in terms of flood quantile prediction and parameter uncertainty, the non-linear optimization model is the most robust when compared to the linear regression methods. Consequently, the regression models obtained are suitable to estimate index floods for regional flood estimation in the Volta River Basin.

### 4. Conclusions

Flood fatalities in West Africa have increased during the last two decades. Thus, efficient flood risk management is urgently needed to reduce the vulnerability of the local population. The first step in any flood management project is to determine the relationship between peak flows and the associated return periods. However, the estimation of flood values with high recurrence intervals, such as extreme floods, for a site of interest poses a great challenge in the Volta River Basin due to the lack of sufficient hydrological information.

We have presented a flood estimation procedure for the Volta River Basin in West Africa using regional flood frequency analysis methods based on L-moments. This study represents a huge step forward in the local context towards improvement of design flood estimates. The selection of the appropriate frequency distributions was based on the identification of homogeneous regions using both the clustering algorithm and statistical tests, L-moment ratio diagrams, quantile-quantile plots and a numerical goodness of fit test (Z-statistic). It was found that GPA and GEV distributions are the most robust flood frequency distributions among five candidate three-parameter distributions. In addition, the relatively flat shape of the flood frequency curves may suggest that flood in the Volta River Basin is caused by an accumulation of rainfall over the monsoon (rainy season), rather than by a storm rainfall. Based on the acceptable results shown in this article, we conclude that the outcomes of this study can be used to predict flood quantiles and the associated recurrence intervals. In addition, the design floods can be used as inputs to hydraulic models to produce flood hazard maps for rivers within the Volta Basin. Finally, due to the evidence of future climate change, further analyses are needed to understand the

effects of climatic variables, such as rainfall, on the variability of L-moments of annual maximum floods in the study area.

**Acknowledgments:** This work is part of the West African Science Service Center on Climate Change and Adapted Land Use project (WASCAL; www.wascal.org), which is funded by the German Ministry of Education and Research (BMBF). The authors are grateful to the national hydrological and meteorological services of Togo and Ghana for providing the discharge and rainfall data. The authors would like to thank the editors and the two anonymous reviewers for the relevant comments and suggestions, which significantly improved the quality of the manuscript.

**Author Contributions:** Kossi Komi conducted this research as a part of his Ph.D. Thesis. Kossi Komi wrote the initial version of the manuscript. Bernd Diekkrüger and Barnabas A. Amisigo helped in improving the manuscript. Fabien C. C. Hountondji proofread and helped in the discussion of the results.

**Conflicts of Interest:** The authors declare no conflict of interest.

### References and Notes

1. Di Baldassarre, G.; Montanari, A.; Lins, H.; Koutsoyiannis, D.; Brandimarte, L.; Blöschl, G. Flood fatalities in Africa: From diagnosis to mitigation. *Geophys Res. Lett* **2010**, doi:10.1029 /2010GL045467.
2. Sivapalan, M.; Takeuchi, K.; Franks, S.W.; Gupta, V.K.; Karambiri, H.; Lakshmi, V.; Liang, X.; McDonnell, J.J.; Mendiondo, E.M.; O'Connell, P.E.; *et.al*. IAHS decade on Predictions in Ungauged Basins (PUB), 2003–2012: shaping an exciting future for the hydrological sciences. *Hydrol. Sci. J.* **2003**, 48, 857–880
3. Cunnane, C. Methods and merits of regional flood frequency analysis. *J. Hydrol*. **1988**, 100, 269–290.
4. Kjeldsen, T. R.; Smithers, J. C.; Schulze, R.E. Regional flood frequency analysis in the KwaZulu-Natal province, South Africa, using the index-flood method. *J. Hydrol*. **2002**, *255*, 194–211.
5. Kachroo, R.K.; Mkhandi, S.H.; Parida, B.P. Flood frequency analysis of southern Africa: I. Delineation of homogeneous regions. *Hydrol. Sci. J*. **2000**, *45*, 437–447
6. Mkhandi, S.H.; Kachroo, R.K.; Gunasekara, T.A.G. Flood frequency analysis of southern Africa: II. Identification of regional distributions. *Hydrol. Sci. J.* **2000**, *45*, 449–464.
7. Padi, T.P.; Di Baldassarre G.; Castellarin A. Floodplain management in Africa: Large scale analysis of flood data. *Phys. Chemis. Earth*. **2011**, *36*, 292–298.
8. Dalrymple, T. *Flood frequency analysis*; Technical report water supply paper 1543-A; US Geological Survey: Washington, DC, USA, 1960.
9. Stedinger, J.R.; Lu L.H. Appraisal of regional and index flood quantile estimators. *Stoch. Hydrol. Hydraul.* **1995**, *9*, 49–75.
10. Burn, D.H. An appraisal of the "region of influence" approach to flood frequency analysis. *Hydrol. Sci. J.* **1990**, *35*, 149–165.
11. Fiorentino, M.; Gabriele, S.; Rossi, F.; Versace, P. Hierarchical approach for regional flood frequency analysis. In *Regional Flood Frequency Analysis*; Singh, V.P., Ed; D. Reidel publishing company: Norwell, MA, USA, 1987.
12. Wiltshire, S.E. Regional flood frequency analysis II: Multivariate classification of drainage basins in Britain, *Hydrol. Sci. J*. **1986**, *31*, 335–346.
13. Gaume, E.; Gaál, L.; Viglione, A.; Szolgay, J.; Kohnová, S.; Blöschl, G. Bayesian MCMC approach to regional flood frequency analyses involving extraordinary flood events at ungauged sites. *J. Hydrol*. **2010**, *394*,101–117.
14. Kuczera, G. A Bayesian Surrogate for Regional Skew in Flood Frequency Analysis. *Water Resour. Res.* **1983**, *19*, 821–832.
15. Ribatet, M.; E. Sauquet, J.G.; Ouarda, T.B. Usefulness of the reversible jump Markov chain Monte Carlo model in regional flood frequency analysis. *Water Resour. Res*. **2007**, doi: 10. 1029/2006WR005525.
16. Castellarin, A. Probabilistic envelope curves for design-flood estimation at ungauged sites. *Water Resour. Res*. **2007**, doi:10.1029/2005WR004384.

## Appendix 1a


17. Cavadias, G.S. Regional flood estimation by canonical correlation. *Proc. 1989 Conf. Can. Soc. Civ. Eng.*, **1989**, *11*, 212–231.
18. Ouarda, T.B.M.J.; Girard, C.; Cavadias, G.S.; Bobée, B. Regional flood frequency estimation with canonical correlation analysis. *J. Hydrol*. **2001**, *254*, 157–173.
19. Hosking, J.R.M.; Wallis, J.R. *Regional Frequency Analysis: An Approach Based on L-Moments.* Cambridge University Press: New York, NY, USA, 1997.
20. Amisigo B.A. Modelling river flow in the Volta Basin of West Africa: A data-driven framework. Ph.D. Thesis, University of Bonn, Bonn, Germany, 2005.
21. Moniod F.; Pouyaud B.; Sechet, P. *Monographies Hydrologiques ORSTOM N05:le Bassin du Fleuve Volta*. Office de la Recherche Scientifique et Technique Outre-Mer: Paris, France, 1977.
22. Hosking, J.R.M. L-moments: analysis and estimation of distributions using linear combinations of order statistics. *J. R. Statist. Soc. B*. **1990**, *52*, 105–124.
23. Ward, J.H. Hierarchical grouping to optimize an objective function. *J. Am. Statist. Assoc*.**1963**, *58*, 236–244.
24. Ouarda, T.B.M.J.; Bâ, K.M.; Diaz-Delgado, C.; Cârsteanu, A.; Chokmani, K.; Gingras, H.; Quentin, E.; Trujillo, E.; Bobée, B. Intercomparison of regional flood frequency estimation methods at ungauged sites for a Mexican case study. *J. Hydrol*. **2007**, *348*, 40– 58.
25. Vogel, R.M.; Fennessey, N.M. L-moment diagrams should replace product moment diagrams. *Water Resour. Res.* **1993**, *29*, 1745–1752.
26. Rosbjerg, D.; Blöschl G.; Burn, H.D.; Castellarin A.; Croke, B.; Di Baldassarre, G.; Iacobellis, V.; Kjeldsen R.T.; Kuczera, G.; Merz, R.; *et.al*. Prediction of floods in ungauged basins. In *Runoff prediction in Ungauged Basins: Synthesis across Processes, Places and Scales*; Blöschl G., Sivapalan M., Wagener T., Viglione A., Savenije, H., Eds; Cambridge University Press: The Edinburgh Building, Cambridge, UK, 2013.
27. Burn, D.H.; Goel, K.N. The formation of groups for regional flood frequency analysis. *Hydrol. Sci. J.* **2000**, *45*, 97–112.
28. Meigh, R.J.; Farquharson, K.A.; Sutcliffe V.J. A worldwide comparison of regional flood estimation methods and climate. *Hydrol. Sci. J*. **1997**, *42*, 225–244.
29. Sutcliffe, J.V.; Farquharson, F.A.K. Flood frequency studies using regional methods. In *Conference for Jacques Bernier*; UNESCO Press: Paris, France, 1996.
30. Lim, Y.H.; Lye, L.M. Regional flood estimation for ungauged basins in Sarawak, Malaysia. *Hydrol. Sci. J.* **2003**, *48*, 79–94.
31. Noto, L.V.; La Loggia, G. Use of L-moments approach for regional flood frequency analysis in Sicily, Italy. *Water Resour. Man*. **2009**, *23*, 2207–2229.
32. Hingray B., Picouet, C.; Musy, A. Hydrologie 2: *une science pour l'ingénieur*; Presses polytechniques et universitaires romandes, Lausanne, Switzerland, 2009. (In French).
33. Pandey, R.G.; Nguyen, V.T.V. A comparative study of regression based methods in regional flood frequency analysis. *J. Hydrol*. **1999**, *225*, 92–101.


**Appendix 1b**

*hydrology*

MDPI

Article

# Integrated Flood Risk Assessment of Rural Communities in the Oti River Basin, West Africa

**Kossi Komi [1,*], Barnabas A. Amisigo [2] and Bernd Diekkrüger [3]**

[1] Graduate Research Program on Climate Change and Water Resources, West African Science Service Center on Climate Change and Adapted Land Use (WASCAL), University of Abomey-Calavi, Cotonou, Abomey-Calavi BP 2008, Benin
[2] CSIR-Water Research Institute, Accra, P.O. Box M 32, Ghana; barnyy2002@yahoo.co.uk
[3] Department of Geography, University of Bonn, Bonn 53115, Germany; b.diekkrueger@uni-bonn.de
* Correspondence: Kossik81@yahoo.fr; Tel.: +229-64-08-20-20

Academic Editor: Luca Brocca
Received: 3 March 2016; Accepted: 15 November 2016; Published: 22 November 2016

**Abstract:** Flood damage in West Africa has increased appreciably during the last two decades. Poor communities are more at risk due to the vulnerability of their livelihoods, especially in rural areas where access to services and infrastructures is limited. The aim of this paper is to identify the main factors that contribute to flood risk of rural communities in the Oti River Basin, Togo. A community-based disaster risk index model is applied. The analyses use primary data collected through questionnaires during fieldwork, the analytic hierarchy process (AHP) method, population and housing census data and flood hazard mapping of the study area. The results showed a moderate level of flood risk despite a high level of hazard and vulnerability for all investigated communities. In addition, the results suggest that decreasing vulnerability through creation of new income-generating opportunities and increasing capacity of communities to manage their own flood risk should be paramount in order to reduce flood risk in the study area. The results of this work contribute to the understanding of flood risk and can be used to identify, assess, and compare flood-prone areas, as well as simulating the impacts of flood management measures in the Oti River Basin.

**Keywords:** community-based disaster risk index; AHP; flood hazard; flood vulnerability

## 1. Introduction

In many parts of the world, extreme floods have been observed and grave consequences on ecosystems, human life and socio-economic activities have been reported. In the last two decades, floods have caused extensive economic damage and loss of life throughout the world. For instance, floods in September 2007 in West Africa caused 23, 46 and 56 deaths in Togo, Burkina Faso and Ghana, respectively [1] and extraordinary floods occurred in 2010 in Pakistan and China [2]. Apart from the effects of human-induced climate change, which is expected to exacerbate this dire situation, many factors contribute to Africa's high vulnerability to disasters, including a high rate of population growth, high levels of poverty, inappropriate use of natural resources, and failures of policy and institutional frameworks [3]. In addition, the main features that characterize an area vulnerable to flood hazards are

the flat topography, the geological conditions, urbanization and poor draining networks [4]. Managing flood risk is important to reduce the damage and adapt to the combined effects of climate and land use changes. With risk defined herein as the probability of harmful consequences, or expected losses and resulting from the interactions between natural or human-induced hazards and vulnerable conditions [5], flood risk can then be managed by reducing the hazard (probability or magnitude) or by reducing the vulnerability of the exposed population.

This approach to managing flood risk is based on the knowledge of the hazards and the physical, social, economic and environmental vulnerabilities to floods that a population faces. Consequently, efficient flood risk management is reliant on a priori assessment of flood hazards. Such assessments give insights into what can be expected, and therefore open up the discussion on how to tackle such situations [6]. Moreover, flood hazard assessment is indispensable for the development of policies and plans to mitigate flood risk [7]. A risk assessment is a methodology to determine the nature and extent of risk by analyzing potential hazards and evaluating existing conditions of vulnerability that could pose a potential threat or harm to people, property, livelihoods and the environment on which they depend [5]. Depending on data availability, the scale of application and the purpose of the risk assessment, several methods have been used to assess flood risk over the last decades. For instance, Ward et al. [8] developed and validated a model cascade to assess flood risk at the global scale. The cascade included hydrological and hydraulic modelling, extreme value statistics and estimation of annual expected impacts. Because of the small time required for the simulations and the good performance of the model cascade, the authors conclude that it could be used to carry out assessment of changes in flood risk. Remote sensing and Geographic Information System (GIS) were used for the delineation of flood zones for flood risk analysis in Ghana [9]. Musungu et al. [10] proposed a methodology of integration of community-based information into a GIS for flood risk assessment of an informal settlement in Cape Town (Republic of South Africa) and Guarín [11] integrated local knowledge into GIS-based flood risk assessment of Triangulo and Mabolo communities in Naga city (Philippines). A Community-Based Disaster Risk Index (CBDRI) approach, developed by Bollin et al. [12], was applied by Adeloye et al. [13] to assess flood risk and vulnerability of rural communities in Malawi (South Africa) and the German Technical Cooperation Agency (GTZ) to assess disaster risks in Africa, Asia, Caribbean, Central America and South America [14]. The CBDRI model was chosen in this study because it can be applied in data sparse areas where data for conventional flood risk assessment are missing.

Traditionally, flood risk is expressed in terms of expected damages and likelihood of occurrence. The flood damage is combined with information on the probability of the flood event and then plotted as return period-damage curve [15, 16]. However, the results obtained using this method would provide neither sufficient information nor the required level of detail for input into flood risk reduction strategies. In addition, the use of damages to assess flood risk suffers from data scarcity, particularly in developing countries where data are usually scarce. The reason is that disaster-related damage figures are not systematically recorded and are often under-recorded, even in developed countries [17, 18]. According to Birkmann [17], highly exposed regions, with high poverty levels and subject to repeated and catastrophic floods, may not necessarily register significant deaths or damage, although these factors make such places highly risky. Moreover, since mortality and damage figures are obtained from actual events, the use of damage assesses actual vulnerability but potential vulnerability is ignored [18].

This study aims at assessing fluvial flood risk of seven rural communities in the study area. Specifically, three research questions are investigated: (i) what are the major factors that contribute to flood in the studied communities? ; (ii) what are the level of flood risk in the Oti River Basin? ; and (iii) what type of measures are required to reduce flood risk in the basin?

This study performs an integrated flood risk assessment for rural communities of the Oti River Basin in Togo, West Africa. This is important because this basin is subject to frequent flooding, and it is the first

time to analyze flood risk in this area. This methodology can be used to support decision-making on possible measures that can be taken and to prioritize areas where actions are required.

## 2. Materials and Methods

### *2.1. Study Area*

In this study, seven communities of the Oti River Basin in Togo (Figure 1a) are investigated. The climate of this area is tropical semi-arid and is characterized by a rainy season starting from April to October with the maximum rainfall occurring in August (Figure 1b) and a dry season from November to March. With a poverty rate of more than 90% (Table 1), these communities are the poorest in the country. Their livelihoods are derived from subsistence farming, animal husbandry and informal labor, all of which are threatened by the impacts of climate change. Most of the dwellings in the studied area are informal self-housing units, poorly planned and made of mud walls, wooden doors and windows. Consequently, many buildings collapse from the force of the flood water.

Heavy rainfall in September 2007 caused the worst flood that Oti River Basin had ever faced. According to the International Federation of Red Cross and Red Crescent Societies (IFRCRCS), by September 2007, 25 people were killed and 97 people were critically injured [19]. In recent years, the most damaging floods were experienced in 2008, 2010 and 2012.

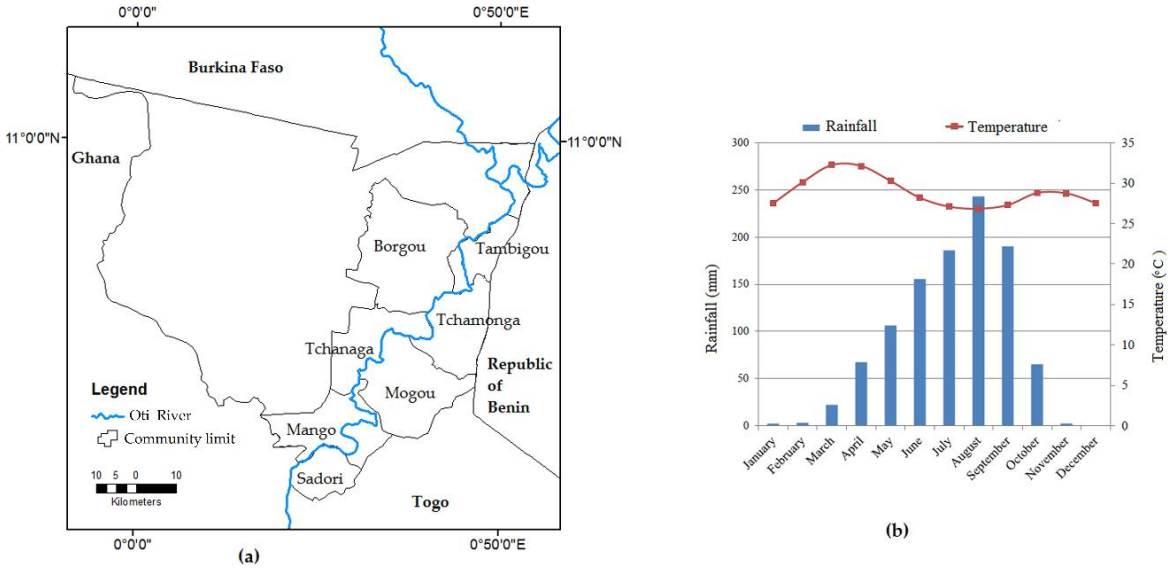


**Figure 1.** (**a**) location of the study area; and (**b**) climate diagram at Mango from 1980 to 2010.

**Table 1.** Socio-economic characteristics of the selected communities.

| Characteristics | Tambigou | Borgou | Tchamonga | Tchanaga | Mango | Mogou | Sadori |
|---|---|---|---|---|---|---|---|
| Density [1] (habitants per km²) | 16 | 17 | 11 | 8 | 29 | 17 | 12 |
| Area (km²) | 164 | 630 | 298 | 267 | 342 | 432 | 156 |
| Literacy level (%) [2*] | 25 | 21 | 18 | 31 | 81 | 22 | 31 |
| Poverty level (%) [2] | 96.7 | 96.3 | 95.9 | 95.8 | 40.8 | 96.2 | 96.5 |
| Area under forest (% of total area) | 21 | 9 | 8 | 24 | 30 | 18 | 71 |
| Rate of access to safe drinking | 7.8 | 10.8 | 42.6 | 1.5 | 84.1 | 39.1 | 2.3 |

## Appendix 1b

| | | | | | | | |
|---|---|---|---|---|---|---|---|
| water (%) [2] | | | | | | | |
| Area prone to flood (% of total area) | 25 | 12 | 19 | 24 | 29 | 18 | 38 |
| Number of housing units [1] | 818 | 3441 | 1031 | 582 | 2808 | 2309 | 459 |

[1] Source: DGSCN [20]; [2] Source: Coulombe et al. [21]; * Literacy level is defined as the percentage of adult population that can read.

*2.2. Conceptual Framework of the Study*

This study applies the CBDRI system, which characterizes the risk of natural disaster via four factors, namely: hazard, exposure, vulnerability, as well as capacity and measures (Equation (1)):

$$R = f(H,V,E,C), \quad (2)$$

where R is the flood risk index and H, V, E, C are indices for hazard, vulnerability, exposure as well as coping capacity, and f denotes the function. In this study, a set of 37 indicators are used to quantify the risk index for a given community (Table 2). All indicators for each of the four factors are integrated into one index (e.g., hazard index).

**Table 2.** The selected factors and indicators used in the analysis (modified from Bollin et al. [12]).

| Factor Component | Indicator Name | Indicator |
|---|---|---|
| HAZARD | | |
| Probability | (H1) Occurrence (experienced events) | Frequency of events in the past 30 years |
| | (H2) Occurrence (possible events) | Probability of possible events. Chances per year |
| Severity | (H3) Intensity (experienced events) | Intensity of the worst event in the past 30 years |
| | (H4) Intensity (possible events) | Expected intensity of possible events |
| EXPOSURE | | |
| Structures | (E1) Number of housing units | Number of housing units (Living quarter) |
| | (E2) Lifelines | % of homes with piped drinking water |
| Population | (E3) Local gross domestic product | Total locally generated GDP in constant currency |
| Economy | (E4) Total resident population | Total resident population |
| VULNERABILITY | | |
| Physical/Demographic | (V1) Density | People per km$^2$ |
| | (V2) Demographic pressure | Population growth rate |
| | (V3) Unsafe settlement | Homes in hazard prone area (ravines, river banks, etc.) |
| | (V4) Access to basic services | % of homes with piped drinking water |
| Social | (V5) Poverty level | % of population below poverty level |
| | (V6) Literacy rate | % of adult population that can read and write |
| | (V7) Attitude | Priority of a population to protect against a hazard |
| | (V8) Decentralisation | Portion of self-generated revenues of the total budget |
| | (V9) Community participation | % of voter turnout at last commune election |
| Economic | (V10) Local resource base | Total available local budget in USS |
| | (V11) Diversification | Economic sector mix for employees |

## Appendix 1b

| | | |
|---|---|---|
| | (V12) Stability | % of businesses with fewer than 20 employees |
| | (V13) Accessibility | Number of interruption of road access in last 5 years |
| Environmental | (V14) Area under forest | % Area of the commune covered with forest |
| | CAPACITY and MEASURES | |
| Physical planning and engineering | (C1) Land use planning | Enforced land use plan or zoning regulation |
| | (C2) Preventive structure | Expected effect of impact-limiting structures |
| | (C3) Environmental management | Measures that promote and enforce nature preservation |
| Societal capacity Economic capacity | (C4) Public awareness programs | Frequency of public awareness programmes |
| | (C5) School curricula | Scope of relevant topics taught at school |
| | (C6) Public participation | Emergency committee with public representatives |
| | (C7) Access to local emergency funds | Release period of national emergency funds |
| | (C8) Access to international emergency funds | Access to international emergency funds |
| | (C9) Insurance market | Availability of insurance for buildings |
| Management and institutional capacity | (C10) Risk management committee | Meeting frequency of a commune committee |
| | (C11) Risk map | Availability and circulation of risk maps |
| | (C12) Emergency plan | Availability and circulation of emergency plans |
| | (C13) Early warning system | Effectiveness of early warning system |
| | (C14) Institutional capacity building | Frequency of training for local institutions |
| | (C15) Communication | Frequency of contact with district level risk institutions |

*2.3. Data Collection*

The application of CBDRI method requires a questionnaire (Table S1) to be administrated at the commune level. In total, seven communities—Sadori, Mango, Mogou, Tchamonga, Tchanaga, Tambigou and Borgou (Figure 1a) in the Oti and Kpendjal prefectures of Togo—were selected for this study because of their proximity to the Oti River. In each community, one questionnaire was completed. In order to get reliable information, only knowledgeable people (members of the local development committee, formal community leader, teacher, etc.) were contacted to fill out the questionnaire. However, some data such as population density (V1), population growth rate (V2), number of housing units (E1) access to basic services (V4) and literacy levels (V6) were obtained from Population and Housing Census data of 2010 [20] and literature. In addition, the percentages of forested area for each community area and flood-prone areas were derived from the FAO (Food and Agriculture Organization) land cover database [22] and NASA MODIS data, respectively. Since the data regarding the hazard factor should be obtained from scientific sources [12], the information on the experienced flood hazards was obtained from the literature while the probability and severity of the possible flood hazard (H2 and H4 ) were obtained through flood hazard mapping of the Oti River Basin.

*2.4. Estimation of the Vulnerability, Exposure, Capacity and Measure Indices*

To assess the vulnerability, exposure, as well as capacity and measures indices of a risk index for a given community, many steps were followed. The first step consisted of making the different measurement of each indicator (e.g., 10,000 residents, 10% literacy level) comparable using a scale. The scaling was done by assigning a score (S) of one, two or three according to the level of the indicator—low,

medium, or high, respectively. A zero value was given if the indicator does not apply for a commune. In a second step, the scores are multiplied by a specific weight (W) of each indicator. The CBDRI model was developed in such a way that the total sum of weights for each of the four factors is equal to 3, so that the factor indices range between 0 and 10. Finally, separate indices were calculated for each factor using the following linear Equations (2)-(5):

$$V = W_{V1}S_{V1} + W_{V2}S_{V2} + W_{V3}S_{V3} + ..... + W_{V4}S_{V4}, \quad (2)$$

$$E = W_{E1}S_{E1} + W_{E2}S_{E2} + W_{E3}S_{E3} + W_{E4}S_{E4}, \quad (3)$$

$$C = W_{C1}S_{C1} + W_{C2}S_{C2} + ... + W_{C23}S_{C23}, \quad (4)$$

$$H = W_{H1}S_{H1} + W_{H2}S_{H2} + W_{H3}S_{H3} + W_{H4}S_{H4}, \quad (5)$$

where V, E, C and H are the values of the vulnerability, exposure, capacity and measures indices and hazard, respectively; $S_{xi}$ refers to the scaled value of the indicator for $Xi$, and $W_{xi}$ is the weight applied to the indicator $Xi$.

*2.5. Estimation of the Indicator Weight*

In the present study, the analytical hierarchy process (AHP) method was employed to compute weights for the different indicators considered in the CBDRI model. The AHP method, which was developed by Saaty [23], is a multi-criteria, mathematically based method which uses a set of pairwise comparison matrices to estimate the relative importance of different criteria and alternatives, among which the best decision is made. Saaty's AHP model has attracted the interest of many researchers (e.g., [7,24–29]) because it has the advantage of incorporating a test for checking the consistency of a choice, thus reducing the uncertainty in the evaluation process.

In order to compute the weights for each indicator, the AHP starts creating a pairwise comparison matrix $M = (B_{ij})$. Each numerical value $B_{ij}$ of $M$ represents the relative importance of the $i$th indicator in comparison with the $j$th indicator. If $B_{ij} > 1$, then the $i$th indicator is more important than the $j$th indicator, whereas if $B_{ij} < 1$, then the $i$th indicator is less important than the $j$th indicator. If two indicators have the same importance, then $B_{ij} = 1$. The numerical values satisfy the condition given in Equation (6) [23]:

$$B_{ij} * B_{ji} = 1. \quad (6)$$

Moreover, the relative importance between two criteria was measured based on a numerical scale from 1 to 9 as follows: 1 = $i$ and $j$ are equally important, 3 = $i$ is slightly more important than $j$, 5 = $i$ is strongly important than $j$, 7 = $i$ is very strongly more important than $j$, 9 = $i$ is extremely more important than $j$, and 2, 4, 6, 8 are intermediate values between the previous scales [23]. After building the matrix $M$, a normalized pairwise comparison matrix was derived by dividing each value $B_{ij}$ by the sum of all values of that column. Finally, the relative weight ($W_{AHP}$) vector was estimated by averaging the values on each row of the normalized pairwise comparison matrix. The AHP method requires all indicator weights to satisfy the condition shown in Equation (7) [30]:

$$\sum_{i=1}^{n} W_{AHP} = 1. \quad (7)$$

The AHP method provides the possibility to check consistency of the estimated weights. This is done with the consistency ratio ($CR$), which is shown in Equation (8) [30]:

$$CR = CI/RI, \quad (8)$$

where $CI$ is the consistency index which is obtained by first computing the scalar $\lambda_{max}$ as the average of the elements of the vector whose $i$th element is the ratio of the $i$th element of the vector ($M$*$W_{AHP}$) to the corresponding element of the vector $W_{AHP}$ [30]. Then, $CI$ is calculated using the Equation (9):

## Appendix 1b

$$CI = \frac{\lambda_{max} - n}{n - 1}, \quad (9)$$

where $\lambda_{max}$ is the largest eigenvalue of the matrix and $n$ is the number of indicators. *RI* is a constant that depends on $n$. When $CR < 0.1$, the evaluation is consistent, and reliable results can be expected from the AHP model [23].

In this study, four pairwise comparison matrices (Tables 3–6) were constructed for the weight estimations of the different indicators used in the CBDRI model. Furthermore, $W_{AHP}$ was multiplied by three to get the final weights ($W_{xi}$) of each indicator.

**Table 3.** The weights estimated from the analytical hierarchy process model and the final weights for the indicators of the hazard factor. For the definition of H1, H2, H3 and H4, see Table 2.

| | **H1** | **H2** | **H3** | **H4** | $\boldsymbol{W_{AHP}}$ | $\boldsymbol{W_{xi}}$ |
|---|---|---|---|---|---|---|
| H1 | 1 | 1 | 1/3 | 2 | 0.2 | 0.6 |
| H2 | 1/2 | 1 | | 2 | 0.18 | 0.54 |
| H3 | 3 | 3 | 1 | 2 | 0.47 | 1.41 |
| H4 | 1/2 | 1/2 | 1/2 | 1 | 0.15 | 0.45 |
| CR = 0.01 | | | | | | |

**Table 4.** The weights estimated from the analytical hierarchy process model and the final weights for the indicators of the exposure factor. For the definition of E1, E2, E3 and E4, see Table 2.

| | **E1** | **E2** | **E3** | **E4** | $\boldsymbol{W_{AHP}}$ | $\boldsymbol{W_{xi}}$ |
|---|---|---|---|---|---|---|
| E1 | 1 | 2 | 2 | 1/3 | 0.22 | 0.66 |
| E2 | 1/2 | 1 | 1/2 | 1/5 | 0.1 | 0.3 |
| E3 | 1/2 | 2 | 1 | 1/3 | 0.15 | 0.45 |
| E4 | 3 | 5 | 3 | 1 | 0.52 | 1.56 |
| CR = 0.02 | | | | | | |

**Table 5.** The weights estimated from the analytical hierarchy process model and the final weight for the indicators of the vulnerability factor. For the definition of V1, V2…V14, see Table 2.

| | **V1** | **V2** | **V3** | **V4** | **V5** | **V6** | **V7** | **V8** | **V9** | **V10** | **V11** | **V12** | **V13** | **V14** | $\boldsymbol{W_{AHP}}$ | $\boldsymbol{W_{xi}}$ |
|---|---|---|---|---|---|---|---|---|---|---|---|---|---|---|---|---|
| V1 | 1 | 1 | 1/2 | 2 | 1/2 | 3 | 2 | 3 | 2 | 1 | 2 | 3 | 2 | 2 | 0.10 | 0.3 |
| V2 | | 1 | 1/2 | 2 | 1/2 | 3 | 2 | 3 | 2 | 1 | 2 | 3 | 2 | 2 | 0.10 | 0.3 |
| V3 | | | 1 | 3 | 2 | 5 | 3 | 5 | 3 | 2 | 3 | 5 | 3 | 3 | 0.17 | 0.51 |
| V4 | | | | 1 | 1/2 | 2 | 1 | 2 | 1 | 2 | 1 | 2 | 1 | 1 | 0.06 | 0.18 |
| V5 | | | | | 1 | 3 | 2 | 3 | 2 | 2 | 2 | 3 | 2 | 2 | 0.12 | 0.36 |
| V6 | | | | | | 1 | 1/2 | 1 | 1/2 | 1/3 | 1/2 | 1 | 1/2 | 1/2 | 0.03 | 0.09 |
| V7 | | | | | | | 1 | 2 | 1 | 1/2 | 1 | 2 | 1 | 1 | 0.05 | 0.15 |
| V8 | | | | | | | | 1 | 1 | 1/3 | 1/2 | 1 | 1/2 | 1/2 | 0.03 | 0.09 |
| V9 | | | | | | | | | 1 | 1/2 | 1 | 2 | 1 | 1 | 0.05 | 0.15 |
| V10 | | | | | | | | | | 1 | 2 | 3 | 2 | 2 | 0.09 | 0.27 |

## Appendix 1b

| | | | | | | |
|---|---|---|---|---|---|---|
| V11 | 1 | 2 | 1 | 1 | 0.05 | 0.15 |
| V12 | | 1 | 1/2 | 1/2 | 0.03 | 0.09 |
| V13 | | | 1 | 1 | 0.05 | 0.15 |
| V14 | | | | 1 | 0.05 | 0.15 |
| CR = 0.01 | | | | | | |

**Table 6.** The weights estimated from the analytical hierarchy process model and the final weights for the indicators of the capacity and measure factor. For the definition of C1, C2…C15, see Table 2.

| | **C1** | **C2** | **C3** | **C4** | **C5** | **C6** | **C7** | **C8** | **C9** | **C10** | **C11** | **C12** | **C13** | **C14** | **C15** | $W_{AHP}$ | $W_{xi}$ |
|---|---|---|---|---|---|---|---|---|---|---|---|---|---|---|---|---|---|
| C1 | 1 | 2 | 3 | 2 | 2 | 3 | 1 | 1 | 2 | 3 | 2 | 2 | 1/3 | 2 | 2 | 0.10 | 0.3 |
| C2 | | 1 | 2 | 1 | 2 | 2 | 1/2 | 1/2 | 1 | 2 | 1 | 1 | 1/3 | 1 | 1 | 0.06 | 0.18 |
| C3 | | | 1 | 1/2 | 1/2 | 1 | 1/3 | 1/3 | 1/2 | 1 | 1/2 | 1/2 | 1/5 | 1/2 | 1/2 | 0.03 | 0.09 |
| C4 | | | | 1 | 1 | 2 | 1/2 | 1/2 | 1 | 1/2 | 1 | 1 | 1/3 | 1 | 1 | 0.05 | 0.15 |
| C5 | | | | | 1 | 2 | 1/2 | 1/2 | 1 | 2 | 1 | 1 | 1/3 | 1 | 1 | 0.05 | 0.15 |
| C6 | | | | | | 1 | 1/3 | 1/3 | 1/2 | 1 | 1/2 | 1/2 | 1/5 | 1/2 | 1/2 | 0.03 | 0.09 |
| C7 | | | | | | | 1 | 1 | 2 | 3 | 2 | 2 | 1/3 | 2 | 2 | 0.10 | 0.3 |
| C8 | | | | | | | | 1 | 2 | 3 | 2 | 2 | 1/3 | 2 | 2 | 0.10 | 0.3 |
| C9 | | | | | | | | | 1 | 2 | 1 | 1 | 1/3 | 1 | 1 | 0.05 | 0.15 |
| C10 | | | | | | | | | | 1 | 1/2 | 1/2 | 1/5 | 1/2 | 1/2 | 0.03 | 0.09 |
| C11 | | | | | | | | | | | 1 | 1 | 1/3 | 1 | 1 | 0.05 | 0.15 |
| C12 | | | | | | | | | | | | 1 | 1/3 | 1 | 1 | 0.05 | 0.15 |
| C13 | | | | | | | | | | | | | 1 | 3 | 3 | 0.18 | 0.54 |
| C14 | | | | | | | | | | | | | | 1 | 1 | 0.05 | 0.15 |
| C15 | | | | | | | | | | | | | | | 1 | 0.05 | 0.15 |
| CR = 0 | | | | | | | | | | | | | | | | | |

*2.6. Estimation of the Flood Hazard Index*

In this study, the indicators of the experienced hazard (H1 and H3) were assessed by answering the corresponding questions based on the literature (e.g., [31, 32]). In contrast, the possible hazard components (H2 and H4) of the risk index were characterized in terms of the floodplain inundation level of the 50-year flood, which were obtained through hydraulic modelling with the sub-grid model of LISFLOOD-FP hydraulic model [33] and regional flood frequency analysis performed by Komi et al. [34]. The 50-year flood was chosen because it provides a plausible measure of flood-affected populations [35]. The application of the sub-grid solver of LISFLOOD-FP requires the specification of the streamlines of the river, floodplain topography, river widths, river bank elevation, inflow hydrographs and downstream boundary conditions. In addition, the sub grid channel solver of LISFLOOD-FP has four parameters, namely: the Manning's friction coefficient separately for channel and floodplain, the exponent ($p$), and coefficient ($r$) of the hydraulic geometry. Due to the lack of detailed hydrological data, tributaries of the Oti River Basin were not considered in the flood inundation modelling. For further details on the calibration of LISFLOOD-FP hydraulic model, the reader is referred to Bates et al. [36]. Finally, the flood hazard severity was estimated based on the categorization proposed by Dinh et al. [37] as shown in Table 7. Since each community area has many flood severity classes (FC) to a particular extent, an average flood severity index (FSI) was used to estimate the average flood severity of a given community area. The FSI takes into account the areal extent of a flood's depth and was calculated using Equation (10) [13]:

## Appendix 1b

$$\mathbf{FSI} = \frac{\sum_{i=1}^{n}(\boldsymbol{FC})_i \boldsymbol{A_i}}{\sum_{i=1}^{n} \boldsymbol{A_i}}, \quad (10)$$

where $A_i$ is the areal extent of the flood severity class $i$, $n$ is the number of flood severity classes and $(FC)_i$ was represented by the mean depth of the flood severity class (Table 7). Then, the flood hazard index (H) was estimated using Equation (5).

**Table 7.** Categorization of flood hazard severity [36].

| Flood Depth (m) | Hazardseverity | Definition of Hazard Severity |
|---|---|---|
| 0–0.2 | Very low | The damage to property is expected to be very low |
| 0.2–0.5 | Low | The number of casualties due to floods, in terms of death or injuries, is insignificant, and the damage to property is expected to be relatively low |
| 0.5–1.0 | Medium | Causalities, in terms of death and injuries are considerable, relative to the number of people living in the area under study. |
| 1.0–2.0 | High | Damage to property is extensive and the probability of having dead and injured people is high. |

*2.7. Estimation of the Flood Risk Index*

To calculate the overall flood risk index (R) in the community based system, Equation (11) was used [38]. In this equation, a constant coefficient of 0.03 was multiplied by each factor in order to maintain the same scale between 0 and 10 as for the individual factor indices [12]:

$$R = 0.03\{H * V * E[0.1(1-a)C + a]\}, \quad (11)$$

where $a$ is a constant ($0 \leq a \leq 1$) used to reduce the total flood risk value and it is assumed to be 0.75 [38]. In addition, this equation is based on the conventional mathematical expression of risk as a convolution of hazard, vulnerability and exposure. The coping capacity (C) was added as a reduction factor [38]. Finally, the values of the risk index were grouped into five categories (very low, low, moderate, high and very high) as shown in Table 8.

**Table 8.** Categorization of the flood risk index used in this study.

| Range of the Flood Risk Index | Risk Zone |
|---|---|
| 0–2 | Very low |
| 2–4 | Low |
| 4–6 | Moderate |
| 6–8 | High |
| 8–10 | Very high |

## 3. Results

*3.1. Scores of the Indicators*

As it is expected, there are differences in the scores assigned to some of the indicators in this case study. For example, 57.15%, 28.57% and 14.29% of the studied communities score, respectively, low, medium and high levels for 'lifelines' indicator and 14.29%, 57.15% and 28.57% of the communities score,

respectively, low, medium and high levels for the 'area under forest indicator' (V14). However, these communities have almost the same scores for many indicators, for instance those which characterize the hazard and the social vulnerability. Moreover, the scores obtained for most of the capacity and measures indicators are relatively low and consequently high for the vulnerability indicators. All communities score low levels for many indicators of the 'coping capacity factor (e.g., C2, C7, C9, C10, C11 and C12) and high levels for many indicators of the vulnerability factor such as poverty level and literacy rate. The low scores for the capacity and measures indicators highlight the insufficiency of social, economic and institutional capacities to cope with extreme floods in the Oti River Basin (Togo).

*3.2. Possible Flood Hazardousness*

Figure 2 shows the 50-year flood hazard map simulated by the hydraulic model (LISFLOOD-FP). This result is used to estimate the severity of the possible flood hazard (H4). When the set of thresholds applied in Table 7 are considered, all community areas fall in the high flood severity category. Sadori has the highest flood depth while Mango has the lowest (Table 9). This difference in simulated flood depth can be explained by the spatial variability in the local topography and the soil property (permeability) of the studied villages. In addition, it is worth noting that the flood depth in the communities may be higher than simulated, given that flooding from tributaries was not considered in this study.

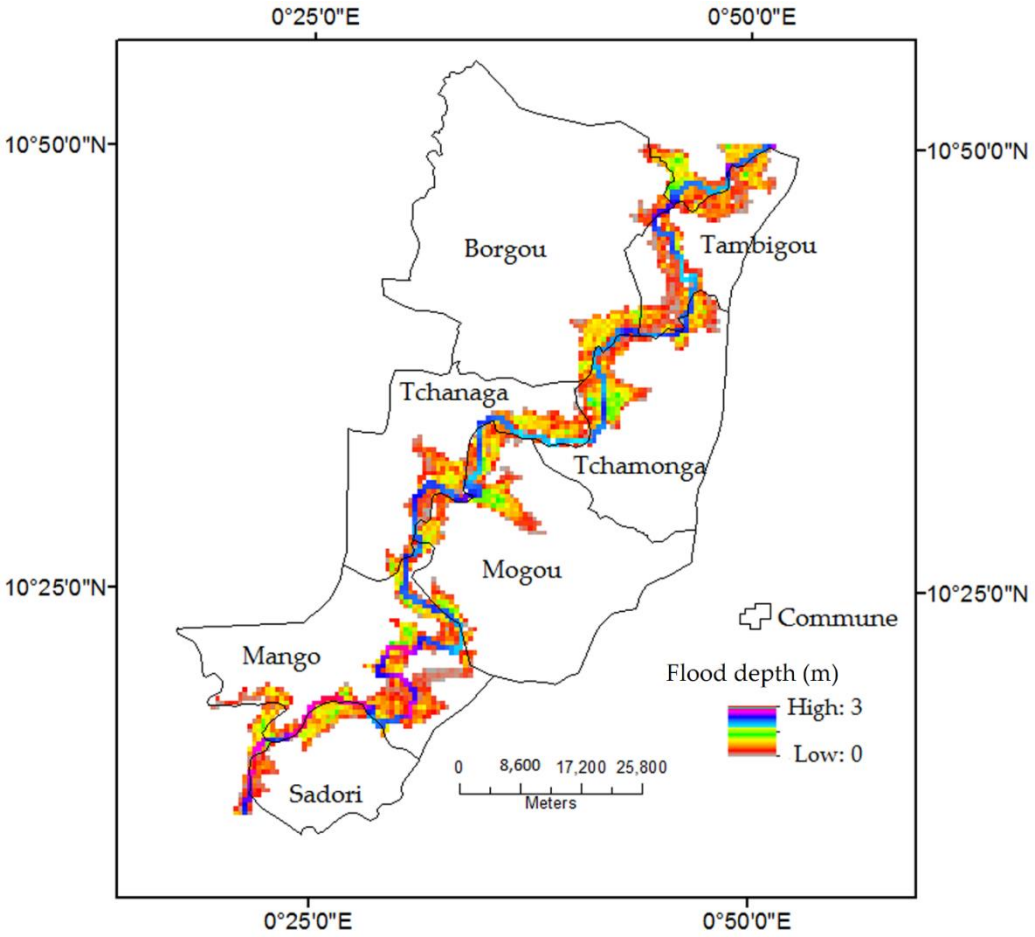


**Figure 2**. Simulated 50-year flood map of the Oti River Basin in Togo.

**Table 9.** Averaged flood depth for the 50-year flood at the different communities in the Oti River Basin.

## Appendix 1b

| Community | Averaged Flood Depth (m) | Severity |
|---|---|---|
| Borgou | 1.57 | High |
| Tambigou | 1.53 | High |
| Tchanaga | 1.56 | High |
| Tchamonga | 1.54 | High |
| Mogou | 1.60 | High |
| Mango | 1.52 | High |
| Sadori | 1.62 | High |

*3.3. Indices of the Risk Factors*

Figure 3 shows the indices of the four factors that contribute to the risk in the CBDRI model. The high level of hazard index can be explained by the repeated and catastrophic floods that have impacted the communities of the Oti River Basin during the last two decades (1998, 2007, 2008 and 2010) and the high level of simulated flood depth, while the observed elevated vulnerability index (V) is mainly due, for instance, to the high poverty level of the communities, insufficiency of access to safe drinking water and the little awareness of the majority of the community members regarding their own flood risk.

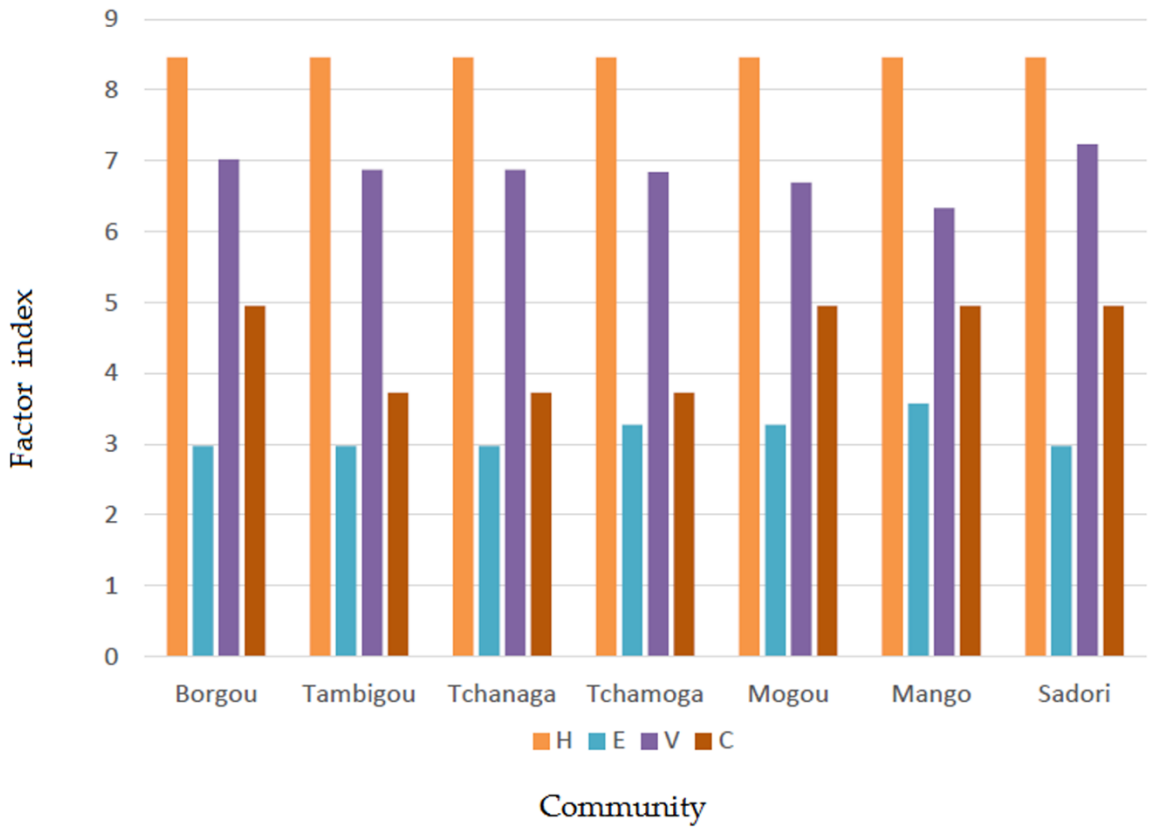

## Appendix 1b

**Figure 3.** Computed indices of the four risk factors for the different communities. C, H, V and E stand for capacities, hazard, vulnerability and exposure indices.

*3.4. Flood Risk Index*

As it is shown in Table 10, flood risk in all studied communities is moderate when we consider the classification shown in Table 8. This moderate level of flood risk is associated with a combination of high indices of flood hazard and vulnerability and low indices of capacities and exposure. In addition, Mango has the highest flood risk index (5.01), while the lowest flood risk index is estimated at Tambigou and Tchanaga (4.36). The small difference (0.65) between the highest and lowest flood risk indices is an indication of the relative homogeneity of flood risk across these communities.

**Table 10.** Flood risk index of the different communities.

| Communities | Borgou | Tambigou | Tchanaga | Tchamoga | Mogou | Mango | Sadori |
|---|---|---|---|---|---|---|---|
| Risk index | 4.62 | 4.36 | 4.36 | 4.78 | 4.85 | 5.01 | 4.76 |

**4. Discussion**

In the present work, a community based disaster risk index system and a simulated 50-year flood hazard map were used to assess quantitatively and qualitatively flood risk for rural communities of the Oti River Basin in Togo (West Africa). Thirty seven (37) indicators of flood risk were considered for the analysis and Saaty's AHP (analytical hierarchy process) method was applied to estimate the weights of the indicators.

The results showed that the hazard, vulnerability, coping capacity factors are the most important factors in increasing flood risk in the study area. For instance, as shown in Figure 4, the hazard and vulnerability indices are high in all the studied communities. The low index of capacity and measures factor is associated with the insufficiency of the strategies and capacity to mitigate flood risk**.** For instance, the people interviewed pointed out the absence of flood risk management committees at the village level, non-access to local emergency funds and insurances for house owners. In addition, education and culture of flood risk management are not part of the school curricula. Apart from Sadori, Mango and Borgou, the investigated communities lack early warning systems and emergency plans for floods, although advanced warning systems for floods are very helpful in reducing flood risk and providing emergency response personnel time to prepare for and mitigate damages [39, 40]. Consequently, decreasing vulnerability and increasing capacity of the communities to manage their own flood risk should be paramount in order to mitigate flood risk in the study area. For instance, due to the high poverty level in the majority of the community areas (Table 1), creating diverse income-generating opportunities could be essential to reduce the vulnerability of the local population. The results of this study showed the need for non-structural measures to reduce the negative consequences of floods in the study area. These measures include the implementation of advanced early flood warning systems for all the flood-prone communes and public education about flood risk, real involvement of wide range of local actors in national efforts to manage flood risks so that they can contribute as much as possible to the reduction of flood risks in their own localities, and a creation of a culture of awareness in which the population realises the negative impacts of floods on development. Moreover, actions to discourage settlements in flood-prone areas and building codes to make houses more resilient to flooding are useful to mitigate flood risk in the Oti River Basin.

Furthermore**,** the relative homogeneity observed in the majority of the vulnerability and coping capacity is reasonable because the studied communities are almost the same in their social and economic profiles as shown by their poverty levels (Table 1). In addition, their economic capacities for disaster risk

management are also the same: all are funded by non-governmental organisation in the case of flood disasters. They are managed at the top by a central government (lack of decentralization). For this reason, a large difference in vulnerability and capacities in the Oti River Basin at the village scale is unexpected.

The presented flood risk indices summarize complex information about flood risk in a simple way that is easy for non-experts to understand and use in flood risk management policies [12]. However, there are some issues that need to be considered. First, the majority of the data are subjective as they were collected from selected local residents. In addition, the results are dependent on the selected indicators, their categorization, the set of thresholds and the spatial scale of application. Second, the selected indicators are only a simplification of key elements of flood risks and vulnerabilities that we wanted to measure. They are not real measures of these elements themselves. Finally, the return period associated with the simulated flood hazard severity is 50 years. Given the significant contribution of the hazard factor to the total flood risk, the results will differ if floods with lower or higher return periods than 50 years are considered.

## 5. Conclusions

The risk of riverine flood to community facilities in the Oti River Basin is expected to increase due to the combined effects of climate change and land use changes, economic development and population growth. In 2005, the World Conference on Disaster Reduction emphasized the necessity to incorporate disaster risk assessment into rural planning and management in order to mitigate disaster risk [41]. This study performed a comprehensive flood risk assessment of rural communities in the Oti River Basin of Togo and identified the relative contributions of hazard, exposure, vulnerability**,** as well as capacity and measure factors to flood risk. While the flood risk for all communities studied is moderate, there were high levels of hazards, vulnerability and a lack of capacity and measures, whereas the exposure is relatively low. The outcomes of this study provide community members as well as government officials with empirical risks and vulnerability evidence. Consequently, the information provided by the community-based disaster risk index system can be used to support decision-makers at local and national levels in order to analyze and understand the flood risk to which a community is exposed. In addition, periodic application of the proposed method can be a measure to examine the projects undertaken to manage flood risks. In order to reduce flood risk in the Oti River Basin, decreasing vulnerability through creation of new income-generating opportunities and increasing capacity of communities to manage their own flood risk should be paramount.

**Supplementary Materials:** The following are available online at www.mdpi.com/link, Table S1: questionnaire used in the Community-based Disaster Risk Index, modified from Bollin et al. [12].

**Acknowledgments:** This work is part of the West African Science Service Center on Climate Change and Adapted Land Use project (WASCAL; www.wascal.org), which is funded by the German Ministry of Education and Research (BMBF). The authors would like to thank the editors and the two anonymous reviewers for the relevant comments and suggestions, which significantly improved the quality of the manuscript.

**Author Contributions:** Kossi Komi conducted this research as a part of his Ph.D. thesis. Kossi Komi wrote the initial version of the manuscript. Bernd Diekkrüger and Barnabas A. Amisigo supervised the work and helped in improving the manuscript.

**Conflicts of Interest:** The authors declare no conflict of interest.

### Abbreviations

The following abbreviations are used in this manuscript:

| | |
|---|---|
| AHP | Analytical Hierarchy Process |
| CBDRI | Community-Based Disaster Risk Index. |

## Appendix 1b

| | |
|---|---|
| DGSCN | Direction Générale de la Statistique et de la Comptabilité Nationale (Togo). |
| FAO | Food and Agriculture Organization. |
| GTZ | German Technical Cooperation Agency. |
| IFRCRCS | International Federation of Red Cross and Red Crescent Societies |
| IPCC | Intergovernmental Panel on Climate Change. |
| ISDR | International Strategy for Disaster Reduction. |
| NASA | National Aeronautics and Space Administration (United State of America). |

### References


1. Tschakert, P.; Sagoe, R.; Ofori-Darko, G.; Codjoe, S.N. Floods in the Sahel: An analysis of anomalies, memory, and anticipatory learning. *Clim. Chang*. **2010**, *103*, 471–502.
2. Guha-Sapir, D.; Vos, F.; Below, R.; Ponserre, S. *Annual Disaster Statistical Review 2010: The Numbers and Trends*; CRED: Brussels, Belgium, 2011.
3.Mulugeta, G.; Ayonghe, S.; Daby, D.; Dube, O.; Gudyanga, F.; Lucio, F.; Durrheim, R. *Natural and Human-Induced Hazards and Disasters in Sub-Saharan Africa*; ICSU Regional Office for Africa: Pretoria, South Africa, 2007.
4.Skilodimou, H.; Livaditis, G.; Bathrellos, G.; Verikiou–Papaspiridakou, E. Investigating the flooding events of the urban regions of Glyfada and Voula, Attica, Greece: A contribution to Urban Geomorphology. *Geogr. Ann. A* **2003**, *85*, 197–204.
5. International Strategy for Disaster Reduction (ISDR). *Living with Risk: A Global Review of Disaster Reduction Initiatives*; United Nations: New York, NY, USA; Geneva, Switzerland, 2004.
6.Moel de, H.; Jongman, B.; Kreibich, H.; Merz, B.; Penning-Rowsell, E.; Ward, J.P. Flood risk assessments at different spatial scales. *Mitig. Adapt. Strateg. Glob. Chang.* **2015**, *20*, 865–890.
7.Bathrellos, G.D.; Karymbalis, E.; Skilodimou, H.D.; Gaki-Papanastassiou, K.; Baltas, E.A. Urban flood hazard assessment in the basin of Athens Metropolitan city, Greece. *Environ. Earth Sci*. **2016**, *75*, 319.
8.Ward, J.P.; Jongman, B.; Weiland, S.F.; Bouwman, A.; Beek van, R.; Bierkens, P.F.M.; Ligtvoet, W.; Winsemius, C.H. Assessing flood risk at the global scale: Model setup, results, and sensitivity. *Environ. Res. Lett*. **2013**, *8*, 044019.
9. Forkuo, E.K. Flood hazard mapping using Aster image data with GIS. *Int. J. Geomat. Geosci.* **2011**, *1*, 932–950.
10. Musungu, K.; Motala, S.; Smit, J. Using Multi-criteria Evaluation and GIS for Flood Risk Analysis in Informal Settlements of Cape Town: The Case of Graveyard Pond. *S. Afr. J. Geomat*. **2012**, *1*, 92–108.
11. Guarín, P.G. Integrated Local Knowledge into GIS-Based Flood Risk Assessment. The Case of Triangulo and Mabolo Communities in Naga City (Philippines). Ph.D. Thesis, International Institute for Geo-Information Science and Earth Observation (ITC), Enschede, The Netherlands, 2008.
12. Bollin, C.; Cardenas, C.; Hahn, H.; Vasta, K.S. *Natural Disasters Network: Comprehensive Risk Management by Communities and Local Governments*; Inter-American Development Bank: Washington, DC, USA, 2003.
13. Adeloye, J.A.; Mwale, D.F.; Dulanya, Z. A metric-based assessment of flood risk and vulnerability of rural communities in the Lower Shire Valley, Malawi. *Proc. IAHS* **2015**, *370*, 139–145.
14. Gesellschaft für Technische Zusammenarbeit. *Community-Based Disaster Risk Management Approach: Experience Gained in Central America*; Deutsche Gesellschaft für Technische Zusammenarbeit (GTZ): Eschborn, Germany, 2003.
15. Meyer, V.; Scheuer, S.; Haase, D. A multicriteria approach for flood risk mapping exemplified at the Mulde River, Germany. *Nat. Hazards* **2009**, *48*, 17–39.
16. Apel, H.; Thieken, H.A.; Merz, B.; Blöschl, G. Flood risk assessment and associated uncertainty. *Nat. Hazards Earth Syst. Sci*. **2004**, *4*, 295–308.
17. Birkmann, J. Risk and vulnerability indicators at different scales: Applicability, usefulness and policy implications. *Environ. Hazards* **2007**, 7 20–31
18. Gall, M. Indices of Social Vulnerability to National Hazards: A Comparative Evaluation. Ph.D. Thesis, University of South Carolina, Columbia, SC, USA, 2007.
.19. International Federation of Red Cross and Red Crescent Societies (IFRCRCS) *West Africa: Flood in Ghana and Togo, Emergency Appeal No MDR61002*; IFRCRCS: Geneva, Switzerland, 2007.

## Appendix 1b


20. Direction Générale de la Statistique et de la Comptabilité Nationale (DGSCN) *Fourth Population and Housing Census in Togo, Republic of Togo*; DGSCN: Lomé, Togo ,2010. (In French)
21. Coulombe, H.; Gentry, A.; Amouzouvi, K. TOGO: Mapping of Poverty 2011, Beyond Productions, Lomé, Togo; 2011. (In French). Available at http://www.togoinfo.tg/publications-togoinfo-tg/finish/7-quibb/12-cartographie-de-pauvrete-2011/0 (last accessed on December 1, 2015)
22. Food and Agriculture Organization of the United Nations (FAO). Land Cover Map of Togo. 2013. Available online: http://data.fao.org/map?entryId=3af5c4ff-865e-4274-af69-4283cf41d41b (accessed on 30 September 2015).
23. Saaty, T.L. A scaling method for priorities in hierarchical structures. *J. Math. Psychol*. **1977**, *15*, 234–281.
24. Saaty, T.L. How to make a decision: The Analytic Hierarchy Process. *Eur. J. Oper. Res.* **1990**, *48*, 2–26.
25. Marinoni, O. Implementation of the analytical hierarchy process with VBA in ArcGIS. *Comput. Geosci.* **2004**, *30*, 367–646.
26. Omkarprasad, V.; Sushil, K. Analytic hierarchy process: An overview of applications. *Eur. J. Oper. Res.* **2006**, *169*, 1–29.
27. Bathrellos, G.D.; Gaki-Papanastassiou, K.; Skilodimou, H.D.; Papanastassiou, D.; Chousianitis, K.G. Potential suitability for urban planning and industry development by using natural hazard maps and geological—Geomorphological parameters. *Environ. Earth Sci.* **2012**, *66*, 537–548.
28. Bathrellos, G.D.; Gaki-Papanastassiou, K.; Skilodimou, H.D.; Skianis, G.A.; Chousianitis, K.G. Assessment of rural community and agricultural development using geomorphological-geological factors and GIS in the Trikala prefecture (Central Greece). *Stoch. Environ. Res. Risk Assess.* **2013**, *27*, 573–588.
29. Danumah, H.J.; Odui, N.S.; Saley, M.B.; Srarzynski, J.; Thiel, M.; Kwaku, A.; Kwame, K.F.; Akpa, Y.L. Flood risk assessment and mapping in Abidjan district using multi-criteria analysis (AHP) model et geoinformation techniques, (Cote d'ivoire). *Geoenviron. Dis.* **2016**, *3*, 10.
30. Saaty, L.T. Decision making with the analytic hierarchy process. *Int. J. Serv. Sci.* **2008**, *1*, 83–98.
31. Ministry of Environment and Forestal Resources. *National Adaptation Strategies to Climate Change*; Ministry of Environment and Forestal Resources: Togo, Lomé, Togo, 2009. (In French)
32. Paeth, H.; Fink, H.A.; Pohle, S; Keis, F.; Mächel, H.; Samimi, C. Meteorological characteristics and potential causes of the 2007 flood in sub-Saharan Africa. *Int. J. Climatol*. **2011**, *31*, 1908–1926.
33. Neal, J.; Schumann, G.; Bates, P. A subgrid channel model for simulating river hydraulics and floodplain inundation over large and data sparse areas. *Water Resour. Res*. **2012**, *48*, W11506.
34. Komi, K.; Amisigo, A.B.; Diekkrüger, B.; Hountondji, C.C.F. Regional Flood Frequency Analysis in the Volta River Basin, West Africa. *Hydrology* **2016**, *3*, 5.
35. Hirabayashi, Y.; Kanae, S. First estimate of the future global population at risk of flooding. *Hydrol. Res. Lett*. **2009**, *3*, 6–9.
36. Bates, P.D.; Trigg, M.; Neal, J.; Dabrowa, A. *LISFLOOD-FP: User Manual, Code Release 6.0.4*; School of Geographical Sciences, University of Bristol: Bristol, UK, 2013.
37. Dinh, Q.; Balica, S.; Popescu, I.; Jonoski, A. Climate Change Impact on Flood Hazard, Vulnerability and Risk of the Long XuyenQuadrangle in the Mekong Delta. *Int. J. River Basin Manag*. **2012**, *10*, 103–120.
38. Davidson, R.; Lambert, K. Comparing the Hurricane Disaster Risk of U.S. Coastal Counties. *Nat. Hazards Rev.* **2001**, *2*, 132–142.
39. Givati, A.; Gochis, D.; Rummler, T.; Kunstmann, H. Comparing One-Way and Two-Way Coupled Hydrometeorological Forecasting Systems for Flood Forecasting in the Mediterranean Region. *Hydrology* **2016**, *3*, 19.
40. Massari, C.; Brocca, L.; Ciabatta, L.; Moramarco, T.; Gabellani, S.; Albergel, C.; De Rosnay, P.; Puca, S.; Wagner, W. The Use of H-SAF Soil Moisture Products for Operational Hydrology: Flood Modelling over Italy. *Hydrology* **2015**, *2*, 2–22.
41. International Strategy for Disaster Reduction (ISDR). Hyogo Framework for Action 2005–2015: Building the Resilience of Nations and Communities to Disasters. In Proceedings of the World Conference on Disaster Reduction, Kobe, Hyogo, Japan, 18–22 January 2005. .

## Appendix 3.1

**Appendix 3.1** Site characteristics used in the development of the regression models. The data in boldface were obtained from Moniod et al. (1977). P is the mean annual rainfall, $Q_m$ is the mean annual daily maximum discharge, A the area and S the mean slope.

| Number | Site name | Record periods | P (mm) | $Q_m$ ($m^3/s$) | A ($km^2$) | S (%) |
|---|---|---|---|---|---|---|
| 1 | Nwokuy | 1954-1973 | **1,085** | **103.53** | **14,800** | 0.70 |
| 2 | Boromo | 1955-1973 | **850** | **126.23** | **35,000** | 0.40 |
| 3 | Lawra | 1951-1973 | **906** | **591.78** | **66,820** | 1.10 |
| 4 | Bui | 1954-1973 | **960** | **1270** | **96,000** | 1.47 |
| 5 | Bamboi | 1950-1973 | **1,348** | **1,329.42** | **134,200** | 0.11 |
| 6 | Yakala | 1956-1973 | **837** | **341.83** | **31,680** | 1.19 |
| 7 | Nangodi | 1958-1973 | **917** | **309.71** | **11,570** | 1.41 |
| 8 | Nakpanduri | 1958-1972 | **925** | **107.32** | **1,530** | 1.47 |
| 9 | Pwalugu | 1958-1973 | **1,156** | **1,274.56** | **63,350** | 1.09 |
| 10 | Yagaba | 1958-1973 | **1,156** | **316.21** | **10,600** | 0.45 |
| 11 | Nawuni | 1953-1973 | **1,156** | **1,704.62** | **92,950** | 1.05 |
| 12 | Yapei | 1951-1967 | **1,348** | **1,846.94** | **102,170** | 1.11 |
| 13 | Tiele | 1961-1973 | **973** | **54.38** | **836** | 1.56 |
| 14 | Porga | 1963-1989 | 949 | 306.66 | **22,280** | 0.33 |
| 15 | Mandouri | 1959-1979 | 930 | 565.57 | **29,100** | 0.80 |
| 16 | Borgou | 1960-1987 | 1,004 | 110.54 | **2,280** | 0.99 |
| 17 | Mango | 1953-1989 | 1,055 | 796.59 | **35,650** | 0.33 |
| 18 | Titira | 1962-1987 | 1,161 | 542.38 | **3,695** | 0.89 |
| 19 | Naboulgou | 1962-1987 | 1,153 | 524.42 | **5,470** | 1.153 |
| 20 | Koumangou | 1959-1987 | 1,076 | 421.62 | **6,730** | 0.70 |
| 21 | Lama-kara | 1954-1987 | 1,220 | 396.32 | **1,560** | 2.52 |
| 22 | Saboba | 1959-2002 | 1,072 | 1,800 | **53,090** | 1.44 |
| 23 | Sabari | 1959-2007 | 1,216 | 2,020.71 | **58,670** | 0.49 |

**Appendix 3.2.** Input tables and maps used in LISFLOOD hydrological model (.Van der Knijff et al., 2008)

| **LAND USE** | | |
|---|---|---|
| **Table** | **Name** | **Description** |
| Crop Coefficient | cropcoef.txt | Crop coefficient for each land use class [-] |
| Manning roughness | n.txt | Manning's roughness for each land use class [-] |
| **SOIL TEXTURE** | | |
| **Table** | **Name** | **Description** |
| TabThetaSat | thetas.txt | Saturated volumetric soil moisture content |
| TabThetaRes | thetar.txt | Residual volumetric soil moisture content |
| TabLambda | lambda | Pore size index |
| TabGenuAlpha | alpha | Van Genuchten parameter α |
| TabKSat | ksat | Saturated conductivity |

| GENERAL | | |
|---|---|---|
| **Maps** | **Name** | **Description** |
| Mask | area.map | Boolean map that defines model boundaries |
| **TOPOGRAPHY** | | |
| **Maps** | **Name** | **Description** |
| LDD | ldd.map | This file contains flows direction from each cell to its steepest neighbor (value 1-9). |
| Grad | gradient.map | Slope gradient |
| **LAND USE** | | |
| **Map** | **Name** | **Description** |
| Land use | landuse.map | Map with land use classes |
| Forest | forest.map | Forest fraction for each cell.Values range from 0(no forest ) to 1(100% forest) |
| Direct runoff fraction | directrf.map | Urban fraction for each cell.Values range from 0(no urban area) to 1 (100% urban) |

**Appendix 3.2**

**Appendix 3. 2** (continued)

| **SOIL** | | |
|---|---|---|
| **Maps** | **Name** | **Description** |
| Texture 1 | soiltex1.map | Soil texture class layer 1 (upper layer) |
| Texture 2 | soiltex 2.map | Soil texture class layer 2 (lower layer) |
| Soil depth | soidep.map | Soil depth to bedrock or groundwater [cm] |

| **CHANNEL GEOMETRY** | | |
|---|---|---|
| **Maps** | **Name** | **Description** |
| Channels | Chan.map | Map with Boolean 1 for all channel pixel, and Boolean 0 for all other pixels on the mask map. |
| ChanGrad | changrad.map | Channel gradient |
| ChanMan | chanman.map | Manning's roughness coefficient for channels |
| ChanLength | chanleng.map | Channel length [m] |
| Channel bottom width | chanbw.map | Channel bottom width [m]. |

| **METEOROLOGICAL VARIABLES** | | |
|---|---|---|
| **Maps** | **Prefix** | **Description** |
| Precipitation | pr | Precipitation intensity [mm $day^{-1}$] |
| E0 | e | Daily potential evaporation rate from free water surface |
| ES0 | es | Daily potential evaporation rate from bare soil surface |
| ET0 | et | Daily potential reference evapotranspiration |

| **DEVELOPMENT OF VEGETATION OVER TIME** | | |
|---|---|---|
| **Maps** | **Prefix** | **Description** |
| LAI | lai | Pixel-average leaf area index [$m^2$ $m^{-2}$] |

| **DEFINITION OF INPUT/OUTPUT TIME SERIES** | | |
|---|---|---|
| | | |
| **Maps** | **Name** | **Description** |
| Gauges | Outlets.map | Nominal map with locations at which discharge time series are reported |
| Sites | Sites.map | Nominal map with locations at which discharge time series of intermediate variables are reported. |

**Appendix 3.3** The Community-based Disaster Risk Index, modified from (Bollin et al., 2003)

| | | | | |
|---|---|---|---|---|
| **1. Hazard** | | | | |
| | **Experienced hazard** | | | |
| **1.1** | **(H1) Occurrence** | | | |
| | How often did an emergency with this hazard happen in the past 30 years | | | |
| | 0-1 Times | Low | | |
| | 2-3 Times | Medium | | |
| | > 3 Times | High | | |
| **1.2** | **(H2) Intensity** | | | |
| | What was the intensity of the worst event in the last 30 years? | | | |
| | No persons killed, only damages to houses and infrastructure | Low | | |
| | Few persons killed, destruction of some houses and infrastructure | Medium | | |
| | More than few persons killed, destruction of many houses and infrastructure | High | | |
| **2. EXPOSURE** | | | | |
| | **STRUCTURES** | | | |
| **2.1** | **(E1) number of housing units.** | | | |
| | Total number of housing units | | | |
| | < 10,000 | Low | | |
| | 10.000 - 100.000 | Medium | | |
| | > 100.000 | High | | |
| **2.2** | **(E2) lifelines** | | | |
| | % of homes with piped drinking | | | |
| | <20% | Low | | |
| | 20%-50% | Medium | | |
| | >50% | High | | |
| **2.2** | **Economy** | | | |
| | **(E3) average income per capita/year** | | | |
| | <$1,022 | Low | | |
| | $1,022-$4,015 | Medium | | |
| | >$11/capita/year | High | | |
| 2.3 | **Population** | | | |
| | **(E4) Resident population** | | | |
| | Total number of population living in the commune. | | | |
| | < 50,000 | Low | | |
| | 50,000 – 500,000 | Medium | | |
| | > 500,000 | High | | |

**Appendix 3.3**(Continued)

| 3. VULNERABILITY | | | | |
|---|---|---|---|---|
| **3.1** | **Physical/demographic** | | | |
| | **(V1) Density** | | | |
| | How many people per $km^2$ live in the | | | |
| | <100 | Low | | |
| | 100-500 | Medium | | |
| | >500 | High | | |
| | **(v2) Demographic pressure** | | | |
| | Population growth rate | | | |
| | <2% | Low | | |
| | 2-4% | Medium | | |
| | >4% | High | | |
| | **(V3) Flood-prone areas** | | | |
| | % of the total area prone to flood | | | |
| | < 10% | Low | | |
| | 10-30% | Medium | | |
| | >30% | High | | |
| | **(V4) Access to basic services** | | | |
| | Rate of access to safe drinking water | | | |
| | >50 % | Low | | |
| | 20-50 % | Medium | | |
| | < 20 % | High | | |
| **3.2** | **Social** | | | |
| | **(V5) Poverty level** | | | |
| | Percent of population below poverty level ($1/DAY) | | | |
| | <10% | Low | | |
| | 10-30% | Medium | | |
| | >30% | High | | |
| | **(V6) Literacy** | | | |
| | Percentage of adult population able to read and write | | | |
| | >70% | Low | | |
| | 40-70% | Medium | | |
| | <40 | High | | |
| | **(V7) Attitude** | | | |
| | What priority does the general population give the protection against a flood hazard? | | | |
| | High priority. Protection against a hazard | Low | | |
| | Concerned, but only if a disaster has hit. | Medium | | |
| | Not concerned. Other issues (food, work) | High | | |
| | **(V8) Decentralization** | | | |
| | What is the portion of self-generated revenues of the total available | | | |
| | >50% | Low | | |
| | 20-50% | Medium | | |
| | <20% | High | | |

**Appendix 3**.3 (Continued)

| | | | | |
|---|---|---|---|---|
| | **(<br>V9) Community participation** | | | |
| | % voter turnout on last commune | | | |
| | >70% | Low | | |
| | 50-70% | Medium | | |
| | <20% | High | | |
| **3.3** | **Economic** | | | |
| | **(V10) Local resource base** | | | |
| | **Does the community have a budget** | **Yes/no** | | |
| | Enough to help the most affected | Low | | |
| | Insufficient | High | | |
| | **(V11) Diversification** | | | |
| | Source of livelihood comes from one, two or three | | | |
| | Mix of 3 sectors | Low | | |
| | Mix of 2 sectors | Medium | | |
| | More than 80% in 1 sector (e.g. | High | | |
| | **(V12) Small business** | | | |
| | Percentage of businesses with fewer than 20 employees | | | |
| | <50% | Low | | |
| | 50-80% | Medium | | |
| | >80% | High | | |
| | **(V13) Accessibility** | | | |
| | How often in the last 5 years was the commune isolated through interruption of access roads for more than 2 days | | | |
| | 0- time | Low | | |
| | 1-5 times | Medium | | |
| | >5 times | High | | |
| 3.4 | **Environmental** | | | |
| | **(V14) Area under forest** | | | |
| | How much of the total territory of the commune is covered with forest? | | | |
| | >30% | Low | | |
| | 10-30% | Medium | | |
| | <10% | High | | |
| | | | | |

Appendix 3.3

| 4. CAPACITIES AND MANAGEMENT | | | | |
|---|---|---|---|---|
| 4.1 | Physical planning and engineering | | | |
| | (C1) Landuse planning | | Their enforcement is | Evaluation |
| | Does a land use plan or zoning regulations exists that keeps local production and housing out of hazardous areas? | YES/NO<br>If YES, explain | Low | Low |
| | | | High | High |
| | (C2) Preventive measures | | Expected effect on damage | |
| | Do flood exposure-limiting mechanisms/structures exist (dykes, retaining walls, dams, barrages, rock fall barriers, terraces, drainage)? | YES/NO<br>If YES, explain | Low | Low |
| | | | Medium/high | Medium/high |
| | (C3) Environmental management | | Number of activities and project | |
| | Are there activities to promote and enforce conservation of natural resources in risk areas (e.g. protection of water reserves, natural resources, desertification control techniques, reforestation) | YES/NO<br>If YES, explain | Few | Low |
| | | | Some | Medium |
| | | | Many | High |
| 4.2 | Societal measures | | | |
| | (C4) Public awareness | | Frequency | |
| | Are the public awareness programs executed? | YES/NO<br>If YES, what are these programmes | Once | Low |
| | | | sometimes | Medium |
| | | | regular | High |
| | (C5) School curriculum | | The topics are taught at | |
| | Are risk, disaster, environment and development topics part of taught lessons at school? | YES/NO<br>If YES, explain | One grade only | Low |

**Appendix 3.3**

**Appendix 3.3** (Continued)

| | | | | |
|---|---|---|---|---|
| | **(C6) Public participation** | | **It is composed of** | |
| | Is the public represented as member in the risk management/ emergency committee? | **YES/NO If YES, explain** | Only level 1 | Low |
| | | | Level 2 | Medium |
| | | | Level 3 of the society | High |
| | Level 1: administration (mayor's office, planning department | | | |
| | Level 2: relevant response institutions (police, fire brigade, education, emergence health) | | | |
| | Level 3: the public (business, civil society, NGO'S) | | | |
| | **(C7) Access to national emergency fund** | | **How fast can it be released/received** | |
| | Is there access to a national/ district emergency fund? | **YES/NO If YES, explain** | >7days | Low |
| | | | 3-5 days | Medium |
| | | | <3 days | High |
| | **(C8) Access to international emergency funds** | | **Access to funds is:** | |
| | Is there access to international emergency funds? | **YES/NO If YES, explain** | Difficult | Low |
| | | | Easy | High |
| | **(C9) Insurance market** | | Use | |
| | Is disaster risk insurance coverage for buildings available? | **YES/NO If YES, explain** | Not common | Low |
| | | | Common | High |
| **4.3** | **Management and institutional measure** | | | |
| | **(C10) Risk management** | | **Meeting frequency:** | |
| | Does a community risk management or emergency committee exist, that deals with prevention, mitigation, Preparedness and response? | **YES/NO If YES, explain** | Only during Emergency | Low |
| | | | Once a year | Medium |
| | | | At least quarterly | High |

**Appendix3.3** (Continued)

| | | | | |
|---|---|---|---|---|
| | **(C11) Risk map** | | **The map is available at** | |
| | Does a risk map exist? | **YES/NO If YES, explain** | Only level1 | Low |
| | | | Also at level 2 | Medium |
| | | | Also at level 3 | High |
| | Level 1: administration (mayor's office, planning department) | | | |
| | Level 2: relevant response institutions (police, fire brigade, education, emergence health) | | | |
| | Level 3: the public (business, civil society, NGO'S) | | | |
| | **(C12) Emergency plan** | | **Availability of maps at different levels:** | |
| | Is there a worked out and circulated emergency plan? | **YES/NO If YES, explain** | One | Low |
| | | | Few | Medium |
| | | | many | High |
| | **(C13) Early warning system** | | Does it work | |
| | Is an early warning system in place? | **YES/NO If YES, explain** | Low | Low |
| | | | Medium | Medium |
| | | | High | High |
| | **(C14) Institutional capacity building** | | | |
| | Do local institutions (administration, police, fire brigade, hospitals, building sector) receive training on risk management? | **YES/NO If YES, explain** | Sometimes | Low |
| | | | Often | Medium |
| | | | Constant | High |
| | **(C15) Communication** | | | |
| | Is there coordination with national level risk management organizations (national committees, government etc.)? | **YES/NO If YES, explain** | Sometimes | Low |
| | | | Often | Medium |
| | | | constant | High |

# REFERENCES

**Adeloye J. A., Mwale D.F. and Dulanya Z. (2015).** A metric-based assessment of flood risk and vulnerability of rural communities in the Lower Shire Valley, Malawi. Proc. IAHS, 370, 139–145, 2015.

**Alexander D. (1993)**. Natural disasters.New York Chapman and Hall

**Allen R.G., Pereira L.S., Raes D. and Smith M. (1998)**. Irrigation and Drainage Paper 56, FAO , Rome, 333 pages

**Amarnath G., Umer Y. M., Alahacoon N., and Inada Y. (2015)**. Modelling the flood-risk extent using LISFLOOD-FP in a complex watershed: case study of Mundeni Aru River Basin, Sri Lanka. Proc. IAHS, 370, 131–138. doi:10.5194/piahs-92-1-2015

**Amisigo A. B. (2005).** Modelling river flow in the Volta Basin of West Africa: A data-driven framework, Ph.D. thesis, Ecology and Development Series No. 34, University of Bonn, Germany.http://www.zef.de/fileadmin/webfiles/downloads/zefc_ecology_development/ecol_dev_34_text.pdf.

**Apel H., Thieken A.H., Merz B., Blöschl G. (2004)**. Flood risk assessment and associated uncertainty. Natural Hazards Earth System Science 4:295-308.

**Apel H., Merz B., and Thieken A. H.:(2008).** Quantification of uncertainties in flood risk assessments, J. River Basin Manage., 6, 149–162.

**Apel H., Aronica G.T., Kreibich H., Thieken A.H. (2009)**. Flood risk analyses-how detailed do we need to be? Natural Hazards, 49:79-98

**Ardoin-Bardin, S. (2004).** Variabilité hydroclimatiaque et impacts sur les ressources en eau des grands bassins hydrographiques en zone soudano-sahélienne, thèse de Doctorat, Université de Montpellier II, Montpellier, France.

**Aronica, G., Bates, P. D., and Horritt, M. S. (2002).** Assessing the uncertainty in distributed model predictions using observed binary pattern information within GLUE, Hydrol. Process., 16, 2001–2016. DOI:10.1002/hyp.398.

**Barry B., Obuobie, E., Andah, W., Pluquet, M. (2005).** The Volta River Basin: Comparative study of river basin development and management, draft. Available at

**References**

http://www.iwmi.cgiar.org/assessment/research_projects/river_basin_development_and_management/projects_locations/volta_river_burkina_faso_ghana.htm, accessed on July 12, 2013

**Bates B.C., Kundzewicz W. Z., Wu S. and Palutikof P.J. (2008)**. Climate Change and Water. Technical Paper of the Intergovernmental Panel on Climate Change, IPCC Secretariat, Geneva, 210 pp.

**Bates P. D., and De Roo J.P.A. (2000).** A simple raster-based model for flood inundation simulation, Journal of Hydrology, 236(1–2), 54–77.

**Bates P.D., Horrit M.S., Hunter N.M., Mason D. and Cobby D. (2005).** Numerical modelling of floodplain flow. In Bates P.D., lane S.N. and Ferguson R. I. (eds), computational Fluid Dynamics: Applications in Environmental Hydraulics, Chichester: John Wiley Sons, 271-304.

**Bates P. D., M. S. Horritt, and Fewtrell J.T. (2010)**. A simple inertial formulation of the shallow water equations for efficient two-dimensional flood inundation modelling, J. Hydrol., 387(1–2), 33–45.

**Bates P. D, Trigg M., Neal J. and Dabrowa A. (2013)**. LISFLOOD-FP: user manual, code release 6.0.4, School of Geographical sciences, University of Bristol, United Kingdom.

**Bathrellos G.D., Karymbalis E., Skilodimou H.D., Gaki-Papanastassiou K. and Baltas, E.A. (2016).** Urban flood hazard assessment in the basin of Athens Metropolitan city, Greece. Environ. Earth. Sci., 75 (4): 319

**Baugh C.A., Bates P.D., Schumann G., Trigg M.A. (2013)**. SRTM vegetation removal and hydrodynamic modelling accuracy- Water Resources. Reserach., 2013.

**Beven K., Leedal D., McCarthy S. (2011)**. Framework for assessing uncertainty in fluvial flood risk mapping, FRMRC Research Report SWP1.7. Available at www.floodrisk.org.uk (accessed on August 15, 2016).

**Blaikie P., Cannon T., Davis I. and Wisner B. (1994)**. At risk natural hazards, people's vulnerability and disasters.London Routledge

**Bodis K. (2009).** Development of a data set for continental hydrologic modelling, JRC scientific and technical reports, EUR 24087 EN-2009.

**Bohle H.G. (2001).** Vulnerability and criticality: perspectives from social geography. IHDP Update, 2/2001,1-7

**Bollin C.; Cardenas, C.; Hahn, H. and Vasta, K. S. (2003).** Natural Disasters Network:

**References**

Comprehensive Risk Management by Communities and Local Governments, Washington D.C.: Inter-American Development Bank.

**Bormann H. and Diekkrüger B. (2003).** Possibility and limitations of regional hydrological models applied within an environmental change study in Benin (West Africa); Physics and Chemistry of the Earth; Vol. 28: pp. 1323–1332

**Brooks N., Adger N.W.and Kelly M. (2005)**. The determinants of vulnerability and adaptive capacity at the national level and the implications for adaptation. Global Environmental Change Part B. Environmental Hazard, 15, 151-163.

**Burn D.H. and Goel K.N. (2000)**. The formation of groups for regional flood frequency analysis. Hydrological Sciences - Journal - des Sciences Hydrologiques, 45 (1), 2/2000

**Cardona O.D., Aalst K.M., Birkmann J., Fordham M., McGregor G., Perez R., Pulwarty S.R., Schipper F.L.E. and Sinh T.B. (2012).** Determinants of risk: exposure and vulnerability. In Managing the Risks of Extreme and Disasters to Advance Climate Change Adaptation [Field C.B., Barros V., Stocker F.T., Qin D., Dokken J.D., Ebi L. K. , Mastrandrea D.M., Mach J.K., Plattner K. G., Allen K.S., Tignor M. and Midgley M.P. (eds)]. A Special Report of Working Groups I and II of the Intergovernmental on Climate Change (IPCC). Cambridge University Press, Cambridge , UK, and New York, USA, pp.65-108.

**Chow V.T. (1956)**. Hydrologic Studies of Floods in the United States, International Association of Scientific Hydrology Publication, vol 42, pp. 134-170.

**Chow V. T. (1959)**. Open channel hydraulics. Mc-Graw Hill: New York.

**Coulombe H., Gentry A., Amouzouvi K., (2011).**TOGO: cartographie de la pauvreté 2011, Beyond productions, Togo.

**Cutter S.L. (1993)**. Living with risk. London: Edward Arnold.

**Cutter S. L.; Boruff, B. J. and Shirley, W. L. (2003).** Social vulnerability to environmental hazards, Social Science Quarterly, 84(2) 242-261

**Dartmouth Flood Observatory. http://www.floodobservatory.colorado.edu**-University of Colorado-United States of America, accessed the 5th March 2015.

**Davidson R. and Lambert K. (2001)**. Comparing the Hurricane Disaster Risk of U.S. Coastal counties. Natural Hazards Review, 2(3): 132-142

**DGSCN (2010)**. Quatrième Recensement Général de la Population et de l'Habitat au Togo, République Togolaise.

**References**

**De Roo A. P. J. and Schmuck G. (2002).** Assessment of the effects of engineering land use and climate scenarios on flood risk in the upper-Oder catchment, European Commission, EUR 20276 EN. Available at http://publications.jrc.ec.europa.eu/repository/handle/JRC23436

**Di Baldassarre G., Schumann G., and Bates P. D. (2009)**. A technique for the calibration of hydraulic models using uncertain satellite observations of flood extent, J. of Hydrol., 367, 276–282. doi:10.1016/j.jhydrol.2009.01.020

**Di Baldassare G. (2012).** Floods in a changing climate: inundation modelling. Cambridge University Press, the Edinburgh Building, Cambridge CB2 8RU, UK.

**Dinh Q.; Balica S.; Popescu I. and Jonoski, A. (2012)**. Climate Change Impact on Flood Hazard, Vulnerability and Risk of the Long XuyenQuadrangle in the Mekong Delta,International Journal of River Basin Management, 10(1) 103-120.

**Dutta D. and Nakayama K. (2008)**. Effects of spatial grid resolution on river flow and surface inundation simulation by physically based distributed modelling approach, hydrological processes, 23, 534–545 (2009), DOI: 10.1002/hyp.7183

**Elkhrachy I. (2015)**. Flash Flood Hazard Mapping Using Satellite Images and GIS Tools: A case study of Najran City, Kingdom of Saudi Arabia (KSA) The Egyptian Journal of Remote Sensing and Space Sciences (2015) 18, 261–278.

**FAO/UNESCO (1995, 2003).** The Digitized Soil Map of the World and Derived Soil Properties. (version 3.6) , Land and Water Development Division, Food and Agriculture Organization of the United Nations (FAO), Rome.

**FAO (2013).** Land cover map of Togo. Available at http://data.fao.org/map?entryId=3af5c4ff-865e-4274-af69-4283cf41d41b and accessed on September 30, 2015.

**Forkuo E. K. (2011)**. Flood hazard mapping using Aster image data with GIS, International Journal of Geomatics and Geosciences, 1 (4), pp 932 – 950.

**Gaillard J.C. (2010)**. Vulnerability, capacity and resilience: Perspectives for climate and development policy, Journal of International Development, 22, 218-232.

**Goula B. T. A., Savané I., Konan B., Fadika V. and Kouadio G. B. (2006).** Impact de la variabilité climatique sur les ressources hydriques des bassins versants du N'Zo et du N'Zi en Côte d'Ivoire (Afrique tropicale humide). *Vertigo,* **7** (1) : 1 - 12.

**Goula B. T. A., Kouassi F.W., Fadika V., Kouakou K. E. Kouadio G. B., Koffi K., Bamory K., Doumouya I. and Savané I. (2009).** Impacts du changement et de la variabilité climatiques

sur les eaux souterraines en zone tropicale humide : Cas de la Côte d'Ivoire. *IASH Publication*, 334 : 190 - 202

**Granger K., Jones T., Leiba M, Scott G. (1999).** Community risk in Cairns: a multi-hazart risk Assessment, AGSO cities project Report no. 1

**Greenwood J.A, Landwehr J.M, Matalas N.C., Wallis J.R. (1979)**. Probability weighted moments: definition and relation to parameters of several distributions expressable in inverse form. Water Resources Research 15:1049–1054. doi:10.1029/WR015i005p01049

**GTZ (2003).** Community-based disaster risk management approach: Experience gained in Central America. Deutsche Gesellschaft für Technische Zusammenarbeit (GTZ), Dag-Hammarskjöld-Weg 1-5, Postfach 5180, 65726 Eschborn, Germany.

**Guarín P. G. (2008).** Integrated local knowledge into GIS-based flood risk assessment. The case of Triangulo and Mabolo communities in Naga city (Philippines), Ph.D thesis, International Institute for Geo-Information Science and Earth Observation (ITC), Enschede, The Netherlands.

**He H.Y., Cloke H.L., Wetterhall F., Pappenberger F, Freer J., Wilson M. (2009).** Tracking the uncertainty in flood alerts driven by ensemble weather predictions.Meteorological applications, 16: 91-101

**Hingray B., C. Picouet, A. Musy (2009)**. Hydrologie 2: une science pour l'ingénieur, Presses polytechniques et universitaires romandes.

**Hirabayashi, Y. and Kanae , S. ( 2009)**. First estimate of the future global population at risk of flooding. Hydro Res Lett. , 3:6–9; DOI: 10.3178/HRL.3.6

**Horritt M.S., Bates P.D. (2001)**. Predicting floodplain inundation: raster-based modelling versus the finite element approach. Hydrological. Process 15:825–842.

**Horritt M.S. (2005)**. A methodology for the validation of uncertain flood inundation models. J. Hydrol., 326 (2006) 153–165, doi:10.1016/j.jhydrol.2005.10.027.

**Hosking J.R.M. (1990).** L-moments: analysis and estimation of distributions using linear combinations of order statistics. J Royal Statistical Society B Methodological 52:105–124

**Hosking, J.R.M., and Wallis, J.R., (1997**). Regional Frequency Analysis: An Approach Based on L-Moments, Cambridge University.

**ICSU Rgeional Office for Africa (2007).** Natural and Human-induced Hazards and disaster in sub-saharan Africa, 32.

**IFRCRCS (1998)**.TOGO: FLOODS, information bulletin No2 (final)

**References**

**IFRCRCS (2007).** West Africa: Flood in Ghana and Togo, emergency appeal No MDR61002.

**IPCC (2001)**. IPCC Third Assessment Report. Synthesis Report, Cambridge University Press, Cambridge UK.

**IPCC (2012).** Managing the Risks of Extreme Events and Disasters to Advance Climate Change Adaptation. A Special Report of Working Groups I and II of the Intergovernmental Panel on Climate Change [Field, C.B., V. Barros, T.F. Stocker, D. Qin, D.J. Dokken, K.L. Ebi, M.D. Mastrandrea, K.J. Mach, G.-K. Plattner, S.K. Allen, M. Tignor, and P.M. Midgley (eds.)]. Cambridge University Press, Cambridge, UK, and New York, NY, USA, 582 pp.

**IPCC (2014).** IPCC's fifth assessment report (AR5). Available at www.ipcc.ch (last accessed November 4, 2016).

**ISDR (2004).** Living with risk: A global review of disaster reduction initiatives. New York and Geneva: United Nations.

**ISDR (2005)**. Hyogo Framework for Action 2005-2015: Building the resilience of nations and communities to disasters, World Conference on Disaster Reduction: 18-22 January 2005, Kobe, Hyogo, Japan.

**ISDR (2009)**. Terminology on Disaster Risk Reduction. United Nations International Strategy for Disaster Reduction, Geneva, Switzerland.

**Jiang X. and Tatano H. (2015).** A rainfall design method for spatial flood risk assessment: considering multiple flood sources, Hydrology and Earth System. Science. Discuss., 12, 8005–8033, 2015, doi:10.5194/hessd-12-8005-2015.

**Kalyanapu A. J., Burian S. J. and McPherson T. N. (2009)**. Effect of land use-based surface roughness on hydrologic model output. Journal of Spatial Hydrology, Vol.9, No.2, 21 pages.

**Kates R.W. (1985)**. The interaction of climate and society. In Climate impact assessment, SCOPE 27 [Kates W.R., Ausubel H.J. and Berberian M. (eds)].New York: Wiley,3-36.

**Kelman I. (2003).** Defining risk, Flood Risk Net Newsletter, Issue 2, winter 2003.

**Knight F.H. (1921)**. Risk, Uncertainty, and Profit. Boston M.A.: Hart, Schaffner and Marx; Houghton Mifflin Company [online] available at http://www.econlib.org/library/Knight/knRUP1.html (Last accessed on November 4, 2016)

**Komi K., Amisigo A. B., Diekkrüger B., Hountondji C. C. F. (2016).** Regional flood frequency analysis in the Volta River Basin. Hydrology, 3, 5. DOI: 10.3390/hydrology3010005.

**References**

**Koriche A. S. (2012).** Remote sensing based hydrological modelling for flood early warning in the upper and Middle Awash River Basin. Master Thesis, Faculty of Geo-Information, Science and Earth Observation, University of Twente (Netherlands).

**Le Barbe L., Lebel T., Tapsoba D. ( 2002).** Rainfall variability in West Africa during the years 1950–90. Journal of Climate 15, 187–202.

**Leopold L. B., and Maddock J. T. (1953)**. The hydraulic geometry of stream channels and some physiographic implications, U.S. Geological. Survey. Prof. Pap., 252, 56 pp.

**Lim Y. H., Lye L. M. (2003).** Regional flood estimation for ungauged basins in Sarawak, Malaysia. Hydrol Sci J 48(1):79–94. doi:10.1623/hysj.48.1.79.43477.

**Maidment D. R. (1992).** Handbook of Hydrology, McGraw-Hill Education Publiher, United States, 1143 pages.

**Marinoni O. (2004)**. Implementation of the analytical hierarchy process with VBA in ArcGIS. Computer Geosciences Journal. 30:367-646

**McCartney, M., Forkuor G., Sood A., Amisigo B., Hattermann F., and Muthuwatta L. (2012).**The Water Resource Implications of Changing Climate in the Volta River Basin, IWMI Research Report 146, Colombo, Sri Lanka, doi:10.5337/2012.219, 2012.

**McCuen H. R., Johnson A. P. and Ragan M. R. (2002)**. Highway hydrology, US department of transportation, publication No.FHWA-NHI-02-001

**Mechler R. S., Hochrainer A., Aaheim H., Salen H. and Wreford A. (2010)**. Modelling economic impacts and adaptation to extreme events: Insights from European case studies. Mitigation and Adaptation Strategies for Global Change, 15 (7), 737-762.

**Meigh R.J., Farquharson K.A. and Sutcliffe V. J. (1997).** A worldwide comparison of regional flood estimation methods and climate, Hydrological Sciences-Journal, 42(2) April 1997.

**Mentzafou A. and Dimitriou E. (2015)**. Flood risk assessment for a heavily modified urban stream, Proceedings of the 11th Kovacs Colloquium, Paris, France, June 2014, IAHS Publ. 366, 2015, doi:10.5194/piahs-366-147-2015.

**MERF (2009)**. Plan d'Action National d'Adaptation (PANA) aux changements climatiques. Ministère de l'Environnement et des Ressources Forestières (MERF), Togo.

**Merz B., Thieken A.H. and Gocht M. (2007).** Flood risk mapping at the local scale: concepts and challenges. In Flood risk management in Europe [Begum S., Stive M.J.F. and Hall J.W. (eds)]. Advances in natural and technological hazards research. Springer Netherlands, 231-251

**References**


**Merz B., Thieken A.H. (2009)**. Flood risk curves and uncertainty bounds. Natural Hazards. 51:437-458.

**Mitchell J.K. (1989)**. Hazards research. In Geography in America [Gaile G.L. and Willmott J.C.Columbus, OH: Merrill, 410-424

**Mohr I. K. and Thorncroft D.C. (2006).** Intense convective systems in West Africa and their relationship to the African easterly jet, Q. J. R. Meteorol. Soc. (2006), **132**, pp. 163–176, doi: 10.1256/qj.05.55

**Moniod F., Pouyaud B. and Sechet P. (1977),** Hydrological monographs $N^0$5:Volta River Basin, Office de la Recherche Scientifique et Technique Outre-Mer, Paris, 1714 pages (In French)

**Moores J. R., Cole J.S., Bell A. V., Jones A. D. (2006)**. Issues in flood forecasting: ungauged basins, extreme floods and uncertainty, IAHS Publ. 305, 2006.

**Moss R.H., Brenkert L.A. and Malone L.E. (2001).** Vulnerability to Climate Change: A Quantitative Approach. Technical Report PNNL-SA-33642, Pacific Northwest National Laboratories, Richland,WA.

**Musungu K., Motala S., Smit J. (2012).** Using Multi-criteria Evaluation and GIS for Flood Risk Analysis in Informal Settlements of Cape Town: The Case of Graveyard Pond, South African Journal of Geomatics, Vol. 1, No. 1, January 2012.

**Neal J. Schumann G., and Bates P. D. (2012)**. A sub-grid channel model for simulating river hydraulics and floodplain inundation over large and data sparse areas. Water Resources Research 48, W11506, doi: 10.1029/2012WR012514

**Nicholson S. E. (2001)**. Climatic and environmental change in Africa during the last two centuries. Clim. Res. **17,** 123-144.

**Noto L. V., La Loggia G., (2009)**. Use of L-moments approach for regional flood frequency analysis in Sicily, Italy. Water Resources Management, 23(11), 2207-2229.

**OCHA (2016)**. http://www.unocha.org/ (last accessed on September 15, 2016)

**Omkarprasad, V. and Sushil K. (2006)**." Analytic hierarchy process: an overview of applications". European Journal of Operational Research, 169(1):1-29

**Omotosho J. B., 1985**: The separate contributions of squall lines, thunderstorms and the monsoon to the total rainfall in Nigeria. Journal of Climatology, **5,** 543–552.

**References**

**Ouarda T.B.M.J., Ba M.K., C. Diaz-Delgado C., A. Carsteanu A., Chokmani K., Gingras H., Quentin E., Trujillo E. and Bobée B. (2007).** Intercomparison of regional flood frequency estimation methods at ungauged sites for a Mexican case study. Journal of Hydrology 348, 40–58. doi:10.1016/j.jhydrol.2007.09.031.

**Paeth H., Fink H. A., Pohle S, Keis F., Mächel H. and Samimi C. (2011).** Meteorological characteristics and potential causes of the 2007 flood in sub-Saharan Africa. Int. J. Climatol., 31: 1908–1926 (2011) .doi: 10.1002/joc.2199 space–time variability of rainfall on basin flood response, Journal of Hydrology. 514 (2014) 313–327, http://dx.doi.org/10.1016/j.jhydrol.2014.04.014.

**Pandey R.G.; Nguyen V.T.V. (1999).** A comparative study of regression based methods in regional flood frequency analysis. Journal of Hydrology 225, 92–101.

**PDNA_Benin (2011)**. Flood in Benin: Post Disaster Needs Assessment, Republic of Benin,84p (In French)

**Pebesma J.E. (2014).** Gstat user's manual, version 2.5.1, Utrecht University, available at http://www.gstat.org (accessed on June 10, 2014).

**Peters M. and Tetzlaff G. (1988).** The structure of West African squall lines and environmental moisture budget, Meteorol. Atmos. Phys. 39, 74-84 (1988)

**Rosbjerg D., Blöschl G., Burn H.D., Castellarin A., Croke B., Di Baldassarre G., Iacobellis V., Kjeldsen R.T., Kuczera G.,Merz R., Montanari A., Morris, D., Ouarda J.M.B.T., Ren L., Rogger M., Salinas L.J., Toth E. and Viglione A. (2013).** Prediction of floods in ungauged basins. In Blöschl G., Sivapalan M., Wagener T., Viglione A., Savenije H., Eds. Runoff prediction in Ungauged Basins: Synthesis across Processes, Places and Scales, Cambridge University Press, The Edinburgh Building, Cambridge CB2 8RU, UK.

**Romanowicz R. and Beven K. (2003)**. Estimation of flood inundation probabilities as conditioned on event inundation maps. Water Resources Research, 39(3), 1073-1085.

**Rose A. (2004).** Economic principles, issues, and research priorities in hazard loss estimation. In Modelling Spatial and Economic Impacts of Disasters [Okuyama,Y. and S.E. Chang (eds)]. Springer, New York.

**Roudier P., Ducharne A., and Feyen L. (2014)**. Climate change impacts on river discharge in West Africa: a review, Hydrology and Earth System Sciences Discussion., 11, 2483–2514, 2014. doi:10.5194/hessd-11-2483-2014

**References**

**Saaty T.L. (1977)**. A scaling method for priorities in hierarchical structures. J. Math. Psychol., 15: 234-281

**Saaty L.T. (2008)**. Decision making with the analytic hierarchy process. Int. J. Service Sciences 2008, Vol.1,No1

**Safaripour M., Monavari M., Zare M., Abedi Z., Gharagozlou A. (2012).** Flood risk assessment using GIS (case study: Golestan province, Iran), Pol. J.Environ. Stud. Vol.21, No 6 (2012), 1817-1824.

**Sayama T., Ozawa G., Kawakami T., Nabesaka S. and Fukami K. (2012)**. Rainfall–runoff–inundation analysis of the 2010 Pakistan flood in the Kabul River basin, Hydrological Sciences Journal, 57:2, 298-312, doi: 10.1080/02626667.2011.644245.

**Sayers B.P., Hall W.J. and Meadowcroft C. I. (2002).** Towards risk-based flood hazard management in the UK. Proceedings of ICE, Pages 36–42 Paper 12803

**Sayers P.B.m Gouldby B.P., Simm J.D., Meadowcroft J., Hall J. (2003)**. Risk, performance and uncertainty in flood and coastal defense-a review. Wallingford: DEFRA/Environment Agency.

**Schumann G.and Di Baldassarre G. (2010).** The direct use of radar satellites for event-specific flood risk mapping, Remote Sensing Letters, 1:2, 75-84, DOI:10.1080/01431160903486685

**Schumann G. J. P.; Neal J.C.; Voisin N.; Andreadis K. M.; Pappenberger F.; Phanthuwongpakdee N.; Hall A. C. and Bates, P. D. (2013).** A first large-scale flood Inundation forecasting model, Water Resources. Research. 10.1002/wrcr.20521.

**Shaw M. E., Beven J.K., Chappell A. N., Lamb R. (2011).** Hydrology in practice, 4th edition, Spon Press, United Kingdom.

**Simonovic P. S. (2012).** Floods in a changing climate: Risk management. Cambridge University Press, the Edinburgh Building, Cambridge CB2 8RU, UK.

**Sintondji L. (2005):** Modelling the rainfall-runoff process in the Upper Ouémé catchment (Terou in Benin republic) in a context of global change: extrapolation from the local to the regional scale. PhD Thesis in Hydrology and Environmental management of the Mathematics and the Natural Sciences Faculty of the University of Bonn. Shaker Verlag GmbH. P.O. Box 101818. D- 52018 Aachen Germany

**Skøien J. O., Merz R., and Blöschl G. (2006).** Top-kriging: geostatistics on stream networks, Hydrology and Earth System Sciences, 10(2), 277–287, doi: 10. 5194/hess-10- 277-2006.

**References**

**Stedinger J. R. and Lu L. H. (1995).** Appraisal of regional and index flood quantile estimators. Stoch HydrolHydraul 9(1):49–75. doi:10.1007/BF01581758

**Stenchion P. (1997).** Development and disaster management The Australian Journal of Emergency Management, vol. 12, no. 3, Spring 1997, pp. 40-44.

**Sultan B. and Janicot S. (2003).** The West African Monsoon Dynamics. Part II: The ‘‘Preonset’’ and ‘‘Onset’’ of the Summer Monsoon, Journal of climate, Vol 16, No 21.

**Sultan B., Janicot S. and Diedhiou A. (2003).** The West African Monsoon dynamics. Part I: documentation of intraseasonal variability, Journal of climate, Vol 16, No 21.

**Sutcliffe J.V.; Farquharson F.A.K. (1996).** Flood frequency studies using regional methods. In Conference for Jacques Bernier; UNESCO Press: Paris, France.

**Thiemig V., Bisselink B., Pappenberger F. and Thielen J. (2015).** A pan-African medium-range ensemble flood forecast system, Hydrol. Earth Syst. Sci., 19, 3365–3385, 2015. doi:10.5194/hess-19-3365-2015

**Thompson A. and Clayton J. 2002**. The role of geomorphology in flood risk assessment, Proceedings of ICE, Civil Engineering 150 May 2002, Pages 25–29 Paper 12771.

**Trigg M. A., M. D. Wilson, P. D. Bates, M. S. Horritt, D. E. Alsdorf, B. R. Forsberg, and. Vega C. M. (2009).** Amazon flood wave hydraulics. Journal of Hydrology, 374(1–2), 92–105.

**Tschakert P., Sagoe R., Ofori-Darko G., and Codjoe S. N. (2010).** Floods in the Sahel: an analysis of anomalies, memory, and anticipatory learning. Climatic Change, 103(3-4), 471–502. doi:10.1007/s10584-009-9776.

**UNEP-GEF Volta Project (2012)**. Volta Basin Transboundary Diagnostic Analysis, UNEP/GEF/Volta/RR 4/2012.

**UNIDRO (1991).** Managing Natural Disasters. Phenomena. Effects and Options. A Manual for Policy Makers and Planners. UN, NY.

**Van Der Knijff, J. and De Roo A. P. J. (2008).** LISFLOOD – Distributed Water Balance and Flood Simulation Model, Revised User Manual. EUR 22166 EN/2 , Luxembourg: Office for Official Publications of the European Communities

**Van Deursen W. and Wesseling C. (2009).** PCRaster version 2 Manual, University of Utrecht, Netherlands. Available at http://pcraster.geo.uu.nl/ (accessed on November 21, 2013).

**Ward J.H. (1963),** Hierarchical grouping to optimize an objective function. J Am Statistical Association, 58:236–244. doi:10.2307/2282967

**Ward J. P., Jongman B., Weiland S. F., Bouwman A., Beek van R., Bierkens P.F.M., Ligtvoet W. and Winsemius C. H. (2013).** Assessing flood risk at the global scale: model setup, results, and sensitivity, Environ. Res. Lett. 8 (2013) 044019 (10pp). doi:10.1088/1748-9326/8/4/044019

**Watts M. J. and Bohle H.G. (1993)**. The space of vulnerability: the causal structure of hunger and famine. Progress in Human Geography 17, 43-67

**Wilson M., Bates P., Alsdorf D., Forsberg B., Horritt M., Melack J., Frappart F. and Famiglietti J. (2007).** Modelling large-scale inundation of Amazonian seasonally flooded wetlands. Geophys Res Lett 34:L15404. doi:10.1029/2007GL030156, 2007

**Wisner B., Blaikie, P., Cannon T. and Davis I. (2004).** At Risk: Natural hazards, People's Vulnerability and Disasters, second ed. Routledge, London.

**World Bank (2011)**.Project appraisal document, the World Bank, Report No: 62210-TG.

**Yan K., Pappenberger F., Umer M.Y., Solomatine P.D. and Di Baldassarre G. (2014)**. Regional versus physical based methods for flood inundation modelling in data scarce areas: application to the Blue Nile. 11th International Conference on Hydroinformatics, New York City, USA.

**Yodmani S. (2001).** Disaster preparedness and management. In: Social Proetection in Asia and the Pacific [Ortiz I.D. (eds.)]. Asian Development Bank, Manila,pp.481-502.

http://iridl.ldeo.columbia.edu/SOURCES/.NASA/.GES-DAAC/.TRMM_L3/.TRMM_3B42/.v7/.daily/.precipitation/, , accessed on June 26, 2014.

https://climatedataguide.ucar.edu/climate-data/cru-ts321, accessed on April 12, 2015.

http://www.iiasa.ac.at/Research/LUC/luc07

http://Landsaf.meteo.pt

http://www.floodobservatory.colorado.edu, accessed on February 10, 2015.

http://www.isric.org/sites/default/files/major_soils_of_the_world, accessed on December 8, 2015

http://www.engineeringcivil.com, accessed on November 7, 2016.